



UNIVERSITY OF PAVIA

PHD COURSE IN PSYCHOLOGY, NEUROSCIENCE AND DATA  
SCIENCE

DOCTORATE CYCLE: XXXV

*Curriculum: Data Science and biomedicine*

PATHOLOGICAL FEATURES OF COVID-19  
INFECTION: A POST-MORTEM APPROACH  
BASED ON AN EXTENSIVE AUTOPTIC  
SAMPLING PROTOCOL

SUPERVISOR:  
PROF. P. POLITI

PhD Candidate:  
**Matteo Moretti**

## ABSTRACT

**Introduction:** Coronavirus disease 19 (COVID-19) is caused by the severe acute respiratory syndrome coronavirus 2 (SARS-CoV-2). Due to the resultant serious public health crisis, the attention of the scientific community was turned towards COVID-19. Despite the importance of post-mortem studies in the understanding of pathophysiology, autopsies have been generally discouraged by government regulations. This study consists of the pathological analysis of samples of select organs obtained during autopsies of deceased COVID-19 subjects, performed by forensic pathologists of the Unit of Legal Medicine of Pavia.

**Aims:** to describe COVID-19 pathology across different tissues to clarify the disease's pathophysiology.

**Materials and methods:** autopsic cases were selected based on the presence of SARS-CoV-2 infection. Lungs, kidneys, hearts, and brains from nine COVID-19 autopsies were compared by using antibodies against SARS-CoV-2, macrophages-microglia, T-lymphocytes, B-lymphocytes, and activated platelets. Alzheimer's Disease pathology was also assessed. PCR techniques were used to verify the presence of viral RNA in brain.

**Results and discussion:** we selected 9 COVID-19 cases. They had a short clinical course (0–32 days) and their mean age was 77.4 y/o. Hypoxic changes and inflammatory infiltrates were present across all tissues. The lymphocytic component in the lungs and kidneys was predominant over that of other tissues ( $p < 0.001$ ), with a significantly greater presence of T-lymphocytes in the lungs ( $p = 0.020$ ), which showed the greatest presence of viral antigens. The heart showed scant SARS-CoV-2 traces, foci of activated macrophages, and rare lymphocytes. The brain showed scarce SARS-CoV-2 traces, prominent microglial activation, and rare lymphocytes. The pons exhibited the highest microglial activation ( $p = 0.017$ ). Microthrombosis was significantly higher in COVID-19 lungs ( $p = 0.023$ ) compared with controls. The most characteristic pathological features of COVID-19 were an abundance of T-lymphocytes and microthrombosis in the lung and relevant microglial hyperactivation in the brainstem. Data obtained in this study could potentially offer a better understanding of how this recently identified pathology affects the human body and specific organs, with the goal of improving clinical management of affected patients and improving strategies for disease prevention.

# INDEX

ABSTRACT .....	2
INDEX .....	3
1. INTRODUCTION AND BACKGROUND .....	5
1.1. Characteristics of SARS-CoV 2 .....	6
1.1.1. Structure and targets .....	7
1.1.2. Clinical presentation .....	8
1.1.3. Brain involvement .....	10
1.1.4. Lung involvement .....	12
1.1.5. Kidney involvement .....	13
1.1.6. Liver involvement .....	13
1.1.1. Post-acute COVID-19 syndrome .....	14
1.2. Covid 19 and autopsies .....	15
1.2.1. General overview: the Italian medical examiner system .....	16
1.2.2. The impact of the COVID-19 emergency on medicolegal practices .....	18
2. OBJECTIVES .....	21
3. MATERIALS AND METHODS .....	23
3.1. Study design, setting and participants .....	23
3.2. Case selection .....	23
3.2.1. Inclusion and exclusion criteria .....	24
3.2.2. Control cases .....	24
3.3. Autopsy protocol .....	24
3.4. Samples collection .....	25
3.5. Collection of clinical information .....	26
3.6. Neuropathological investigation .....	27
3.7. Histopathological examinations .....	27
3.8. Immunohistochemical examinations .....	28
3.8.1. Summary of the procedures implemented in the immunohistochemistry laboratory .....	30
3.8.2. Semi-quantitative Analysis .....	31
3.8.3. Statistical evaluation .....	38
3.9. Presence of viral RNA and Trascriptomic evaluations .....	39
4. RESULTS .....	41
4.1. COVID cases overview .....	41

4.2.	General and clinical data of included cases.....	46
4.3.	Histopathology in Lung, Kidney, Heart, Brain .....	49
4.3.1.	Pathological findings in COVID-19 Cases .....	49
4.3.2.	Pathological Findings In Control Non-COVID Cases .....	53
4.4.	Focus on neuropathological investigation .....	58
4.4.1.	Macroscopic and microscopic neuropathological features .....	58
4.4.2.	Semi-quantitative analysis of microglial activation .....	62
4.1.	SARS-CoV 2 detection in frontal cortex.....	65
4.1.1.	Transcriptomic results .....	65
5.	DISCUSSION .....	67
5.1.	COVID-19 Pathology in the Lung, Kidney, Heart and Brain .....	67
5.1.1.	SARS-CoV-2 Antigens .....	68
5.1.2.	Inflammatory Infiltrates .....	70
5.1.3.	Comparison between COVID-19 and other types of pneumonia .....	71
5.1.4.	Comparison between COVID-19 and control brains .....	72
5.1.5.	Microthrombosis .....	73
5.2.	COVID-19-related neuropathology and microglial activation .....	75
5.3.	Presence of viral RNA in brain and trascriptomic evaluations .....	82
5.4.	Limitations and strength of the study .....	85
6.	CONCLUSIONS.....	87
7.	REFERENCES .....	89

# 1. INTRODUCTION AND BACKGROUND

Coronavirus disease 19 (COVID-19), originated at Wuhan city of China in early December 2019 has rapidly widespread with confirmed cases in almost every country across the world and has become a new global public health crisis<sup>1</sup>. The rate of its spreading compelled the World Health Organization (WHO) to declare the state of pandemic on March 11, when over 118,000 cases of the coronavirus illness were reported in over 110 countries and territories around the world. Up to date 19/06/2020 WHO report 642 379 243 confirmed cases, 6 624 118 confirmed deaths<sup>2</sup>.

The first outbreak of COVID-19 was reported in Wuhan, China, on 31th December 2019, but at the time it was not yet associated to the now well-known virus. Only on the 9th of January 2020 the Chinese's Center for Disease Control communicated that the pathological agent was identified, but by then the virus had spread quickly to all the Wuhan region.

The virus was rapidly isolated and sequenced and was officially identified as SARS-CoV-2 by the International Committee on Taxonomy of Viruses on the 11th of February 2020 and data were made available to all the scientific community<sup>3,4</sup>.

The results from analysis of phylogenetic, virological, epidemiological, ecological, clinical data have been crucial to clarify the genomic characterization of the novel virus.

Whole genome sequencing revealed that SARS-CoV-2 phylogenetically has genomic similarities to be placed in the same Betacoronavirus clade like SARS-CoV (severe acute respiratory syndrome coronavirus), MERS-CoV (Middle East respiratory syndrome coronavirus), and SARS-like bat CoV; however, phylogenetic analysis and amino acid sequences have revealed enough differences in SARS-CoV-2 to confer structural and functional difference from other coronaviruses<sup>5</sup>. These viruses have been identified as belonging to the Sarbecovirus subgenus, Betacoronavirus genus, Orthocoronavirinae subfamily, Coronaviridae family (Cornidovirinea: Nidovirales)<sup>1</sup>. Coronaviruses are characterized by frequent genomic

recombination, high prevalence, and wide distribution, and they typically infect the respiratory and digestive tracts of several animal species, as well as humans. All previous human coronaviruses have zoonotic origins, as have the vast majority of human viruses.

## **1.1. Characteristics of SARS-CoV 2**

COVID-19 marked the third introduction of a highly pathogenic and large-scale epidemic coronavirus into the human population in the twenty-first century since the severe acute respiratory syndrome coronavirus (SARS-CoV) in 2002, and Middle East respiratory syndrome coronavirus (MERS-CoV) in 2012<sup>6</sup>. The mortality rates due to SARS-CoV (9.6%) and MERS-CoV (34.3%) are significantly higher than that of SARS-CoV-2 infection (4.4%), but the latter is more easily transmittable, which explains its rapid spread and the massive number of cases worldwide<sup>7</sup>.

Appearance of SARS-CoV, SARS-CoV-2, and MERS viruses is the result of evolutionary events occurring in bat populations with further transfer of viruses to the human directly or through the intermediate vertebrate hosts, ecologically connected with bats. Most of the earliest human cases centred on the Huanan Seafood Wholesale Market in City of Wuhan, China<sup>8</sup>. Within the market, the data statistically located the earliest human cases to one section where vendors of live wild animals congregated and where virus-positive environmental samples concentrated. In a related report, scientists found that genomic diversity before February 2020 comprised two distinct viral lineages, A and B, which were the result of at least two separate cross-species transmission events into humans<sup>9,10</sup>. The precise events surrounding virus spillover will always be clouded, but all of the circumstantial evidence so far points to more than one zoonotic event occurring in Huanan market in Wuhan, China, likely during October–December 2019.

### 1.1.1. STRUCTURE AND TARGETS

SARS-CoV-2 has a single-stranded, positive-sense RNA (+RNA) genome of ~29.9 kb directly working as an mRNA, to initiate viral genome replication and transcription<sup>10</sup>.

SARS-CoV-2 shares 79% genome sequence identity with SARS-CoV<sup>11</sup>.

Since the outbreak of the COVID-19 pandemic in December 2019, the SARS-CoV-2 genome has undergone several mutations. The emergence of such variants has resulted in multiple pandemic waves, contributing to sustaining to date the number of infections, hospitalisations, and deaths despite the swift development of vaccines, since most of these mutations are concentrated on the Spike protein, a viral surface glycoprotein that is the main target for most vaccines<sup>12</sup>.

Genetic similarities of Covid-19 to the virus SARS-CoV-1 include the “spike proteins” that dictate tissue tropism using the angiotensin-converting enzyme type 2 (ACE-2) receptor to bind to cells. For a full understanding of the susceptibility for SARS-CoV-2 infection and the role of ACE2 in clinical manifestations of the disease, it is necessary to study the cell type-specific expression of ACE2 in human tissues. This is a receptor on variety of cells in the human body. The ACE-2 receptor is widely distributed in the body present in the lungs, oral and nasal mucosa, bone marrow and spleen, skin, heart, arteries, kidneys, adipose tissue, reproductive system, and brain<sup>13,14,15</sup>. ACE 2 receptor is also expressed in the central nervous system predominantly in *thalamic nuclei, cerebellum, and inferior olivary nuclei*. Therefore, COVID-19 is broadly characterized as a disease that targets multiple organs, particularly causing acute complications via organ-specific pathogenesis accompanied by destruction of ACE2+ cells, including alveolus, cardiac microvasculature, endothelium, and glomerulus<sup>16</sup>.

The peptidase ACE2 exerts a central regulatory role in inflammatory processes by downregulating the main pro-inflammatory peptides of the Renin-angiotensin system (RAS) and the Kinin kallikrein system (KKS). These two highly integrated signalling systems, whose

receptors act synergistically and strengthen each other, activate the inflammatory response, activate cytokines starting from a central controller of inflammation such as TNF- $\alpha$ , which is activated by the same protease that degrades ACE2 and recruits macrophages and neutrophils. It is being suggested that the main role of ACE2 consists in terminating this inflammatory process. ACE2 degradation or failure to activate it, may exacerbate the inflammatory response leading to organ damage, including oedema, and it may be responsible of the most severe consequences of Covid-19 even after the infection has been resolved<sup>17</sup>.

Under such circumstances, the high expression of ACE2 in predisposing individuals associated with anomalous production of the renin-angiotensin system (RAS) may promote enhanced viral load in COVID-19, which comparatively triggers excessive apoptosis<sup>18,19</sup>.

### *1.1.2. CLINICAL PRESENTATION*

Other than genetic characteristic, COVID, SARS, MERS viruses also present with similar clinical presentation. SARS and MERS have received worldwide attention as important pathogens in respiratory tract infection occasionally accompanied by gastrointestinal manifestations. Clinical symptoms on admission included fever, cough, myalgia and shortness of breath in both SARS and MERS patients, while symptoms of upper respiratory tract infection such as sore throat were also frequent. Atypical symptoms such as diarrhoea and vomiting developed in both SARS and MERS patients. Respiratory distress remaining the primary mechanism leading to increased morbidity and mortality, associated with variable incubation time with symptoms taking from two days to as long as around two weeks to appear<sup>19,20</sup>.

SARS-CoV-2 infection, as well, has caused clusters of severe respiratory illness similar to that of SARS-CoV. The virus causes symptoms such as fever, cough, shortness of breath, leukopenia and bilateral interstitial pneumonia<sup>21</sup>. Although the respiratory system is undoubtedly the main target of SARS-CoV-2, the infection is characterized by a broad spectrum

of clinical manifestations denoting a multiple-organ disease, which has been confirmed by pathologic studies<sup>22,23,24,25</sup>.

The symptoms are observed approximately 5.2 days after the SARS-CoV-2 infection<sup>26</sup>.

The prevalence rates of the most common symptoms were as follows: fever: 84.30%, cough: 63.01%, dyspnoea: 37.16%, fatigue: 34.22% and diarrhea: 11.47%<sup>27</sup>.

Regarding conditions at admission in hospital, the median duration from symptom onset to hospitalisation was longest in the middle-aged group (5 days) and during Wave 1 (7 days). Young patients had least severe disease at admission (7,8%). The incidence of severe disease at admission was lowest during Wave 2. The frequency of some symptoms varied considerably with age. Sore throat was more common among young and middle-aged (patients, and rhinorrhoea was more common among under 18 and young patients. Dyspnoea was most common among middle-aged patients (25%). Muscle pain, headache, and diarrhoea were more common among young and middle-aged patients. Fever, cough, and fatigue were most frequent among middle-aged patients. Taste and smell disorders were most common among young patients<sup>28</sup>.

COVID-19 is particularly detrimental in patients with multiple comorbidities (e. g. cardiovascular diseases, diabetes, obesity, pulmonary disorders, and cancer). In elderly subjects affected by dementia, the Coronavirus disease 2019 (COVID-19) mortality is increased approximately three-fold<sup>29</sup>.

The majority of extant published estimates offer empirical evidence showing that the incubation period for the virus has a median of 5.8 days, which falls into the ranges proposed by the World Health Organization – WHO (0–14 days) and the European Center for Disease prevention and Control - ECDC (2–12 days)<sup>30</sup>. Another study from the Chinese Centers for Disease Control reported 80.9% of persons infected with SARS-CoV-2 were asymptomatic or developed only mild pneumonia yet shed large amounts of virus in the early phase of their

infection, in those becoming symptomatic, the clinical manifestations of COVID-19 were virtually indistinguishable from influenza being initially characterized by fever and cough<sup>31</sup>.

Recent review has stated that the pooled percentage of asymptomatic infections was 32.40% among SARS-CoV-2 Omicron variant-positive individuals. The people who were vaccinated, young (median age < 20 years), had a travel history, and were infected outside of a clinical setting (community infection) had higher percentages of asymptomatic infections<sup>32</sup>.

The most common radiological CT features in patients affected by COVID-19 included ground glass opacities and consolidation involving the bilateral lungs in a peripheral distribution<sup>33</sup>. Lymphopenia was also reported as commonly observed, even more severe lymphopenia being associated with a higher mortality<sup>34</sup>. Elevated acute phase reactants including a variety of cytokines, such as TNF $\alpha$ , IL6, and IL10<sup>35</sup>.

The most prevalent complications were found to be acute respiratory distress syndrome (ARDS) with 33.15%, arrhythmia with 16.64%, acute cardiac injury with 15.68%, heart failure with 11.50%, and acute kidney injury with 9.87%. COVID-19 was associated with a 2-3-fold higher risk of myocarditis compared to patients with respiratory illness without COVID-19<sup>36,37</sup>.

### *1.1.3. BRAIN INVOLVEMENT*

SARS-CoV-2 virus infects multiple organs including the brain. Several clinical studies revealed that patients with COVID-19 infection experience an array of neurological signs ranging in severity from headaches to life-threatening strokes. Although the exact mechanism by which the SARS-CoV-2 virus directly impacts the brain is not fully understood, several theories have been suggested including direct and indirect pathways induced by the virus.

In addition to pneumonia, the virus may induce an uncontrolled cytokine storm (mostly involving IL6, IL1 $\beta$ , TNF), causing a wide range of symptoms, including encephalopathy<sup>38,39</sup>.

Mild symptoms, such as dizziness, lethargy, and psychomotor retardation may be part of the “sickness behaviour”, a nonspecific cytokine-induced syndrome present in several

infectious-inflammatory states due to the activation of innate immunity<sup>40,41</sup>. On the other hand, severe manifestations including confusion, agitation, delirium and seizures may be caused by specific underlying encephalitis. When focusing on patients with dementia, delirium was found to frequently develop during the clinical course of COVID-19, but in some cases, it represented the initial manifestation of the disease and heralded a worse prognosis<sup>42,43</sup>. Neurological manifestations could be immune-mediated or caused by direct viral invasion of the CNS. SARS-CoV-2 may enter the CNS through: (A) the trans-synaptic route, via the cranial nerves en route to the brainstem or via the olfactory bulbs to the basal frontal lobes; or (B) the endothelial-astrocytic route, by crossing the blood brain barrier<sup>38,44</sup>. Previous studies on SARS-CoV-1 pathology reported viral localization in some brain neurons, but the topographical distribution was not described. Nonetheless, there is still no clear evidence of SARS-CoV-2 neurotropism, and the expression of angiotensin converting enzyme-2 (ACE-2) and transmembrane protease serine 2 (TMPRSS2), the main factors allowing the virus to enter cells, is generally low in the human brain<sup>45</sup>. Although viral RNA may be detected in about 50% of cases, immunohistochemical staining has revealed the presence of scant viral proteins limited to isolated neurons and endothelial cells in the medulla oblongata of the CNS. Additionally, no correlation has been found between the severity of neuropathological changes and the presence of viral protein or RNA in the brain. However, it should be considered that the presence of the virus could be influenced by time intervals between initial infection, death, autopsy and subsequent brain processing<sup>46,47</sup>.

Available autopsy data from brains of COVID-19 patients show unspecific findings of brain congestion, oedema, neuronal damage, and inflammatory infiltrates including acute disseminated encephalomyelitis (ADEM)-like features and different patterns of immune-induced meningoencephalitis with meningeal, perivascular, or parenchymal lympho-monocytic infiltrates. Such findings appear attributable more to hypoxic and immune-mediated

phenomena rather than to virus-induced lesions; they do not clearly establish the presence of SARS-CoV-2 in the brain and its role in neuronal damage remains unclear<sup>46,48,49</sup>.

Microglial activation with microglial nodules is often detected. In this regard, it should be considered that the elderly population is the most affected by the severe form of COVID-19, and many patients had pre-existing neurocognitive disorders; thus, brain inflammation changes and consequent neurological manifestations may be greatly influenced by the presence of microglial “priming” due to neurodegeneration. Vascular injuries of either the ischemic or hemorrhagic type are also reported, including macroscopic and microscopic lesions caused by clotting alterations and/or endotheilitis<sup>46,47,50,51,52,53,54,55</sup>.

It has been suggested that astrocytes could be susceptible to SARS-CoV-2 infection through a noncanonical mechanism that involves spike–NRP1 interaction and respond to the infection by remodeling energy metabolism, which in turn, alters the levels of metabolites used to fuel neurons and support neurotransmitter synthesis<sup>56</sup>.

#### *1.1.4. LUNG INVOLVEMENT*

Damage to the lungs is typically marked by diffuse alveolar damage (DAD) of variable degrees and stages (acute–proliferative–fibrotic), with edema and hyaline membrane formation, cytopathic features, and hyperplasia of type-2 pneumocytes, and the presence of SARS-CoV-2 antigens, accompanied by macrophage and lymphocyte infiltration, organizing pneumonia, and frequent superimposed bacterial infection. Moreover, vascular damage is often described with the formation of microthrombi and thrombi, hemorrhagic infarctions, and pulmonary thromboembolism<sup>7,58,59,60,61,62,3,64,65,66,67</sup>. DAD is a key pathophysiological mechanism of lung damage in SARS-CoV-2 infection that is present in 88% of cases; however, it is not pathognomonic for COVID-19. Indeed, DAD with prominent hyaline membrane formation is also very frequent in SARS-CoV (98%) and influenza A/H1N1 (90% in the 2009 pandemic). On the other hand, micro-thrombotic disease has been reported with a similarly high

prevalence among COVID-19 (57%) and SARS (58%) cases, while it is lower for H1N1 (24%) flu cases<sup>68</sup>.

#### *1.1.5. KIDNEY INVOLVEMENT*

The most common renal manifestation in COVID-19 patients is acute kidney injury, proteinuria (>60% of the cases), and haematuria. Acute kidney injury is probably linked to multiple factors including: direct cytopathic damage of kidney tubular and endothelial cells by the virus, as it has greater affinity for the ACE2 receptor; indirect damage by virus-induced cytokine release, indirect damage by excessive activation of T lymphocytes, renal hypoperfusion due to hypovolemia, abnormal coagulation and hyperventilation-relevant rhabdomyolysis<sup>69,70</sup>.

Regarding glomerular pathology, collapsing glomerulopathy emerged as a distinct lesion in these patients. A small subset of cases (4.3%) had thrombotic microangiopathy<sup>71</sup>. The demonstration of viral particles in renal tissue remains debatable and requires further study<sup>72</sup>.

At the kidney level, the main histological findings are acute tubular injury, inflammatory infiltrates, and microvascular occlusion of glomerular and peritubular capillaries, frequently accompanied by arteriosclerosis and glomerular degeneration (pre-existing chronic renal disease)<sup>25,65,66,69,73</sup>.

#### *1.1.6. LIVER INVOLVEMENT*

Severe COVID-19 cases were found to be more associated with liver injury<sup>74</sup>. A potential cause of the hepatic injury may be the systemic effects of COVID-19. COVID-19 sepsis could lead to hypoxic damage and liver ischemia. It elevates liver biochemistries, demonstrating why total serum bilirubin, AST, and ALT levels are higher in severe COVID-19 patients than non-severe patients<sup>75</sup>.

Lobular necroinflammation was described in several cases. Infrequent hepatocyte apoptosis was observed. In addition, mild but not moderate necroinflammatory activity was observed in few cases<sup>76</sup>. Necroinflammatory foci consist of one to several dead and dying hepatocytes with few accompanying lymphocytes and histiocytes. Plasma cells have been rarely encountered. Histological findings strengthen the hypothesis that the derangement of the coagulation process and impairment of blood circulation inside blood vessels or endothelial damage could be the mechanism in the pathogenesis of COVID-19 damage<sup>77,78</sup>.

Although the liver is one of the most important immunological organs in the body, the pathological findings are non-specific and the impairment of liver function does not appear clinically relevant in SARS-CoV-2 infection<sup>79,80,81</sup>.

### *1.1.1. POST-ACUTE COVID-19 SYNDROME*

The involvement of different organs and extent of the lesions can be considered reliable prognostic factors for adverse outcomes in COVID-19 patients and for the development of post-acute COVID-19 syndrome<sup>82</sup>. Indeed, post-acute COVID-19 syndrome, divided into subacute or ongoing symptomatic COVID-19 (4–12 weeks after disease onset) and chronic or post-COVID syndrome (beyond 12 weeks), may affect the lungs, kidneys, heart, and brain with variable severity. Pulmonary outcomes range from a chronic cough to respiratory insufficiency due to fibrosis, renal dysfunction may persist and lead to chronic kidney disease<sup>83</sup>, heart complications include arrhythmias and heart failure<sup>84</sup>, and the so-called “brain fog” affects cognitive functions after the acute phase of the disease<sup>85</sup>.

## 1.2. Covid 19 and autopsies

Autopsy, particularly in emerging and reemerging infectious diseases should be considered mandatory to define the cause and the mechanism of death, thus providing useful clinical and epidemiologic information to improve prevention and provide new therapeutic tools. Autopsy is essential in order to determine the cause of death in decedents who test positive for SARS-CoV-2 and to discriminate between those who died with COVID-19 and who died from COVID-19.

Post-mortem examinations provide valuable information about SARS-CoV-2 pathology and physiology, bringing about useful clinical and epidemiological managements that are anticipated to be effective in guiding therapy and orienting patient care<sup>86</sup>. Equally important, post-mortem samples may solve unanswered questions, for instance the effects of the infection on the lungs and the involvement of other organs<sup>87,88,89</sup>.

The COVID-19 pandemic has caused crucial adjustments in many fields of medicine, specifically in the medico-legal field. Forensic practices related to performing autopsies have been largely affected by the COVID-19 pandemic due to the highly contagious nature of the virus. SARS-CoV-2 is categorized as a hazard group 3 (HG3) coronavirus. This pathogen requires four areas of attention: i) risk assessment, ii) pathological determinations, iii) universal standard preventative measures, and iv) standard operating procedures for handling specific HG3 organisms. If universal preventative measures are effectively used, they mitigate against inaccurate or incomplete data used in risk assessment.

Some authors<sup>90</sup> observed prolonged survival (up to 7 days at room temperature) of SARS-CoV-2 on various surface types in contrast to previous studies with survival times of 3–4 days at room temperature<sup>91</sup>. Despite this, based on the current state of science regarding SARS-CoV-2 transmission via contaminated surfaces and its persistence on environmental surfaces, there is a relatively low risk of fomite transmission<sup>92</sup>.

A proper decontamination after each autopsy of autopsy tables and instruments used in the morgue could guarantee to destroy infectious COVID-19 particles.

### *1.2.1. GENERAL OVERVIEW: THE ITALIAN MEDICAL EXAMINER SYSTEM*

Dissimilar to the U.S. system, in Italy there is no official death investigation agency such as a coroner or medical examiner system that investigates and certifies causes of death. The first Italian legislation about death investigation was issued in 1910, with the “Circolare Fani”<sup>93</sup>. This Ministerial Circular describes in detail the minimum standards for a forensic autopsy. Before that, there were no standardized procedures or rules for forensic autopsies in place. The Circular was written thanks to the work of Prof. Lombroso who, in 1898, inaugurated the first national meeting of Legal Medicine concerning cadaveric examination. The law mandated that two qualified doctors are needed for each autopsy and this practice is still implemented in current criminal casework. No further laws governing the matter were provided after the “Circolare Fani”. Since 2011, a new death certificate, which conforms to European rules dealing with statistical recording (Rule EU 1338/08, 16.12.2008) and was designed by the Italian Institute of Statistics (ISTAT) based on previous Italian rules of law, (Royal Law 1265/34 and Law 285/90) has been in use. Prior to 2011, each Italian death certificate consisted of two categories (natural deaths and violent deaths). Currently, for all natural deaths, disease, injury, and intoxication conditions related to the immediate, intermediate and underlying causes of deaths are synopsisized. Non-natural deaths (fall, hanging, gunshot, and intoxication) are documented to clarify the manner of death.

In Italy, forensic autopsies are performed under one of two different statutes: 1) judicial autopsies (ordered for forensic purposes) and 2) nonjudicial autopsies (ordered for sanitary reasons). These kinds of autopsies may also serve to answer epidemiological questions, as may be found in cases of infectious diseases, environmental problems, etc<sup>94</sup>. Nonjudicial autopsies which are also known as “riscontro diagnostico” which is Italian for “diagnostic validation,”

are regulated by the National Health Service and are requested when the cause of death is unknown or when confirmatory diagnostic investigations are needed. In the U.S., the manner of death is classified as accident, homicide, natural, suicide, or undetermined. In contrast to U.S. death certificates, Italian death certificates do not offer an undetermined manner of death. Judicial autopsies are requested by the Prosecutor or by the Court, if it appears that one's death is related to a crime. This is to enable evidence to be collected. The decision whether or not a judicial autopsy has to be performed is left to the discretion of the Prosecutor, based on preliminary information collected by the police and/or by a medical doctor. Indeed, in every case of unexpected, sudden, unexplained or, above all, violent death, as well as in potential medical malpractice cases, the physician who is asked to fill the death certificates must inform the Judicial Authority<sup>95</sup>. Autopsies, in most cases, are carried out by medical doctors specialized in Legal Medicine employed at University or Public Hospitals, or by other qualified physicians. The Prosecutor usually refers to a Legal Medicine Department of a University or Hospital. According to Italian law, any qualified, registered doctors may be called upon to perform a forensic autopsy, even without any proven specialized training or technical experience in the field<sup>94</sup>.

Despite the European recommendations, and unlike in the United States, in Italy forensic autopsies are not mandatory, even when the cause and/or manner of death are unclear, or when the death may be connected to a crime. Law enforcement officers sometimes decide if an external examination is enough for the death investigation. Due to costs, a problematic declining autopsy rate is occurring in Italy, as well as in other countries<sup>96</sup>. Despite rising costs, autopsy remains the only way to determine with certainty the cause, manner, and time of death. Another problem is that, often, too much time lapses before a judicial autopsy is done, due to the time-consuming obligation to serve notice on every party involved.

### *1.2.2. THE IMPACT OF THE COVID-19 EMERGENCY ON MEDICOLEGAL PRACTICES*

The outbreak of COVID-19 created a global health crisis that has had a deep impact on medicolegal practices in the U.S. and Italy including autopsy recommendations and forensic pathology activity<sup>97</sup>. On January 30, 2020, the WHO declared the outbreak a public health emergency of international concern, warning that “all countries should be prepared for containment”. Due to the large and unexpected number of COVID-19 cases, there is a critical need for swabs for COVID-19 testing and personal protective equipment (PPE) such as gloves, goggles, and masks. During the COVID-19 pandemic, due to the high number of deaths, governments have had limited choices in handling the large volume of bodies. In countries such as the U. S. and Italy, temporary mortuaries big enough to accommodate thousands of bodies have been assembled. Autopsies have been generally discouraged due to the risk of further spreading the disease through the handling and dissection of bodies<sup>99</sup>. To the best of our knowledge, to date, there has been no scientific confirmation of disease transmission from a body to a medical examiner after an autopsy of a COVID-19 case, even if, in April, a published article was misinterpreted by the media<sup>100,101</sup>. As the coronavirus pandemic has unfolded, forensic pathologists have played (and are still playing) an important role because they are called on to investigate and determine the causes of deaths that are unexpected or unnatural, including deaths that occur at home.

According to CDC recommendation<sup>103</sup>, specific contact and airborne precautions should be followed during autopsy for someone who has known or suspected COVID-19 infection. Many of the procedures are consistent with existing guidelines for safe work practices in the autopsy setting. In particular, in cases of SARS-CoV-2 positivity, autopsies must be performed in rooms especially equipped against airborne infections, with negative pressure, and 6-12 air changes per hour.

Italy was the first European country to have a serious outbreak of COVID-19. A circular issued by the Italian Ministry of Health on March 9, 2020 provided an update and replacement of the previous ones and outlined the definition of a suspected, probable, and confirmed case of COVID-19<sup>104</sup>. Deaths in hospitals were generally assessed as natural, though some EU member states have issued their own statements regarding COVID-19. In Italy, death in the context of COVID-19 should be indicated on the death certificate<sup>105</sup>. It is necessary to indicate if the infection is only suspected or if there is a confirmed antemortem diagnosis of coronavirus. It is also recommended that it is indicated on the death certificate if the virus is directly or indirectly connected to the death, or if the death happened from other causes (for example, from a trauma) in a patient with a confirmed positive COVID-19 swab.

In accordance with the directions issued by the Ministry of Health in its circular published in February 2020<sup>105</sup>, at the beginning all certifications recording COVID-19 as the cause of death should be accompanied by an opinion of the Istituto Superiore di Sanità (ISS). A working group has therefore been created to study the cause of death of patients who tested positive for SARS-CoV-2<sup>107</sup>. In most cases, a postmortem examination was not required unless other circumstances make it necessary. Every single case was evaluated based on medical records and the ISTAT death files, recording the patients' causes of death. Data are collected on a web platform (<http://covid-19.iss.it>), which is also used for the national epidemiological and virological surveillance of COVID-19 cases in Italy (coordinated by the ISS and established by the Ministry of Health<sup>108</sup>).

On April 1, 2020, the Italian Ministry of Health<sup>109</sup> published an official document on autopsies during the SARS-CoV-2 epidemic. In conformity with most of the International recommendations, this circular stated that: i) for the entire period of the emergency phase, autopsies or postmortem diagnostic studies should be avoided in cases of COVID-19; ii) the Judicial Authority will evaluate the possibility of limiting the assessment to the external

inspection of the body, in all cases where an autopsy is not strictly necessary for forensic reasons; iii) the Public Health Departments of each Region will give the criteria to limit the execution of autopsy in case it is necessary to find out the cause of death. It is not allowed to perform autopsies only for scientific purposes; and iv) autopsies can only be carried out in rooms with adequate safety conditions.

Also the Italian Group of Forensic Pathologist has developed specific recommendations for performing autopsies<sup>110</sup>. In Italy, there are very few autopsy rooms equipped with the recommended safety standards and it is not possible to perform COVID-19 autopsies in the vast majority of Legal Medicine Departments.

As a matter of fact, in less than two months, medicolegal autopsies have drastically decreased. For example, in two of the most important Institutes of Legal Medicine in Lombardy, in March and in April, the decrease in the number of autopsies being undertaken was approximately 70%<sup>111</sup> compared to the same period in previous years. As the contagion progressed in Italy, stricter rules for the management of the deceased were established. Bodies were not stripped and coated. The transfer of open caskets was prohibited, and coffins were sealed immediately. Funeral ceremonies have also been banned, in order to avoid mass gatherings.

Despite these difficulties, North Italy has conducted one of the first and largest studies regarding the histological analysis of lung tissues of 38 cases who died from COVID-19. The main relevant finding regards the presence of thrombi in small arterial vessels. This important observation fits into the clinical context of coagulopathy which predominates in these patients and which has become one of the main targets of therapy<sup>87</sup>.

## 2. OBJECTIVES

The objective of this study is to comprehensively describe the pathological alterations present in a series of clinically well-documented COVID-19 cases. COVID-19 induces multi-organ damage, the pathological aspects of which are essential for understanding the pathophysiology of the acute disease, as well as its long-term manifestations.

We systematically reviewed published case reports and case series in order to increase our understanding of COVID-19 pathophysiology.

We focused on different aspects of the disease, with the following aims:

- Main objective:
  - to describe how the different organs (in particular brain, lungs, heart and kidneys) are involved and how SARS-CoV-2 spreads and persists throughout the organism.
  - to compare the inflammatory infiltrates of the lungs, the organ massively affected by the viral invasion, with those of the kidneys, heart, and brain, which are non-primary targets for the virus.
  - to emphasize the pathological features specific for SARS-CoV-2 infection through a comparison between COVID-19 and non-COVID lungs,
  - to investigate the role of microthrombosis.
- Secondary objectives:
  - to investigate the presence of SARS-CoV-2 in the brain of elderly patients died of COVID-19 and the possible effect of SARS-CoV-2 infection on transcriptomic profile in frontal cortex comparing COVID-19 patients and matched controls by RNA-seq analysis.

- to analyse the neuropathological alterations, comparing the brains of COVID-19 and matched non-COVID cases, both with and without Alzheimer's disease (AD), to verify where and how SARS-CoV-2 affects the inflammatory response in the brains of older people, and determine whether the inflammatory changes are mainly due to COVID-19 or are also related to the presence of AD neuropathology.

### **3. MATERIALS AND METHODS**

#### **3.1. Study design, setting and participants.**

We performed an observational, case-control study involving all the subjects deceased with COVID-19 undergoing to a forensic or sanitary autopsy performed by the forensic pathologists of the Department of Public Health, Experimental and Forensic Medicine of the University of Pavia (Section of Legal Medicine and Forensic Science) during the entire period of the project.

The study was carried out through the following phases:

- Selection of cases,
- Autopsies,
- Collection of formalin fixed samples in addition to other organs and tissues,
- Hematoxylin-Eosin (H&E) and Immunohistochemistry (IHC) staining of organs, including a neuropathological investigation,
- Optical microscope (Nikon NI-U) reading of histological preparations. The evaluation of the expression of markers was done according to a staging system adapted for this particular purpose.
- Presence of viral RNA and Transcriptomic evaluations.

#### **3.2. Case selection**

Our project involved all the subjects deceased with COVID-19 who underwent a forensic or clinical autopsy at the Department of Public Health, Experimental and Forensic Medicine of the University of Pavia (Section of Legal Medicine and Forensic Science) during the entire period April 2020-August 2021.

### 3.2.1. INCLUSION AND EXCLUSION CRITERIA

The inclusion criteria were:

- SARS-COV-2 infection must be ascertained through a nasopharyngeal swab performed before or shortly after death;
- Continuous refrigeration of the cadaver at 4°C until the time of the autopsy with adequate preservation of the sample material for histological analysis.

The exclusion criteria consisted of a post-mortem interval (PMI) longer than 13 days or inadequate preservation of the cadaver.

### 3.2.2. CONTROL CASES

Matched controls were studied:

- For lung comparison, 5 cases with non-COVID pneumonia were selected from the Unit of Legal Medicine, it was decided to include people who died due to pneumonia (viral or bacterial) in order to compare inflammatory differences in the lungs.
- For neuropathological comparison, 5 non-COVID brains were selected from the Abbiategrasso Brain Bank (ABB) at the Golgi-Cenci Foundation (Abbiategrasso, Milan).
- For transcriptomic comparison, 8 non-COVID-19 cases provided by ABB were selected.

## 3.3. Autopsy protocol

The Departmental Unit of Legal Medicine and Forensic Sciences of the University of Pavia and the ABB (Golgi-Cenci Foundation, Abbiategrasso) provided Autoptic human samples. During the COVID-19 pandemic, autopsies have been generally discouraged by

government regulations. Despite these restrictions, the present COVID-19 cases were subjected to forensic autopsies, ordered by the State Prosecutor in the hypothesis of medical mistakes or failure to comply with hygiene regulations. Autoptic examinations were held in different facility scattered among Italy, including the forensic medicine of Pavia, Piacenza and Torino. They were performed in a room suitable for the examination of cadavers of people who died from infectious diseases (biosafety level 3 -BSL-3- autopsy laboratory), following safety procedures required by the Italian Ministry of Health and the recommendations of the Italian Group of Forensic Pathologist<sup>110</sup>. Standard autopsy protection, together with specific personal protection equipment, have been used (double surgical gloves interposed with a layer of cut-proof gloves, impermeable long-sleeve gown/apron, goggles or face shield, shoe covers, surgical cap, respiratory protection consists of a FP-2 or higher respirator). All procedures that may produce aerosol have been avoided. A minimally invasive protocol was adopted (abdominal organs have been investigated *in situ*).

### **3.4. Samples collection**

The ABB autopsy and sampling protocol<sup>112</sup> was approved by the Ethics Committee of the University of Pavia on October 6th, 2009 (Committee report 3/2009). In accordance with Italian Law, this research was performed on small portions of biological samples routinely taken during autopsies that need to be examined for diagnostic and/or forensic purposes and not only for scientific reason. The various samples (partly preserved in formalin, partly included in paraffin in order to obtain histological sections) are stored for several decades in the Departmental Section of Legal and Forensic Medicine's archive. This study made use of only small portions of these samples, therefore the integrity of the archive itself or the possibility of re-examining, for any need, individual cases was not affected.

In each case, the following samples were collected:

- Whole brain, pituitary gland, dura mater, whole heart, lungs (one sample for each lobe), liver, spleen, pancreas, kidneys, adrenal glands: formalin fixed.
- Hair, blood, urine, liquor, brain (frontal lobe), heart (apex), right lung: stored at -20°C.

In addition, after the brain removal, one slice of anterior frontal lobe was fresh cut into about 10 mm thickness and frozen at -80 degrees C.

All the material relating to individual cases was recorded and catalogued with a specific numerical code and never with the details of the deceased person.

### **3.5. Collection of clinical information**

A retrospective review of medical charts was performed by two forensic medical doctors, a geriatrician, and a neurologist in order to ascertain the clinical history of the selected cases.

The patients were clinically defined for the presence or absence of comorbidities, dementia, delirium, and sepsis. The DSM-5 criteria were used to define the mental state and identify any pre-existing cognitive dysfunction, namely major neurocognitive disorder (major-NCD) to indicate dementia and mild-NCD to designate mild cognitive impairment (MCI). Sepsis was considered a severe bacterial superinfection with at least one positive blood culture.

Information about case were taken in accordance with the Italian law regarding processing of personal data. The reference law is the authorization n9/2016 of the guarantor of privacy, then replaced by Regulation (eu) 2016/679 of the European Parliament and of the Council.

### **3.6. Neuropathological investigation**

Selected cases underwent a complete neuropathological evaluation, carried out by neuropathologists of the Department of Neurology and Neuropathology, Golgi-Cenci Foundation, Abbiategrasso, Milan. Detailed protocols have been described by Poloni et al<sup>113</sup>.

After proper fixation, macrosections were cut from specific areas, obtaining the following samples:

- 2 from the frontal lobe (1 from the anterior frontal area, including the rhinencephalon; and 1 from the posterior area, containing the gyrus cinguli and basal ganglia),
- 1 each from the remaining lobes (parietal, temporal and occipital),
- 1 sample each from the olfactory bulbs, hippocampus and entorhinal cortex, cerebellum, midbrain, pons and medulla oblongata.

### **3.7. Histopathological examinations**

8- $\mu$ m thick paraffin-embedded sections from each organs were collected and stained with Hematoxylin and Eosin (H&E).

Sections include 7 sections of specific brain region (see neuropathological investigations paragraph for details), 1 section per each pulmonary lobe; 5 heart sections from a mid-horizontal slice -anterior and posterior right ventricle, septum, left ventricle, and 1 epicardial coronary-; and 1 section from each kidney, including the cortex and medulla.

H&E staining were performed by technicians of the laboratory of anatomical pathology laboratory of the San Matteo Hospital, Pavia.

The liver, hypophysis, thyroid, spleen, adrenal glands, uterus, or prostate, besides the brain, lungs, heart, and kidneys, were also included in the routine histopathological examination. Upon Hematoxylin–Eosin (H&E) staining, we did not observe any peculiar

features that could be related to COVID-19. Moreover, the subjects of the present study did not show any clinical signs related to a possible liver failure or impairment. Therefore, despite the liver being one of the most important organs of the body, we chose to focus the study on the brain, lungs, heart, and kidneys, for which the clinical picture and the routine H&E staining provided the most interesting results.

At the Department of Neurology and Neuropathology, Golgi-Cenci Foundation & ASP Golgi-Redaelli, selected brain sections were stained with H&E and Luxol Fast Blue (LFB) to evaluate vascular, architectural and structural tissue abnormalities, inflammatory infiltrates, and myelin loss.

### **3.8. Immunohistochemical examinations**

Immunohistochemistry (IHC) was also performed, using the following antibodies:

- SARS-COV-2 coronavirus nucleocapside monoclonal antibody (monoclonal antibody, clone B46F, and Invitrogen Waltham, MA USA; 1:100) to detect the virus in the tissues.
- antiCD68 (polyclonal antibody and Invitrogen; 1:500—brain microglia: monoclonal antibody clone KP1, and Dako Santa Clara, CA 95051 United States; 1:100), antiCD3 (monoclonal antibody, clone SP7, and Invitrogen; 1:200—brain: monoclonal antibody, clone F7.2.38, and Dako; 1:50), antiCD20 (polyclonal antibody and Invitrogen; 1:300—brain: monoclonal antibody, clone L26, and Dako; 1:100) to characterize the leukocytes in the inflammatory infiltrates.
- antiCD42B (monoclonal antibody, clone 42C01, and Invitrogen; 1:100) to detect thrombi.

The use of immunohistochemistry allowed us to highlight the presence of specific target structures and in this case made possible for us to identify Coronavirus antigen in the selected tissues slide when using a specific Covid-19 antibody (Antibodies against the nucleocapsid are produced during the disease and can be used as a marker for the presence of the virus). Other marker were applied to establish the level of inflammation and in which degree or if there is any, the antibody that were chosen for this purpose were against CD3, CD20, CD68.

CD3 is a protein complex that is part of the T cell receptor complex. It is found uniformly in all mature T cells and in virtually no other cell type, making it a useful marker for T cells in tissue sections.

CD20 is found in B lymphocytes, serving as a marker for this cell type. Its presence increases as the cell differentiates, being therefore observed both in immature and mature B cells.

CD42b is a platelet surface membrane glycoprotein to which von Willebrand factor (VWF) binds, initiating signalling events within the platelet that lead to enhanced platelet activation, thrombosis, and haemostasis. Therefore, CD42b is a useful marker for the identification of platelet aggregates and thrombi.

Immunohistochemistry staining on heart, lungs, kidney, liver were prepared in the immunohistochemistry laboratory of the Section of Legal Medicine and Forensic Science (University of Pavia) in collaboration with medico legal residents and students. Immunohistochemistry staining were performed based on a previously described protocol<sup>113</sup>. 5 slides were prepared for each organ, with 15 slides for each case, and with a total of 225 slides.

As already reminded, selected cases underwent a complete neuropathological evaluation at the Department of Neurology and Neuropathology, Golgi-Cenci Foundation & ASP Golgi-Redaelli. To obtain a definite Alzheimer's Disease (AD) diagnosis, selected areas were stained for with AD neurodegenerative markers. 4G8 antibody was used to detect and

grade the extent of  $\beta$ -amyloid deposits (4G8, monoclonal antibody, BioLegend San Diego, CA, USA; 1:1000) and phospho-tau was used to define the stage of phospho-TAU aggregates (AT8, monoclonal antibody, clone MN1020, Thermo Fisher Scientific Waltham, MA, USA; 1:200). Successively, the severity of AD neuropathology was defined according to Montine's scheme (low-intermediate-high AD pathology).

Staining with anti-GFAP (an astrocytes antigen) was also performed on brain sections (polyclonal antibody, and Dako Z0334; 1:1000).

3.8.1. SUMMARY OF THE PROCEDURES IMPLEMENTED IN THE IMMUNOHISTOCHEMISTRY LABORATORY

<b>ANTI-CD3 ANTIBODY</b>	<b>ANTI-CD20 ANTIBODY</b>
<b>Deparaffinization:</b>	<b>Deparaffinization:</b>
<ol style="list-style-type: none"> <li>1) Xylene x2 (10 minutes)</li> <li>2) From alcohol 100% to distilled water (5 minutes)</li> <li>3) Hydrogen peroxide (12 minutes)</li> <li>4) PBS wash x2 (5 minutes)</li> </ol>	<ol style="list-style-type: none"> <li>1) Xylene x2 (10 minutes)</li> <li>2) From alcohol 100% to distilled water (5 minutes)</li> <li>3) Hydrogen peroxide (12 minutes)</li> <li>4) PBS wash x2 (5 minutes)</li> </ol>
<b>Antigen retrieval:</b>	<b>Antigen retrieval:</b>
<ol style="list-style-type: none"> <li>1) Citrate 1:100</li> <li>2) PBS wash x3 (5 minutes)</li> </ol>	<ol style="list-style-type: none"> <li>1) Citrate 1:100</li> <li>2) PBS wash x3 (5 minutes)</li> </ol>
<b>Addition of antibodies:</b>	<b>Addition of antibodies:</b>
<ol style="list-style-type: none"> <li>1) Goat serum 1:75 (20 minutes)</li> <li>2) Rabbit primary antibody 1:200 (overnight 4 °C incubation)</li> <li>3) PBS wash x3 (5 minutes)</li> <li>4) Rabbit secondary antibody 1:200 (30 minutes)</li> <li>5) PBS wash x3 (5 minutes)</li> </ol>	<ol style="list-style-type: none"> <li>1) Goat serum 1:75 (20 minutes)</li> <li>2) Rabbit primary antibody 1:300 (overnight 4 °C incubation)</li> <li>3) PBS wash x3 (5 minutes)</li> <li>4) Rabbit secondary antibody 1:200 (30 minutes)</li> <li>5) PBS wash x3 (5 minutes)</li> </ol>
<b>Detection:</b>	<b>Detection:</b>
<ol style="list-style-type: none"> <li>1) Avidin 1:100 – Biotin 1:100 (1 hour)</li> <li>2) PBS wash x3 (5 minutes)</li> <li>3) Benzidine (DAB) in distilled water (3 minutes)</li> </ol>	<ol style="list-style-type: none"> <li>1) Avidin 1:100 – Biotin 1:100 (1 hour)</li> <li>2) PBS wash x3 (5 minutes)</li> <li>3) Benzidine (DAB) in distilled water (3 minutes)</li> </ol>
<b>Counterstaining:</b>	<b>Counterstaining:</b>
<ol style="list-style-type: none"> <li>1) Hematoxylin</li> <li>2) From distilled water to 100% alcohol (2 minutes)</li> <li>3) Xylene x2 (2 minutes)</li> <li>4) Mounting of slide</li> </ol>	<ol style="list-style-type: none"> <li>1) Hematoxylin</li> <li>2) From distilled water to 100% alcohol (2 minutes)</li> <li>3) Xylene x2 (2 minutes)</li> <li>4) Mounting of slide</li> </ol>

ANTI-CD42b ANTIBODY	ANTI-CD68 ANTIBODY	SARS-COV-2 CORONAVIRUS NUCLEOCAPSID ANTIBODY
<p><b>Deparaffinization:</b></p> <ol style="list-style-type: none"> <li>1) Xylene x2 (10 minutes)</li> <li>2) From alcohol 100% to distilled water (5 minutes)</li> <li>3) Hydrogen peroxide (12 minutes)</li> <li>4) PBS wash x2 (5 minutes)</li> </ol> <p><b>Antigen retrieval:</b></p> <ol style="list-style-type: none"> <li>1) Citrate 1:100</li> <li>2) PBS wash x3 (5 minutes)</li> </ol> <p><b>Addition of antibodies:</b></p> <ol style="list-style-type: none"> <li>1) Horse serum 1:75 (20 minutes)</li> <li>2) Mouse primary antibody 1:100 (overnight 4 °C incubation)</li> <li>3) PBS wash x3 (5 minutes)</li> <li>4) Mouse secondary antibody 1:200 (30 minutes)</li> <li>5) PBS wash x3 (5 minutes)</li> </ol> <p><b>Detection:</b></p> <ol style="list-style-type: none"> <li>1) Avidin 1:100 – Biotin 1:100 (1 hour)</li> <li>2) PBS wash x3 (5 minutes)</li> <li>3) Benzidine (DAB) in distilled water (3 minutes)</li> </ol> <p><b>Counterstaining:</b></p> <ol style="list-style-type: none"> <li>1) Hematoxylin</li> <li>2) From distilled water to 100% alcohol (2 minutes)</li> <li>3) Xylene x2 (2 minutes)</li> <li>4) Mounting of slide</li> </ol>	<p><b>Deparaffinization:</b></p> <ol style="list-style-type: none"> <li>1) Xylene x2 (10 minutes)</li> <li>2) From alcohol 100% to distilled water (5 minutes)</li> <li>3) Hydrogen peroxide (12 minutes)</li> <li>4) PBS wash x2 (5 minutes)</li> </ol> <p><b>Antigen retrieval:</b></p> <ol style="list-style-type: none"> <li>1) Citrate 1:100</li> <li>2) PBS wash x3 (5 minutes)</li> </ol> <p><b>Addition of antibodies:</b></p> <ol style="list-style-type: none"> <li>1) Goat serum 1:75 (20 minutes)</li> <li>2) Rabbit primary antibody 1:500 (overnight 4 °C incubation)</li> <li>3) PBS wash x3 (5 minutes)</li> <li>4) Rabbit secondary antibody 1:200 (30 minutes)</li> <li>5) PBS wash x3 (5 minutes)</li> </ol> <p><b>Detection:</b></p> <ol style="list-style-type: none"> <li>1) Avidin 1:100 – Biotin 1:100 (1 hour)</li> <li>2) PBS wash x3 (5 minutes)</li> <li>3) Benzidine (DAB) in distilled water (3 minutes)</li> </ol> <p><b>Counterstaining:</b></p> <ol style="list-style-type: none"> <li>1) Hematoxylin</li> <li>2) From distilled water to 100% alcohol (2 minutes)</li> <li>3) Xylene x2 (2 minutes)</li> <li>4) Mounting of slide</li> </ol>	<p><b>Deparaffinization:</b></p> <ol style="list-style-type: none"> <li>1) Xylene x2 (10 minutes)</li> <li>2) From alcohol 100% to distilled water (5 minutes)</li> <li>3) Hydrogen peroxide (12 minutes)</li> <li>4) PBS wash x2 (5 minutes)</li> </ol> <p><b>Antigen retrieval:</b></p> <ol style="list-style-type: none"> <li>1) EDTA 1:100</li> <li>2) PBS wash x3 (5 minutes)</li> </ol> <p><b>Addition of antibodies:</b></p> <ol style="list-style-type: none"> <li>1) Horse serum 1:75 (20 minutes)</li> <li>2) Mouse primary antibody 1:100 (overnight 4 °C incubation)</li> <li>3) PBS wash x3 (5 minutes)</li> <li>4) Mouse secondary antibody 1:200 (30 minutes)</li> <li>5) PBS wash x3 (5 minutes)</li> </ol> <p><b>Detection:</b></p> <ol style="list-style-type: none"> <li>1) Avidin 1:100 – Biotin 1:100 (1 hour)</li> <li>2) PBS wash x3 (5 minutes)</li> <li>3) Benzidine (DAB) in distilled water (3 minutes)</li> </ol> <p><b>Counterstaining:</b></p> <ol style="list-style-type: none"> <li>1) Hematoxylin</li> <li>2) From distilled water to 100% alcohol (2 minutes)</li> <li>3) Xylene x2 (2 minutes)</li> <li>4) Mounting of slide</li> </ol>

### 3.8.2. SEMI-QUANTITATIVE ANALYSIS

Semi-quantitative analysis of immunostaining was performed, using sections processed for light microscopy immunocytochemistry. (Nikon NI-U). For each representative slide, 5 areas of 4.7 mm<sup>2</sup> were evaluated (the 4 corners and the center). A low magnification (4x) was used to explore the area and higher magnifications (10-20x) to judge the cell morphology.

To interpret the results of immunohistochemical staining, in this study, a semi-quantitative evaluation system was used.

To quantify the presence of lymphocytes and monocyte–macrophages in the different infiltrates of the various tissues, we effectively applied the method described by Matschke and colleagues based on cell counts<sup>46</sup> (none/4.7mm<sup>2</sup>; rare: 0–9; moderate: 10–49; abundant >49

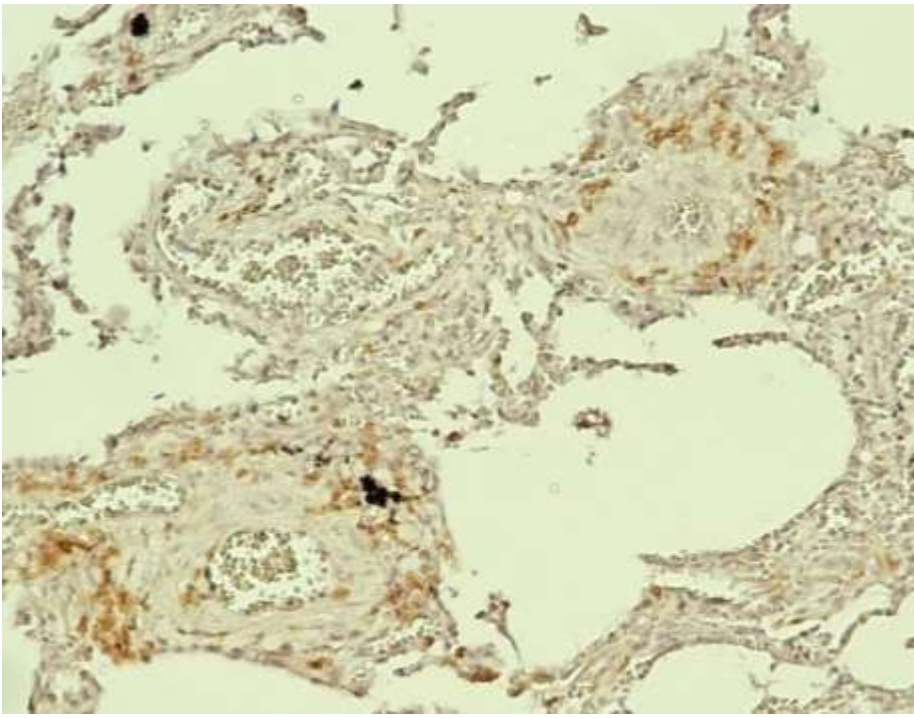
cells). The highest grading observed was then reported. None or rare lymphocytes were considered as a condition of normal immunological surveillance.

To evaluate the activation of brain microglia, a 0–3 scoring method, consolidated in the laboratory of Golgi-Cenci Foundation & ASP Golgi-Redaelli<sup>113</sup>, was applied.

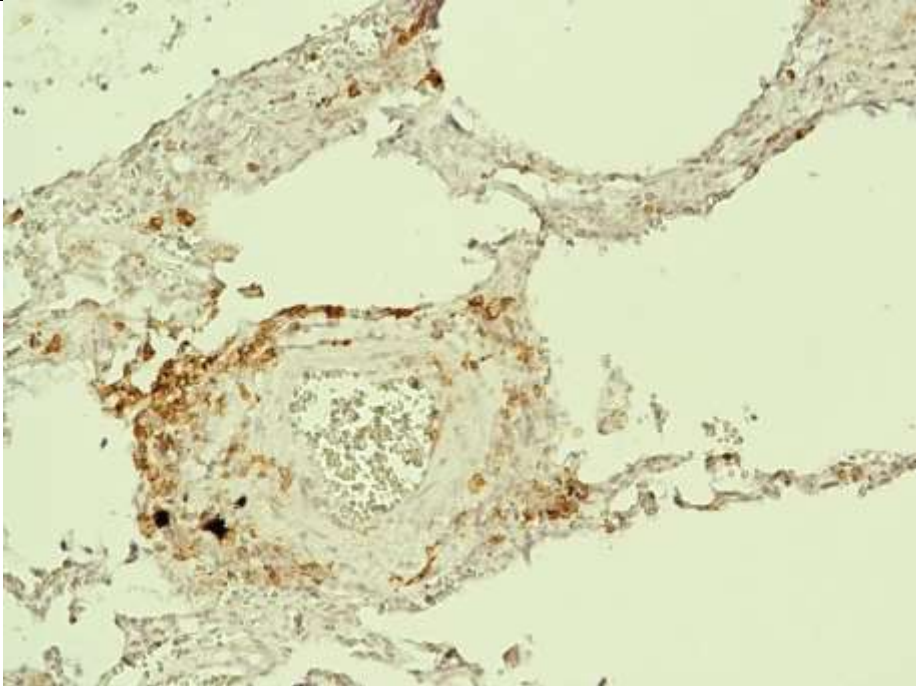
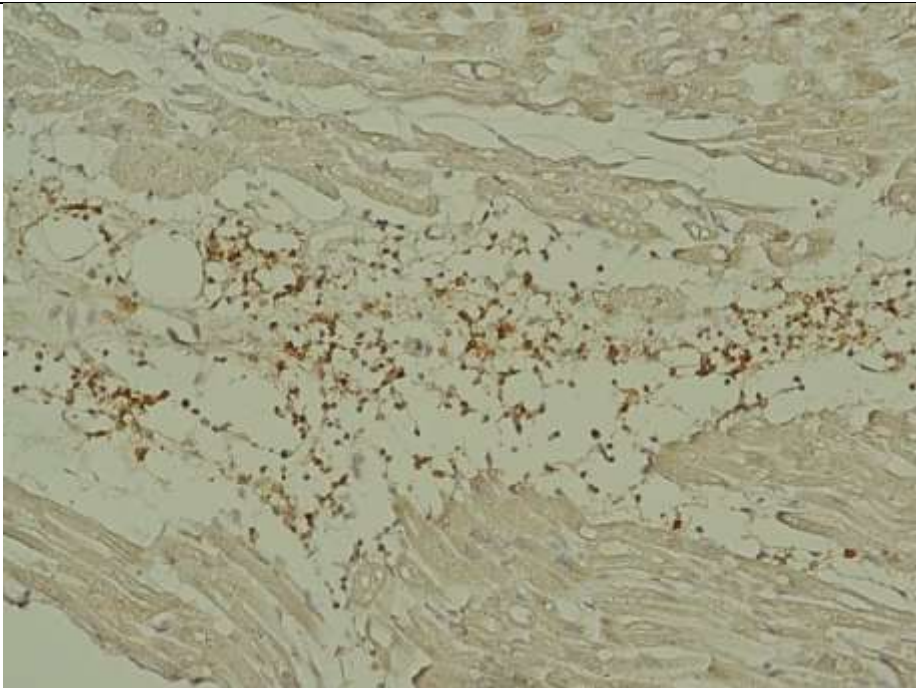
To quantify the microthrombi, the thrombosed capillaries were counted (0/4.7 mm<sup>2</sup> = 0, none; 1/4.7 mm<sup>2</sup> = 1, mild; 2/4.7 mm<sup>2</sup> = 2, moderate; and  $\geq 3/4.7$  mm<sup>2</sup> = 3, severe). Scores of 0–1 (none-mild) were considered not relevant in all tissues and reactions, while scores of 2–3 represented a moderate to severe pathological alteration. Two neurologists with expertise in neuropathology and two pathologists blinded to the clinical history performed the pathological assessment. Whenever discrepancies between the gradings emerged, the area was reassessed together until an agreement was reached.

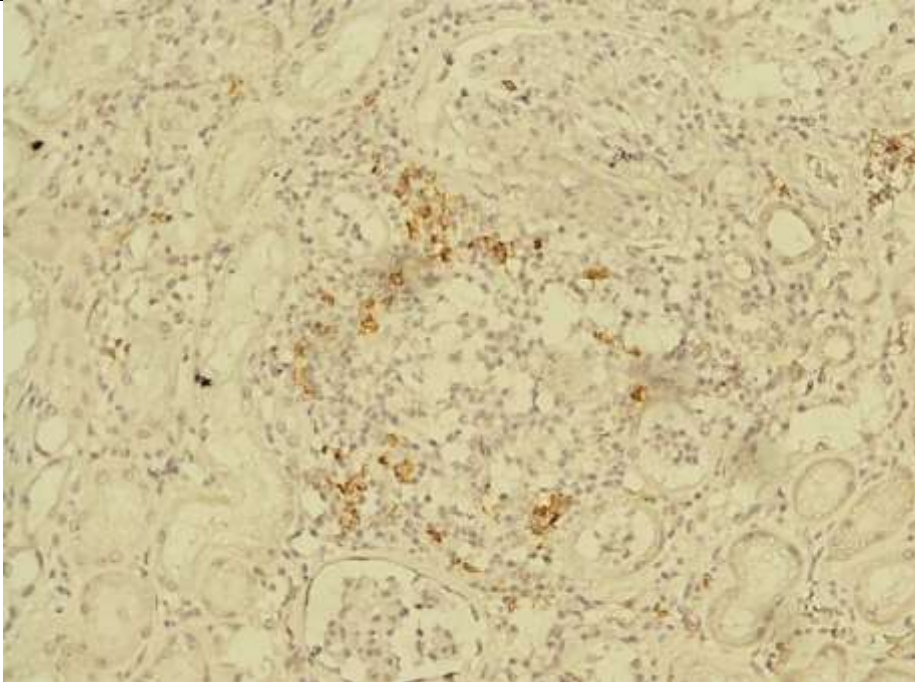
The evaluation scales chosen for each of the antibodies used are described below (table 1, 2, 3, 4, 5). The images used as examples were taken at a magnification of 20x.

**Table 1:** CD3 evaluation

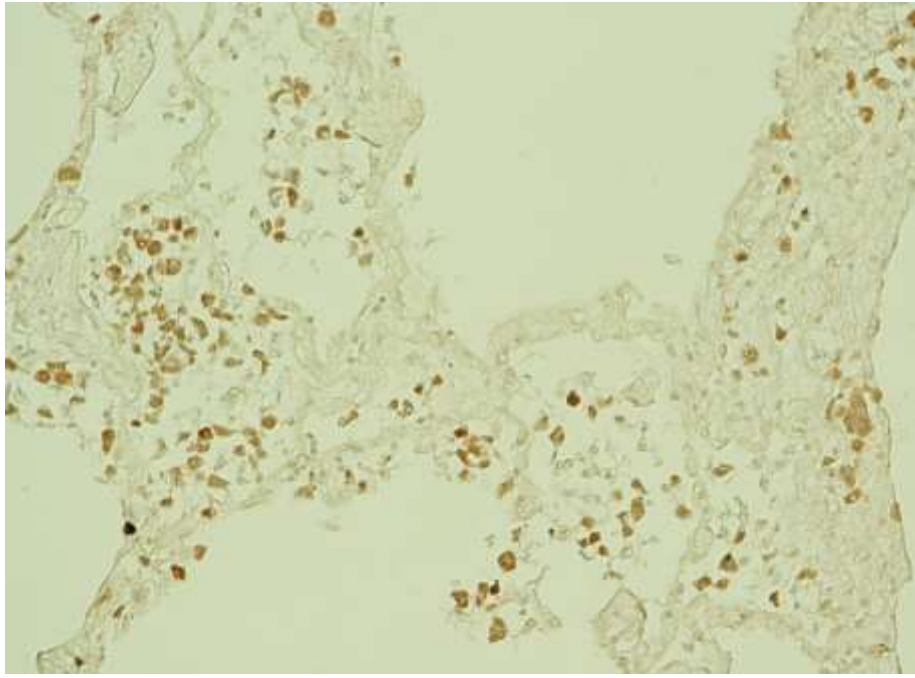
Score	Characteristics	
0	none/4.7mm <sup>2</sup>	
1	Rare: 0–9 cells	
2	Moderate: 10–49 cells	
3	Abundant >49 cells	
		Example of Score 3 with anti-CD3 antibody in lung.

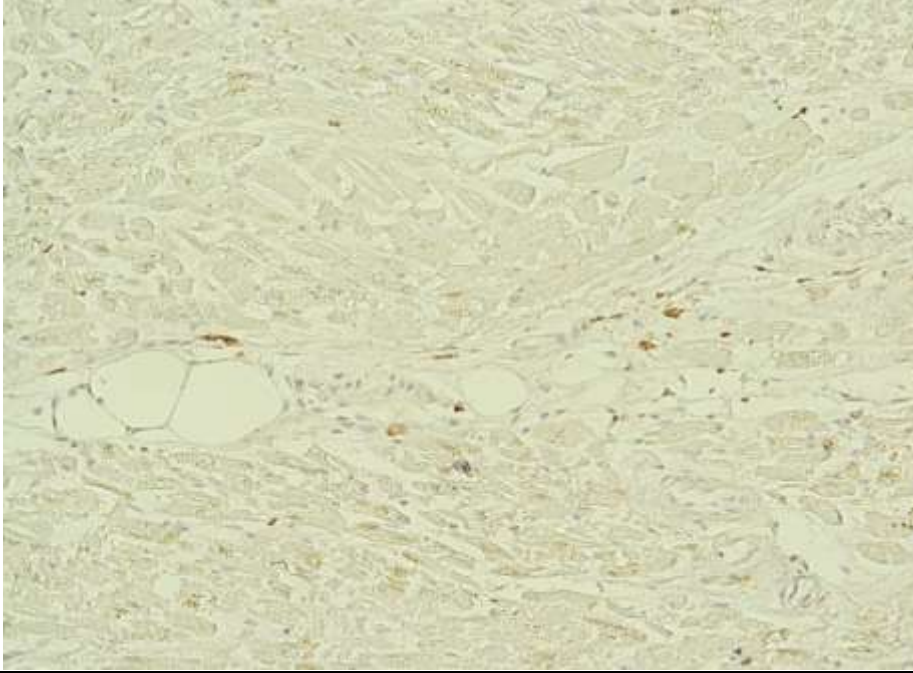
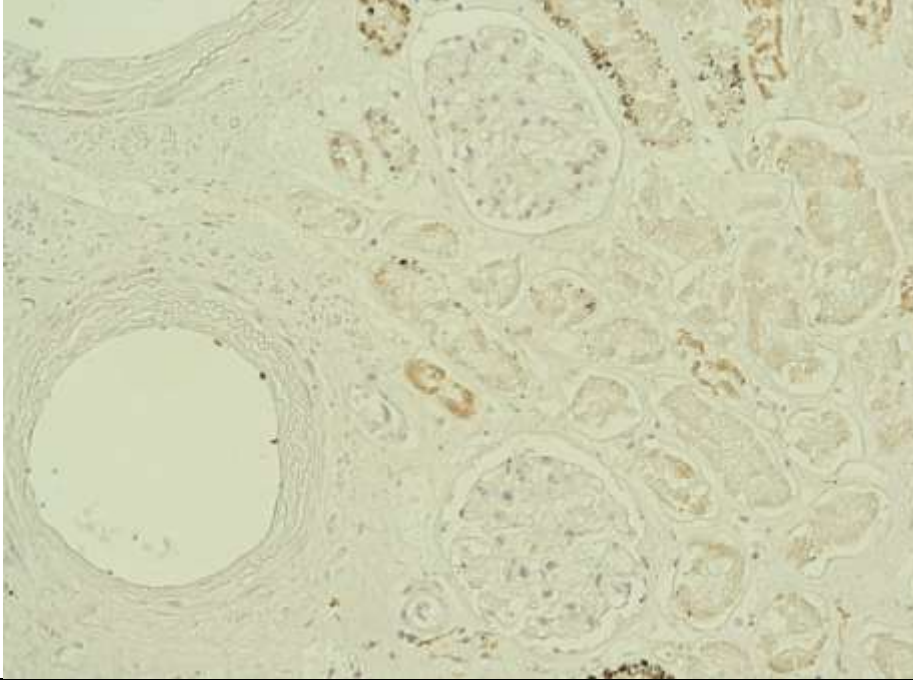
**Table 2:** CD20 evaluation

Score	Characteristics	
0	none/4.7mm <sup>2</sup>	
1	Rare: 0–9 cells	
2	Moderate: 10–49 cells	
3	Abundant >49 cells	
		Example of Score 3 with anti-CD20 antibody in lung.
		
		Example of Score 2 in heart with anti-CD20 antibody.

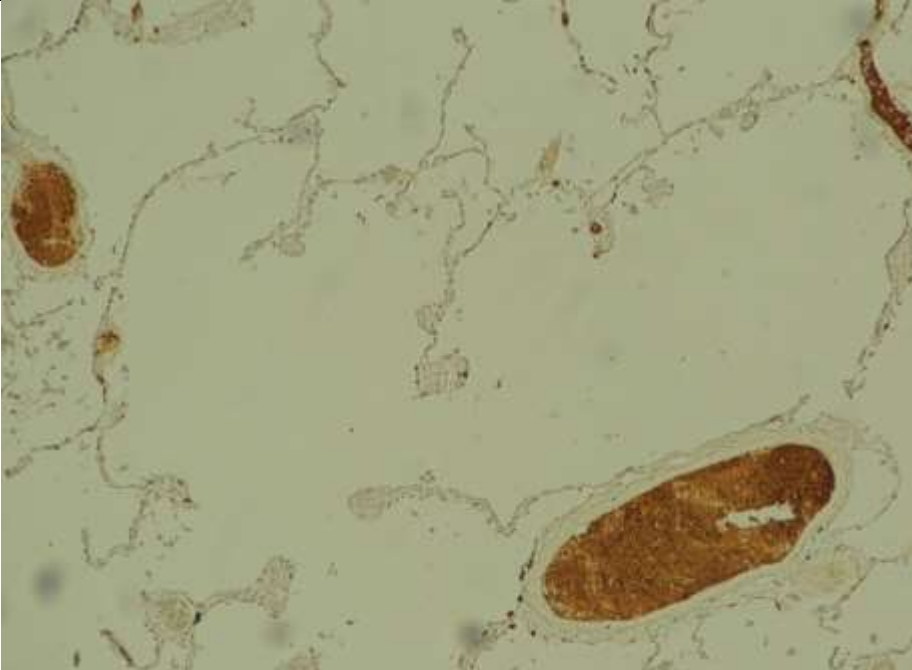
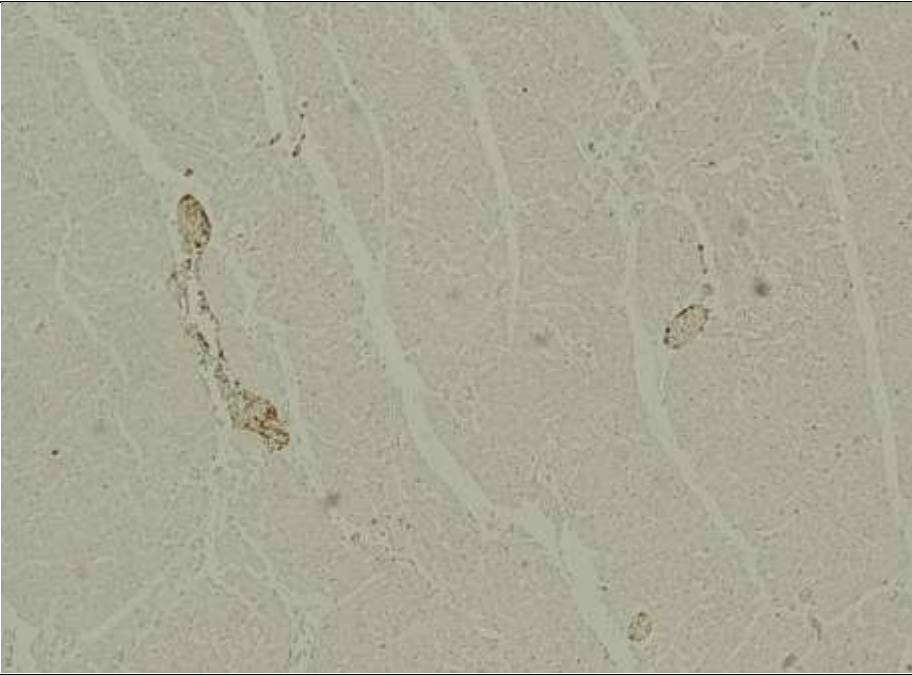
	
	<p>Example of Score 2 in kidney with anti-CD20 antibody.</p>

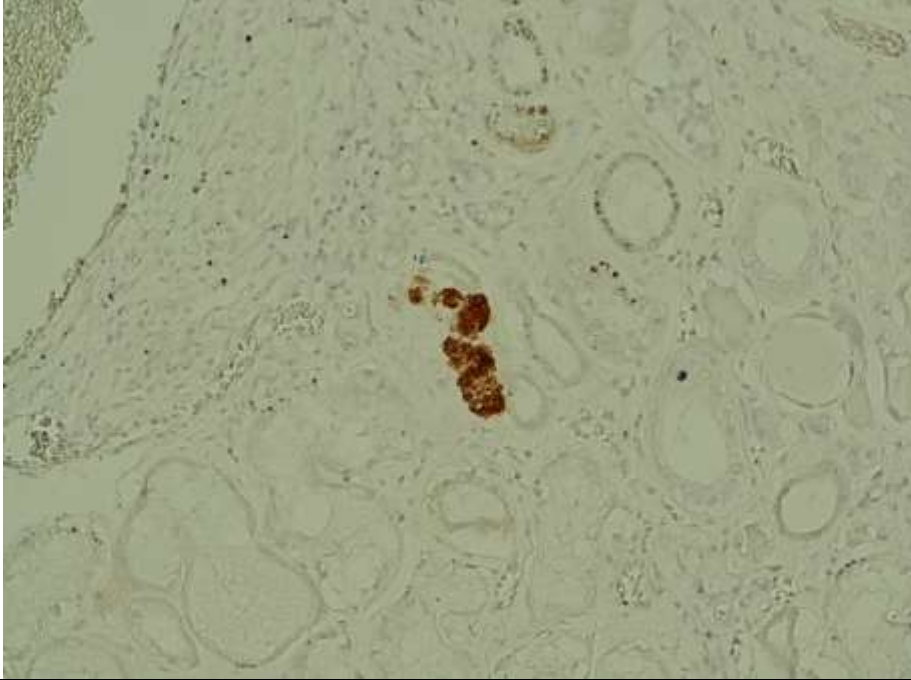
**Table 3:** CD68 evaluation

Score	Characteristics	
0	none/4.7mm <sup>2</sup>	
1	Rare: 0–9 cells	
2	Moderate: 10–49 cells	
3	Abundant >49 cells	
	<p>Example of Score 3 with anti-CD68 antibody in lung.</p>	

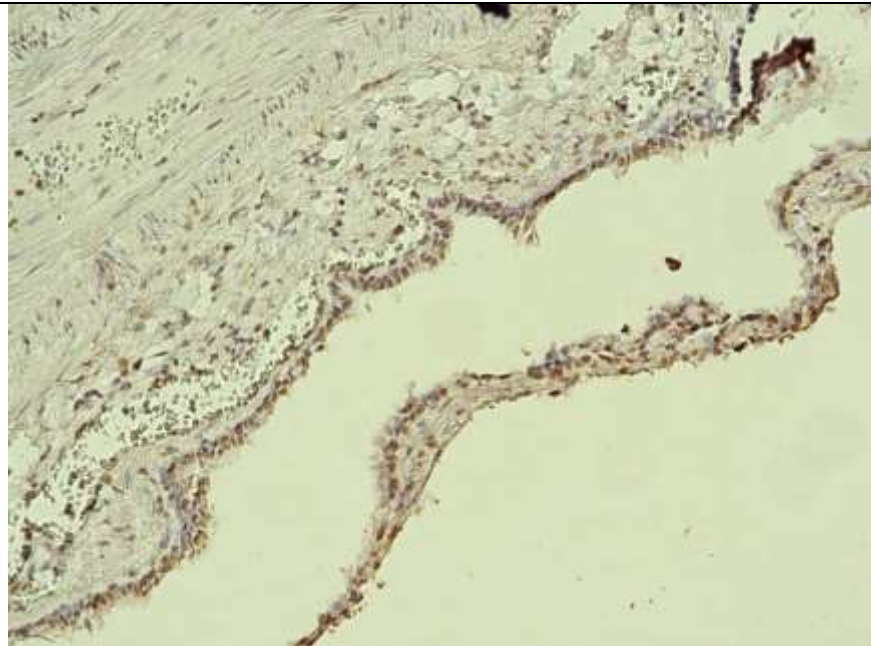
	
<p>Example of Score 2 with anti-CD68 antibody in heart.</p>	
	
<p>Example of Score 1 with anti-CD68 antibody in kidney.</p>	

**Table 4:** CD42b evaluation

Score	Characteristics	
0	0 thrombosed capillaries /4.7 mm <sup>2</sup>	
1	Mild: 1 thrombosed capillary /4.7 mm <sup>2</sup>	
2	Moderate: 2 thrombosed capillaries /4.7 mm <sup>2</sup>	
3	Severe: $\geq 3$ thrombosed capillaries /4.7 mm <sup>2</sup>	
		Example of Score 3 with anti-CD42 antibody in lung.
		
		Example of Score 1 with anti-CD42 antibody in heart.

	
	<p>Example of Score 2 with anti-CD42 antibody in kidney.</p>

**Table 5:** SARS-CoV-2 evaluation

Score		Characteristics	
0	-	Absent staining	
1		Light and focal staining	
2	+	Diffuse staining	
			<p>Example of Score 2 with anti-SARS-CoV-2 nucleocapsid antibody in lung.</p>

		
		<p>Example of Score 2 with anti-SARS-CoV-2 nucleocapsid antibody in heart.</p>
		
		<p>Example of Score 2 with anti-SARS-CoV-2 nucleocapsid antibody in kidney.</p>

### 3.8.3. STATISTICAL EVALUATION

The scores attributed to the reading of the immunohistochemical preparations were statistically evaluated.

For comparison between different organs (brain, lung, heart, kidney) statistical analyses were conducted using R (version 4.2.1; R Core Team; R Foundation, Released 2021,

Vienna, Austria). p-values of  $< 0.05$  were considered significant. Given the ordinal nature of the scores and the low number of cases, a nonparametric statistical test was used. The T and B lymphocyte sum was considered as a further variable. Friedman's test with Durbin–Conover pairwise comparison was used to compare the different tissues within subjects (R package PMCMR). Score differences between the cases and controls for each organ were compared using the Mann–Whitney U test.

Regarding specific neuropathological evaluation, COVID-19 cases (with and without dementia) were compared with the control non-COVID group (also with and without dementia). Moreover, COVID-19 cases were grouped according to the presence or absence of delirium, and sepsis. Regarding delirium, COVID-19 cases were also categorized based on its onset (early, late, and no delirium). Differences in microglial activation (i.e. microglial grading) between groups were compared using Mann-Whitney U test or Kruskal-Wallis, where appropriate. The Mood's Median Test was used to compare microglial activation between COVID-19 cases with and without delirium, and with and without sepsis; this choice was made because the variables, in addition to having a skewed distribution, belong to a very low number of cases. The correlation between microglial activation and AD pathology (Braak and Thal stages) was assessed using Spearman's Rho correlation. p-values  $< 0.05$  were considered significant. All statistical analyses were conducted using SPSS version 26.

### **3.9. Presence of viral RNA and Transcriptomic evaluations**

Fresh frontal sample was frozen for the subsequent quantitative Reverse Transcription-PCR (qRT-PCR) and droplet-digital PCR (ddPCR) analysis for the detection of the viral RNA.

RNA extraction and transcriptomic evaluations were performed at Genomic and Post Genomic Unit, IRCCS Mondino Foundation, Pavia, Italy. Detailed protocols have been described by Gagliardi et al<sup>115</sup>.

In brief, frozen slices from frontal cortex were used for isolation of total RNA by Trizol reagent. Quantification and quality control of RNAs have been done using a Nanodrop ND-100 Spectrophotometer and a 2100 Bioanalyzer; RNAs with a 260:280 ratio of  $\geq 1.5$  and an RNA integrity number of  $\geq 8$  were selected to deep sequencing.

Quantitative polymerase chain reaction (qPCR) and droplet digital PCR analysis (ddPCR) of SARS-CoV-2 were performed in frontal cortex tissues.

The transcriptomic profile of frontal cortex from COVID-19 patients and matched controls by RNA-seq analysis were investigated to characterize the transcriptional signature.

Sequencing libraries of COVID-19 patients and matched controls were prepared.

Gene enrichment analysis was performed on coding genes.

For qPCR validation, PCR oligonucleotide for genes pairs were selected spanning introns to optimize amplification from mRNA templates and avoiding nonspecific amplification products.

## 4. RESULTS

### 4.1. COVID cases overview

A total of 287 autopsy were performed between 17 April 2020 and 30 august 2021. They included 15 autoptic COVID-19 cases

The available circumstantial/anamnestic information, the cause of death, and the anatomopathological data are reported in table 6.

**Table 6:** data about COVID-19 cases (n=15)

<b>Cov 1</b>	
<b>Sex</b>	F
<b>Age</b>	74
<b>Circumstantial/anamnestic data</b>	Hyperhomocysteinemia, restrictive eating disorder, previous postpartum depressive episode, chronic constipation, and neurocognitive decline.
<b>Cause of death</b>	Multiple organ failure, secondary to bilateral pneumonia. Picture suggestive of bacterial pneumonia superimposed on interstitial pneumonia caused by SARS-CoV-2.
<b>Anatomopathological data</b>	Severe cachexia. "Hepaticized" lower and middle lobes of the right lung and lower lobe of the left lung, with mucus and pus. Whitish mucus in the bronchi and trachea. Dilated hilar vessels. Enlarged lymph nodes at the level of the trachea.
<b>Cov 2</b>	
<b>Sex</b>	M
<b>Age</b>	29
<b>Circumstantial/anamnestic data</b>	After coming back from work, the subject had a discussion with his partner. He fall across a glass door and got deep cuts in the lower limbs, involving the popliteal vessels. Positive nasopharyngeal swab performed shortly before death (asymptomatic subject)
<b>Cause of death</b>	Hemorrhagic shock caused by profuse bleeding secondary to stab wounds in the lower limbs.
<b>Anatomopathological data</b>	Pulmonary edema, food in the airways with chromatic alteration in the upper and middle lung lobes. Cerebral and pulmonary edema.

<b>Cov 3</b>	
<b>Sex</b>	M
<b>Age</b>	87
<b>Circumstantial/anamnestic data</b>	Benign prostatic hypertrophy, COPD, type 2 diabetes mellitus. Previous removal of back neuroma. Reduced compliance with drug and dietary therapy, tendency to alcohol abuse. Hospitalizations due to heart failure. Fall with head trauma evidenced by CT scan during ER stay. Positivity for COVID-19 with subsequent aggravation of clinical picture.
<b>Cause of death</b>	Multiple organ failure, secondary to bilateral interstitial pneumonia caused by SARS-CoV-2.
<b>Anatomopathological data</b>	Bilateral pleural adhesions, dense whitish material in the trachea, right bronchus, and distal bronchiolar branches. Thickening of the left pulmonary apex. Diffuse bronchial calcifications. Parenchymal edema.
<b>Cov 4</b>	
<b>Sex</b>	M
<b>Age</b>	67
<b>Circumstantial/anamnestic data</b>	Obesity and ischemic heart disease. Subject went to Emergency Departments due to COVID-19 positivity. Progressive worsening with onset of respiratory insufficiency, tetraparesis, renal insufficiency, paroxysmal atrial fibrillation, necrotic decubitus ulcer, bacterial superinfection.
<b>Cause of death</b>	Acute heart failure during recovery phase from SARS-CoV-2 pneumonia.
<b>Anatomopathological data</b>	Pleural effusion. Abundant mucus in the trachea. Lymphadenomegaly. Pulmonary oedema. Coronary artery bypass with pericardial adhesions.
<b>Cov 5</b>	
<b>Sex</b>	F
<b>Age</b>	94
<b>Circumstantial/anamnestic data</b>	Arterial hypertension, dyslipidemia, diabetes, dysphagia, atrial fibrillation, and femur fracture. Nursing home resident. COVID-19 symptoms with admission to the hospital. Progressive deterioration of clinical condition.
<b>Cause of death</b>	Multiple organ failure resulting from septic shock as a complication of bilateral interstitial pneumonia.
<b>Anatomopathological data</b>	Yellowish mucus in the trachea. Bilateral effusion. Right apical pleural adhesions. Pulmonary distelectasis, with compact areas in the upper and middle lobe of the right lung, and in anterior portions of the left lung. Presence of yellowish exudate in the small bronchial branches.

<b>Cov 6</b>	
<b>Sex</b>	F
<b>Age</b>	90
<b>Circumstantial/anamnestic data</b>	Past history of eating disorder and pelvic fracture. Bilateral hearing loss, significantly reduced walking ability, arterial hypertension, COPD, cataracts, urinary incontinence.
<b>Cause of death</b>	Multiple organ failure following interstitial pneumonia, acute respiratory failure, and bacterial superinfection.
<b>Anatomopathological data</b>	Bilateral reddish effusion, expanded and congested lung. Ectatic hilar vessels. Cardiomegaly, with moderately dilated chambers. Coronary sclerosis with patent lumens. Tracheal hyperemia.
<b>Cov 7</b>	
<b>Sex</b>	F
<b>Age</b>	80
<b>Circumstantial/anamnestic data</b>	Lewy body dementia, severe cognitive impairment, extrapyramidal syndrome, glaucoma, double incontinence, difficulty in standing, bladder prolapse, hearing loss, osteoarthritis.
<b>Cause of death</b>	Respiratory failure due to interstitial pneumonia caused by SARS-CoV-2.
<b>Anatomopathological data</b>	Obesity. Putrefactive veil in the right pleural cavity and in the pericardium. Lung distelectasis, with thickened and congested areas. Sporadic thrombotic-like formations in some distal intraparenchymal vascular branches. Ectatic hilar vessels. Cardiomegaly with dilation of the chambers and velamentous appearance of the anterolateral walls of the right ventricle and the interventricular septum. Tracheal hyperemia. Polyvisceral alterations. Nephrosclerosis.
<b>Cov 8</b>	
<b>Sex</b>	F
<b>Age</b>	83
<b>Circumstantial/anamnestic data</b>	Alzheimer's disease, arterial hypertension, right knee arthroplasty, hysterectomy, unoperated right breast cancer (infiltrating ductal carcinoma with low proliferative index), aortic aneurysm.
<b>Cause of death</b>	Respiratory failure due to interstitial pneumonia caused by SARS-CoV-2.
<b>Anatomopathological data</b>	Cachexia. Cerebral edema. Pallor of the subcutaneous tissues. Bilateral reddish pleural effusion. Expanded, congested lungs. Ectatic hilar vessels. Modestly increased heart size. Coronary sclerosis. Atherosclerosis. Myocardium with greyish and whitish marbling. Right kidney hypoplasia.

	Aneurysmal dilatation of the subrenal aorta, with fibrinous material and thrombus.
<b>Cov 9</b>	
<b>Sex</b>	M
<b>Age</b>	92
<b>Circumstantial/anamnestic data</b>	Hypertensive heart disease, restenosis of left carotid thromboendarterectomy, severe dementia in ischemic cerebral vasculopathy, multi-district arthrosis, left ear keratoacanthoma.
<b>Cause of death</b>	Septic shock due to COVID-19 pneumonia with severe dehydration and multiple organ failure.
<b>Anatomopathological data</b>	Cachexia. Brain atrophy. Right pleural cavity adherence, distelected lungs, congestion of the basal lobes. Expanded and congested lungs. Ectatic hilar vessels. Increased heart size. Calcific thickening of the aortic valve. Calcific coronary sclerosis, with patent lumen.
<b>Cov 10</b>	
<b>Sex</b>	M
<b>Age</b>	81
<b>Circumstantial/anamnestic data</b>	Pacemaker, Guillan Barrè syndrome, bladder catheterization, paraplegia, bladder volvulus surgery. COPD, chronic AF. Heel and sacrum pressure ulcers. Hospitalization for dyspnoea, desaturation, and leukocytosis.
<b>Cause of death</b>	Septic shock due to COVID-19 pneumonia with severe dehydration and multiple organ failure.
<b>Anatomopathological data</b>	Extensive pressure sores to both feet and the sacrum. Edematous brain. Bilateral pleural adhesions. Yellowish mucus in the bronchi and parenchyma. Cardiomegaly. Left ventricle with thinned walls and septum. Pale myocardium. Pacemaker in place. Liver with macronodular surface, yellowish. Dilated gallbladder. Bladder mucosa with hemorrhagic spots.
<b>Cov 11</b>	
<b>Sex</b>	F
<b>Age</b>	89
<b>Circumstantial/anamnestic data</b>	Previous nursing home resident, transferred to hospital after COVID-19 positivity. Severe asthenia, nausea, anorexia, and vomiting. Radiological picture suggestive of SARS-CoV-2 infection. Severe ESBL-producing <i>E. coli</i> and multidrug-resistant <i>Staphylococcus</i> sepsis.
<b>Cause of death</b>	Septic shock related to COVID-19 pneumonia

<b>Anatomopathological data</b>	Extensively thickened and hemorrhagic middle and lower right lung lobes. Diffusely edematous and focally thickened and hemorrhagic left lower lung lobe. Ectasia of the pulmonary arterial vessels. Calcification of the bronchi. Calcific plaques at the circle of Willis. Marbled, yellowish hepatic parenchyma, with moderately increased consistency. Moderate nephrosclerosis. Small cyst in the left lobe of the thyroid gland.
<b>Cov 12</b>	
<b>Sex</b>	F
<b>Age</b>	82
<b>Circumstantial/anamnestic data</b>	Nursing home resident. Subject went to ER due to asthenia and dyspnea. Subsequent worsening of clinical conditions, with radiological picture suggestive of SARS-CoV-2 infection and positive nasopharyngeal swab.
<b>Cause of death</b>	Respiratory failure due to interstitial pneumonia caused by SARS-CoV-2.
<b>Anatomopathological data</b>	Subdural blood petechiae at the vault and at the base of the skull. Brain blood clots / venous thrombi. Roundish neoformation at the level of the middle cranial fossa with continuous peduncle of the dura mater. Brain depression in the right parietal area. Vessels of the Willis affected by atherosclerosis and containing clots / thrombi. Large cardiac vein containing clot / thrombus. Flaccid myocardium. Edematous and congested lungs. Peribronchial lymphadenopathy. Right pulmonary artery containing thrombus. Right kidney affected by probable middle third abscess. Congested kidneys. Hepatic parenchyma with yellowish marbling.
<b>Cov 13</b>	
<b>Sex</b>	F
<b>Age</b>	90
<b>Circumstantial/anamnestic data</b>	Nursing home resident. Worsening dyspnea, hospitalized with a diagnosis of pneumonia. Discharged after stabilization of clinical picture. Chronic HCV, permanent atrial fibrillation, anxious-depressive syndrome.
<b>Cause of death</b>	Thrombosis and pulmonary infarction during COVID-19 recovery.
<b>Anatomopathological data</b>	Cachexia. Thrombotic-like formation inside the transverse sinus of the base of the skull. Collection of brownish fluid in the mediastinal area. Heart of increased volume. Ectatic ascending aorta. Increased caliber of pulmonary hilar vessels. Pseudo-infarct associated with significant edema in the lower lobe of the left lung. Diffuse calcific sclerosis of aorta.
<b>Cov 14</b>	
<b>Sex</b>	F
<b>Age</b>	89

<b>Circumstantial/anamnestic data</b>	Nursing home resident. Cognitive impairment after stroke, dysphagia. Repeated episodes of vomiting in the days before death.
<b>Cause of death</b>	Respiratory failure in patient affected by interstitial pneumonia caused by SARS-CoV-2
<b>Anatomopathological data</b>	Cachexia. Arthritic skeletal deformations. Hiatal hernia with displacement of the stomach into the left pleural cavity and displacement of the mediastinum to the right. Right serous pleural effusion. Aspirated food present throughout the esophagus and in the larynx. Dystelectactic lungs. Nephrosclerosis. Previous cholecystectomy.
<b>Case 15</b>	
<b>Sex</b>	F
<b>Age</b>	88
<b>Circumstantial/anamnestic data</b>	Nursing home resident. Intellectual disability from birth. Former alcoholic. Spondylodiscarthrosis with stiffness in the lower limbs.
<b>Cause of death</b>	Respiratory failure due to pulmonary thromboembolism in patient with interstitial pneumonia caused by SARS-CoV-2
<b>Anatomopathological data</b>	Cachexia. Polyarthrosis with deformities of the four limbs and fingers of the hands. Serous effusion into the pericardial sac and pleural cavities. Bilateral apical pleural thickening, moderately thickened lower lobes, oedema at the left superior lobe. Blood clot in the pulmonary trunk, extending to the right pulmonary artery. Dilatation of the heart chambers, as well as of the pulmonary arterial vessels. Liver with diaphragmatic notches. Biliary stasis. Voluminous uterine fibroid.

## 4.2. General and clinical data of included cases

Nine (4 females, 5 males) of 15 COVID-19 subjects who underwent autopsy between April 2020 and August 2021 were included in this study. 6 cases were excluded for excessive post-mortem interval (PMI) or inadequate preservation of tissues. In addition, 10 matched controls were studied: for lung comparison, 5 cases with non-COVID pneumonia, while, for neuropathological comparison, 5 non-COVID brains were selected including 3 cases with Alzheimer's disease (AD) pathology and 2 with no AD pathology.

The demographic and clinical features of the study participants are shown in Table 7. The nine COVID-19 patients (four females and five males) died 0 to 32 days after diagnosis (mean: 10 days). At death, their mean age was 77.4 (range: 29–94), and the mean postmortem interval was 7 days (range: 3–13). All subjects, except for patient COV2 (a previously healthy young man), had several comorbidities of varying severity, including pulmonary diseases, hypertension, diabetes, obesity, and cancer. None of them had severe heart failure. Six had a history of NCD (four major-NCD and two mild-NCD), five of whom had a clinical course complicated by delirium (three as the first COVID-19 symptom). The other three were cognitively normal. All cases developed severe lymphopenia and typical symptoms (fever–cough–dyspnoea), except for the COV2 case, who was asymptomatic and died from haemorrhagic shock due to accidental trauma. Three had sepsis before death and only one was treated in an intensive care unit; however, none of them underwent orotracheal intubation.

The five cases with non-COVID pneumonia (from the Institute of Legal Medicine) and the five non-COVID ABB controls were matched for age and comorbidities.

These subjects died of either of the following: pneumonia–pulmonary failure, heart failure, cachexia due to terminal dementia, or cancer.

The mean PMI in COVID-19 cases was 7 days (range: 3–13). The mean PMI in ABB cases was 10.5 hours (range: 3–16). The mean PMI in non-COVID pneumonia was 6 days (2–12).

**Table 7:** demographic and clinical features of the study participants

CODE	PMI (days/ hours)	GENERAL AND CLINICAL FEATURES						
		SEX	AGE (y/o)	ANAMNESIS; CAUSE OF DEATH	NCD	DEL	SEP	
COV2	7 d	M	29	NR; hemorrhagic shock	no	no	no	
COV4	5 d	M	67	Obesity, HTN, CVD; CIP, respiratory failure	no	no	yes	
COV6	11 d	F	90	HTN, COPD; respiratory failure	no	no	no	
COV3	7 d	M	87	T2D, CVD; respiratory failure	Mild (VCI)	Hyper/Hypo, (early onset)	no	
COV10	7 d	M	81	AF, paraparesis (previous GBS); respiratory failure	Mild (VCI)	Hypo, (late onset)	yes	
COV1	7 d	F	74	NR; respiratory failure	Major (AD)	Hyper, (early onset)	no	
COV5	3 d	F	94	T2D, HTN, CVD, AF; multiorgan failure	Major (AD + VaD)	Hypo, (early onset)	yes	
COV8	13 d	F	83	HTN; respiratory failure	Major (AD)	no	no	
COV9	6 d	M	92	HTN, cerebrovascular disease; respiratory failure	Major (AD + VaD)	Hyper/Hypo, (late onset)	no	
L1	4 d	F	76	AF; multiorgan failure 7 days after head trauma	no	no	no	
L2	5 d	M	92	HTN, CVD, cerebrovascular disease; respiratory failure	Major (VaD)	Hypo, (late onset)	no	
L3	6 d	F	60	CVD; multiorgan failure 3 days after head trauma	no	no	no	
L4	4 d	M	62	HTN; respiratory failure	no	no	yes	
L5	8 d	M	74	HTN, COPD; multiorgan failure 10 days after intestinal perforation	Major (Ad + VaD)	Hypo, (late onset)	yes	
B1	3 hr	M	79	T2D; liver cancer	no	no	no	
B2	8 hr	M	79	HTN, CVD, cerebrovascular disease; cachexia	Mild (VCI), hemiparesis	no	no	
B3	16 hr	F	83	HTN, CVD, cerebrovascular disease; CHF	Major (AD + VaD)	no	no	
B4	15 hr	F	85	CVD, cerebrovascular disease; CHF	Major (AD + VaD)	Hyper, (prev. ep)	no	
B5	15 hr	F	89	HTN, COPD, cerebrovascular disease; cachexia	Major (AD)	Hyper, (prev. ep)	no	

Note: COVID-19 cases are labelled as ‘COV’, control cases are identified as ‘B’ (Brain Bank) for brain and L (lung control) for lungs; PMI was measured in days (d) or hours (h). Abbreviations (in alphabetical order): AD, Alzheimer’s disease; AF, atrial fibrillation; CHF, chronic heart failure; COPD, chronic obstructive pulmonary disease; CVD, cardiovascular disease; DEL, delirium; GBS, Guillain Barre Syndrome; HTN, hypertension; n/a, not available; NCD, neurocognitive disorder; NR, nothing relevant in medical history; PMI, post mortem interval; prev. ep., previous episode; SEP, sepsis; T2D, type 2 diabetes; VaD, vascular dementia; VCI, mild vascular cognitive impairment.

## **4.3. Histopathology in Lung, Kidney, Heart, Brain**

### **4.3.1. PATHOLOGICAL FINDINGS IN COVID-19 CASES**

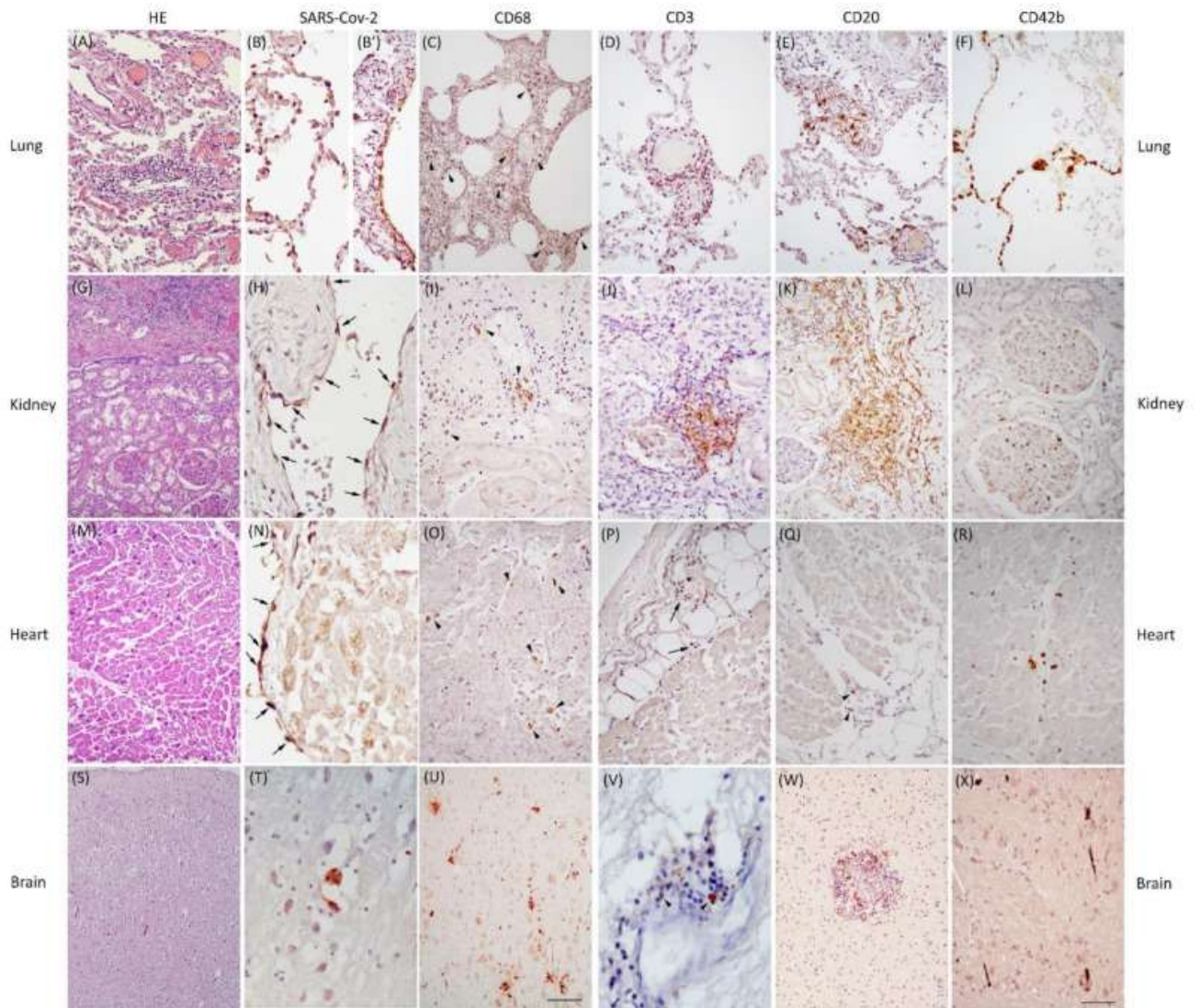
As general autoptic findings, COVID-19 cases showed typical findings, including hypoxic-ischemic damage in multiple organs and diffuse pneumonia with lung congestion or oedema, frequent clots inside the vessels, and alveolar damage often associated with bacterial superinfection.

The general and specific pathological findings of the COVID-19 cases and control cases are summarized in table 8, and their most representative histological details are displayed in figure 1.

**Table 8:** pathological findings of the COVID-19 cases and control cases.

CASE	General pathological features										Specific pathological features																			
	Lung	Kidney	Heart	Brain	Lung					Kidney					Heart					Brain-Frontal Lobe					Brain-Pons					
	(Acute; chronic findings)	(Acute; chronic findings)	(Acute; chronic findings)	(Acute; chronic findings)	TL	BL	AP	VA	TL	BL	AP	VA	TL	BL	AP	VA	TL	BL	AP	VA	TL	BL	AP	VA	TL	BL	AP	VA		
COVID	M IC, AE, interstitial-subpleural I.F., CE, A	Severe C	M A	HA, no AD, no SVD, mild gliosis RA																										
CON1	Severe C, interstitial-subpleural I.F., AE, E, DAD, BS, I.F., CE, A	Severe C, cortical-medullary I.F., BS	M V, BS, M.A., Subepicardial I.F., CH	HA, no AD, SVD, mild gliosis																										
CON5	AE, E, interstitial I.F., A	Cortical I.F.	M IC	HA, low AD, mild gliosis																										
CON3	Severe C, AE, DAD, interstitial I.F., AS, CE, A	Severe C, AGA, cortical-medullary I.F., AS, BS	M V, M.A., I.F., AS	HA, low AD, SVD, mild gliosis																										
CON10	Severe C, AE, BS, interstitial I.F., AS	Severe C, AGA, I.F.	M A, interstitial-subepicardial I.F.	HA, no AD, SVD, perivascular gliosis																										
CON1	C, AE, AH, E, DAD, BS, interstitial I.F., CE	Cortical I.F., BS	M A, BS, I.F.	HA, high AD, perivascular gliosis																										
CON5	Severe C, AH, AE, E, DAD, BS, interstitial I.F., CE, A	Severe C, cortical-medullary I.F., AGA, BS	M V, M.A., subepicardial I.F., CH	HA, intermediate AD, SVD, mild gliosis RA																										
CON8	Severe C, interstitial I.F., CE, A	Cortical-medullary I.F., AS	F	HA, intermediate AD, perivascular gliosis RA																										
CON9	Severe C, AH, interstitial I.F., CE, A	AS	M A, interstitial I.F., AS	HA, intermediate AD, SVD, perivascular gliosis RA																										
C11 / 81	M IC, E, DAD, interstitial I.F., A	n/a	n/a	No AD, no SVD																										
C12 / 82	AE, interstitial-subpleural I.F., CE, A	n/a	n/a	No AD, stroke and SVD																										
C13 / 83	M IC, interstitial I.F., E, DAD, BS	n/a	n/a	Intermediate AD, atrophic, severe gliosis																										
C14 / 84	Severe C, AE, BS, interstitial-subpleural I.F., A	n/a	n/a	High AD, SVD, severe gliosis																										
C15 / 85	M IC, E, BS, interstitial I.F., CE	n/a	n/a	High AD, severe gliosis																										

**Figure 1:** Pathological features of COVID-19.



In the lung, H&E revealed severe congestion, diffuse alveolar damage, and interstitial pneumonia presenting as septal infiltrate shown in the middle of the image (A); SARS-CoV-2 positivity is evident in alveolar pneumocytes showing cytopathic features (B) and in the bronchiolar ciliated epithelium (B'); diffuse interstitial macrophages detected by CD68 antibody (C, arrowheads); T-lymphocyte (D) and B-lymphocyte (E) infiltrates are revealed by CD3 and CD20 reactions, respectively; CD42b marks several microthrombi in capillary and interstitial vessels characterized by a “rosary crown” feature (F). In the kidney, H&E labeled acute glomerular alterations in the lower part of the image and inflammatory infiltrates at the top (G); SARS-CoV-2 immunoreactivity detectable in some vascular endothelial cells (H, arrows); occasional foci of macrophages detected by the CD68 antibody (I, arrowheads); as in the lung, T-lymphocyte (J) and B-lymphocyte (K) infiltrates are revealed by CD3 and CD20 reactions, respectively; occasional microthrombi in the glomerular capillary are marked by CD42b antibody (L). In the heart, H&E stained parenchymal dissociation and myocyte vacuolization in the upper part of the image (M); rare SARS-CoV-2 traces observed in the endocardium (N, arrows); occasional foci of interstitial macrophages labeled by the CD68 antibody (O, arrowheads), rare subepicardial T-lymphocyte (P, arrows) and B-lymphocyte (Q, arrowheads) infiltrates revealed by CD3 and CD20 reactions in the upper and lower parts of the images, respectively; CD42b antibody marks focal and sporadic capillary microthrombi (R). In the brain, H&E revealed diffuse neuronal loss and cortical edema characterized by spongiosis (S); very rare SARS-CoV-2-positive cells detected in the pons (T); amoeboid microglial cells and several microglial nodules identified by the CD68 antibody, mainly in the brainstem (U); rare T and B lymphocytes are observed in the perivascular spaces (V) and in some nodules (W); frequent capillary microthrombi are observed in the brainstem (X). Scale bars: 230  $\mu$ m (S); 162  $\mu$ m (G); 140  $\mu$ m (C,U); 75  $\mu$ m (A,E,F,K,M,P,W); 64  $\mu$ m (D,I,O,Q,R,X); 60  $\mu$ m (J); 52  $\mu$ m (L); 44  $\mu$ m (B'); 39  $\mu$ m (B); and 30  $\mu$ m (H,N,V,T).

The lung samples showed:

- severe capillary congestion, edema, and DAD with cytopathic alterations in type-2 pneumocytes;
- SARS-CoV-2 positivity in alveolar pneumocytes of five cases, ubiquitous alveolar macrophages, interstitial pneumonia with fibrosis and moderate to severe inflammatory septal infiltrates (mainly T-lymphocytes, present in all cases), and frequent superimposed bacterial infection;
- microthrombi and frequent clots inside the vessels in seven cases.

Findings from the kidneys included:

- congestion and acute glomerular alterations in three cases;
- SARS-CoV-2 positivity in the tubular epithelium and the capillary endothelium in three cases, and moderate to severe inflammatory infiltrates (T-lymphocytes and B-lymphocytes in the majority of cases, while macrophages were quite rare in all but one case);
- microthrombi and clots in two cases.

The heart samples revealed:

- hypoxic myocytic injuries;
- sporadic SARS-CoV-2 traces in the endothelial and endocardial cells of one case, perivascular–parenchymal inflammatory infiltrates (prominent only in two cases) characterized by predominant macrophages with no evidence of T-lymphocytes and rare B-lymphocytes;
- relevant microthrombi in only one case.

The neuropathological hallmarks were:

- diffuse cortical edema due to extreme hypoxia with cortical swelling, spongiosis, and severe neuronal rarefaction in the cerebral cortex and hippocampus;
- very limited traces of SARS-CoV-2 antigens in pontine neurons of one case, perivascular and parenchymal inflammatory infiltrates characterized by the enhancement of CD68-positive amoeboid cells (activated microglia), which are more abundant in the pons (all cases) than in the frontal cortex, with a tendency to nodular aggregation and neuronophagia, and very scant B–T lymphocytes as vascular cuffing or inside few nodules;
- frequent microthrombi in the frontal lobe (eight cases) and pons (six cases) with rare ischemic rarefaction of the surrounding tissue.

Apart from COV2, all of the other cases had pre-existing or age-related pathologies. The lungs frequently showed emphysema, dystelectasis, and anthracosis. The kidneys showed glomerulosclerosis and arteriolosclerosis. The heart samples presented with myocardiosclerosis, lipofuscin deposits, and fatty infiltrates. The brain samples showed different degrees of atrophy and AD pathology (six cases showing cortical neuritic plaques associated with microglial activation and astrogliosis with reactive astrocytes), and small-vessel disease (SVD), including enlarged perivascular spaces, arteriolosclerosis, myelin loss, hemosiderin leakage, and microbleeds (five cases).

#### *4.3.2. PATHOLOGICAL FINDINGS IN CONTROL NON-COVID CASES*

The lungs of non-COVID cases showed congestion, edema, and DAD with septal lympho-monocytic infiltrates associated with intra-alveolar fibrinopurulent exudates consisting of neutrophils and macrophages (similar to COVID-19 cases with superimposed bacterial infection). The control brains presented both AD pathology and vascular diseases (SVD and

cerebral infarcts). Similar to the COVID-19 cases with AD, the three controls affected by AD showed severe astrogliosis and cortical microglial nodules with a distribution resembling that of neuritic plaques.

The presence of T-B lymphocytes as a whole (sum of scores) was similar in the lungs and kidneys, albeit with a significantly greater presence of T lymphocytes in the lungs ( $p = 0.020$ ; Figure 2B, Table 9). The lymphocyte component within the inflammatory infiltrates of lungs and kidneys was clearly predominant over that of other tissues ( $p < 0.001$ ), as well as the presence of the viral antigen, particularly in the type-2 pneumocytes and bronchiolar epithelial cells. The heart had relevant inflammatory foci in only two cases, characterized by the presence of macrophages, the substantial absence of lymphocytes, and very rare SARS-CoV-2 traces in the endothelium–endocardium.

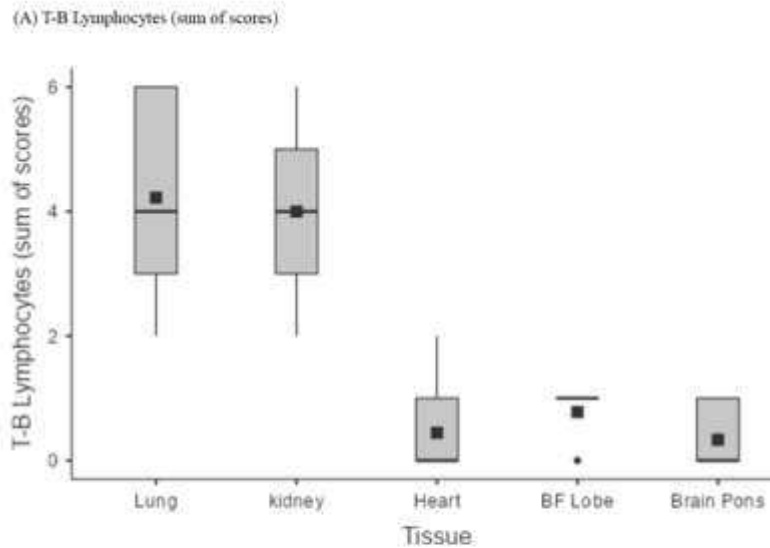


**Figure 2:** Lymphocytic infiltrates. (A) Box plot comparing the sum of the B and T lymphocyte scores across lungs, kidneys, heart, brain frontal lobe (BF), and pons (BP); the lymphocyte component within the inflammatory infiltrates of lungs and kidneys was clearly predominant over that of other tissues ( $p < 0.001$ ); (B) box plot showing a comparison between T lymphocyte scores in the lungs and in the kidneys; The presence of T-B lymphocytes as a whole (sum of scores) was similar in the lungs and kidneys, albeit with a significantly greater presence of T lymphocytes in the lungs ( $p = 0.020$ ).

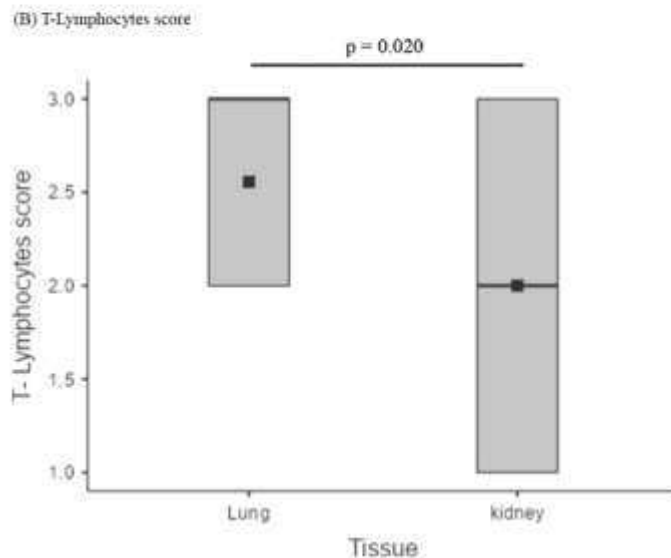


**Table 9:** Summary of statistical analyses.

	$\chi^2$	p.value
Friedman rank sum test	31.8	<0.001
<hr/>		
Pairwise comparisons (Durbin-Conover)	t	p.value
Sum of T-B Lymphocytes Lungs VS Kidneys	0.438	0.665
Sum of T-B Lymphocytes Lungs VS Heart	10.506	<.001
Sum of T-B Lymphocytes Lungs VS Brain frontal lobe	8.536	<.001
Sum of T-B Lymphocytes Lungs VS Brain pons	11.162	<.001
Sum of T-B Lymphocytes Kidneys VS Heart	10.068	<.001
Sum of T-B Lymphocytes Kidneys VS Brain frontal lobe	8.098	<.001
Sum of T-B Lymphocytes Kidneys VS Brain frontal pons	10.725	<.001

Comparing lung T-B lymphocytes between COVID-19 cases and controls, there was no significant difference (Figure 3A); nonetheless, the T-component was considerably more represented in COVID-19 pneumonia ( $p = 0.010$ ).

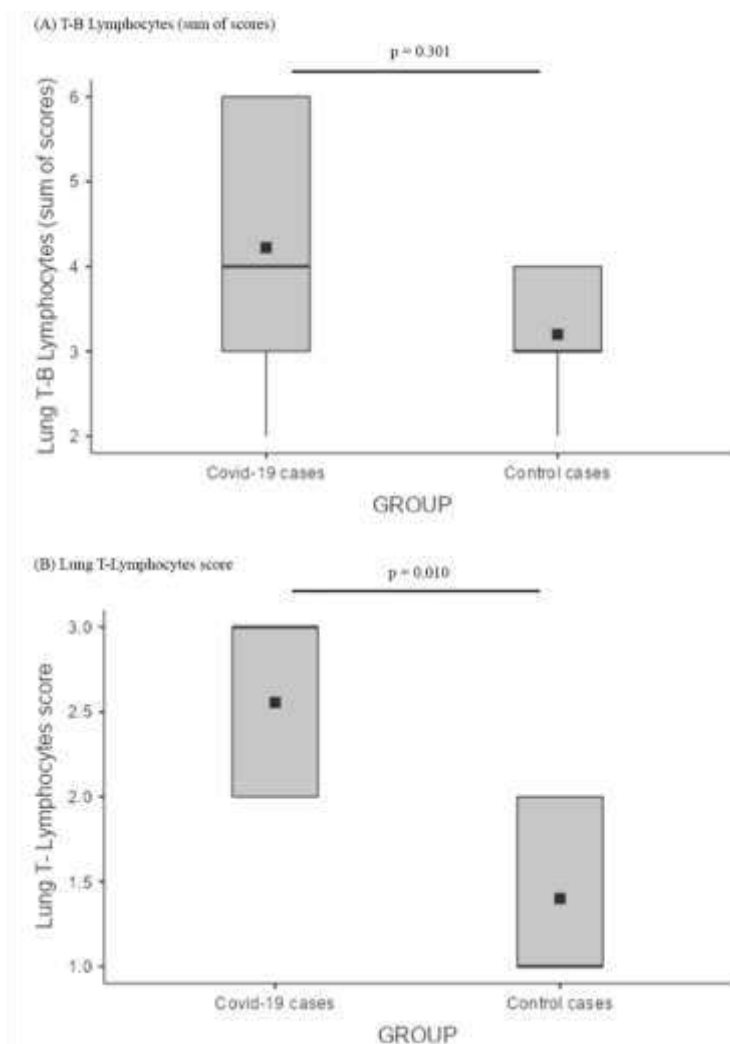


**Figure 3:** Comparison of lymphocytic infiltrates among the lungs of cases and controls. (A) Box plot describing the comparison between the lung B–T lymphocyte of COVID-19 cases versus control cases; lung T-B lymphocytes (sum of scores) did not show any significant difference; (B) lung T lymphocyte score comparison among COVID-19 cases and control cases according to a box plot demonstrated that the T-component was considerably more represented in COVID-19 pneumonia ( $p = 0.010$ ).

As for the brain, the preponderance of microglial activation (innate immunity) over the lymphocytic response (adaptive immunity) was distinct. In the frontal lobe, this phenomenon did not differ between COVID-19 cases and controls; these two groups showed similar levels of microglial activation, probably reflecting an inflammatory boost related to the presence of neurodegeneration (Figure 4A). On the other hand, the significantly greater microglial activation in the pons of COVID-19 cases (Figure 4B), associated with traces of viral antigen (Figure 1T), emerged as a specific topographical phenomenon within the brain ( $p = 0.017$ ; Figure 4B). Microthrombosis assumed a clinico-pathological relevance only in the lungs, with a significant prevalence of pulmonary microthrombi in COVID-19 cases (Figure 5;  $p = 0.023$ ) in comparison with non-COVID pneumonia.

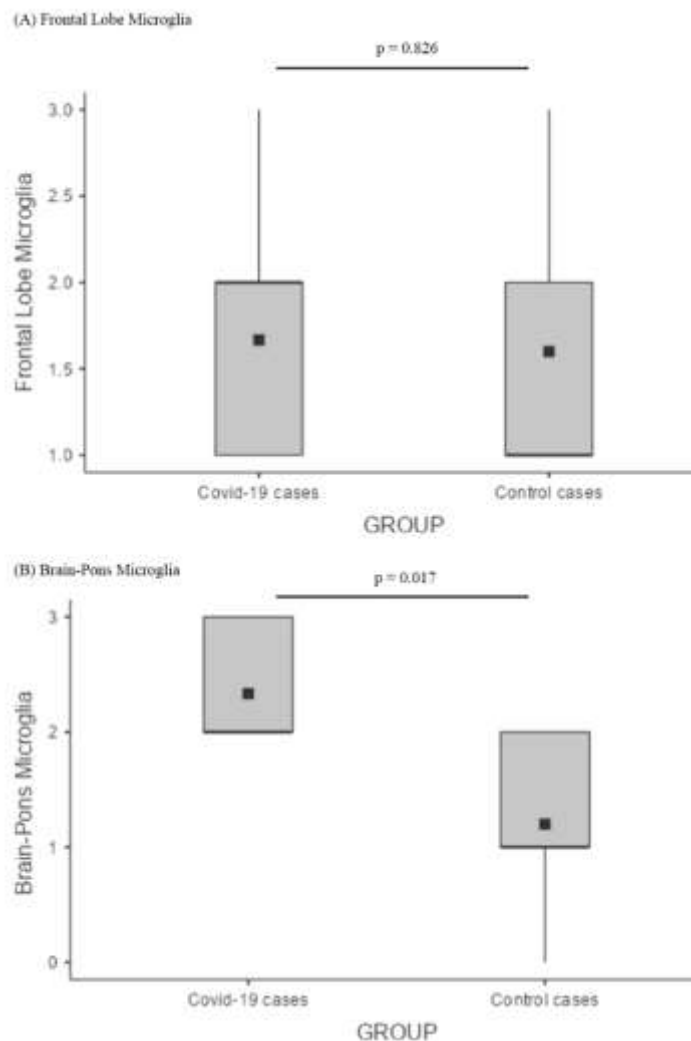


**Figure 4:** Comparison of microglial activation between the brains of cases and controls. (A) In the frontal lobe, microglial activation (innate immunity) did not differ between COVID-19 cases and controls; (B) Comparison of pontine microglia between COVID-19 cases and control cases by a box plot showed a significantly greater microglial activation in the pons of COVID-19 cases ( $p = 0.017$ ).

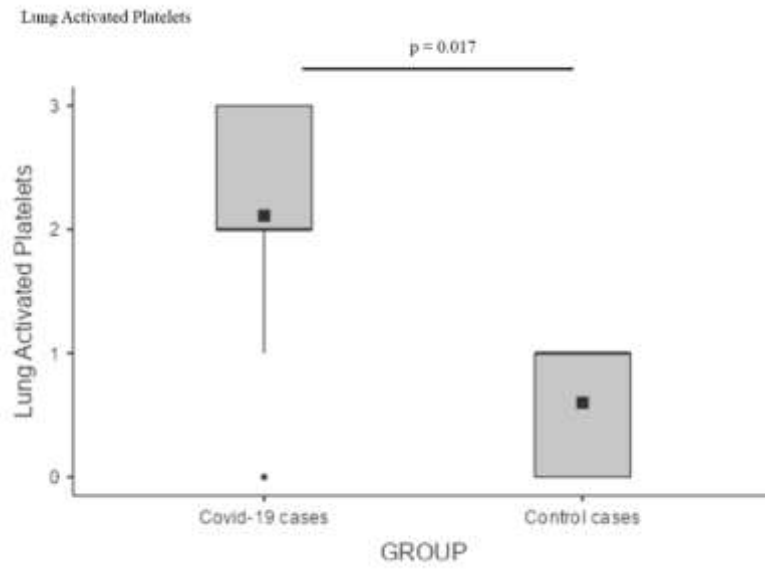


**Figure 5:** Box plot comparing activated platelets between the lungs of cases and controls demonstrating a predominance of pulmonary microthrombi in COVID-19 cases ( $p = 0.023$ ).

## 4.4. Focus on neuropathological investigation

This part of the study was coordinated and mainly managed by Emanuele Poloni and Valentina Medici, with the collaboration of Mauro Ceroni, Antonio Guaita (Department of Neurology and Neuropathology, Abbiategrosso Brain Bank, Golgi-Cenci Foundation) and other colleagues.

### 4.4.1. MACROSCOPIC AND MICROSCOPIC NEUROPATHOLOGICAL FEATURES

#### 4.4.1.1. COVID-19 brains

All COVID-19 brains did not show gross abnormalities, thrombosis of the large vessels or infarcts. Brain atrophy and enlarged perivascular spaces were observed in the 4 cases with dementia. Some of the most representative microscopic details of the COVID-19 cases are displayed in Figure 6. In all cases, microscopic examination showed diffuse moderate to severe brain oedema (Figure 6A) commonly seen as unspecific hypoxic and agonal change. H&E staining indicated loss of neurons in the cerebral cortex and hippocampus, and reveals inflammatory infiltrates (sporadically in the meninges and consistently in the brain tissue) forming perivascular cuffing (Figure 6B) and parenchymal nodules which are also identified by the CD68 microglial marker, particularly in the brainstem, cortex and hippocampus but also in basal ganglia (Figure 6C) and subependymal zone, (Figure 6D,E). In five out of nine cases, small vessel disease (SVD) was observed, including enlarged perivascular spaces, arteriolosclerosis, hemosiderin leakage and microbleeds in the cortex and basal ganglia. In addition, myelin loss in subcortical and deep white matter was detected by LFB (Figure 6F). Different degrees of AD pathology were noted in 6 cases, and a definite AD diagnosis was made in 4. The distribution of neuritic plaques in the cortex and hippocampus was comparable to that of microglial nodules. In 7 cases, rare perivascular T&B lymphocytes and sporadic B-lymphocytes in some inflammatory nodules were found (Figure 6G–I), with no particular

differences between AD and non-AD cases. None of the COVID-19 cases showed clear IHC positivity for SARS-CoV2, except for Cov3, which exhibited very few SARS-CoV-2-positive cells with neuronal morphology in the lower brainstem (Figure 6J,K). The microvasculature was characterized by a continuous and intense perivascular profile with no relevant alterations in the vascular endothelium. Unexpectedly, frequent foci of tuft-like capillary proliferation were present in the brainstem of 6 COVID-19 cases (Figure 6L,M; anti-CD34): in two cases tufts were abundant (COV1,9: tufts in at least 3 of the 5 areas examined) while in others cases they were moderate (COV2,5,6: tufts in 2 areas) or rare (COV10: scant tufts in 1 area). These capillary tufts were observed in areas containing neuronal aggregates rather than fibers. GFAP immunoreactivity revealed astrogliosis associated with reactive astrocytes, especially in subjects with dementia (Figure 6N,N'). Enhanced labelling around blood vessels (enhanced astrocytic endfeet) was a peculiar feature in some COVID-19 cases (Figure 6O).

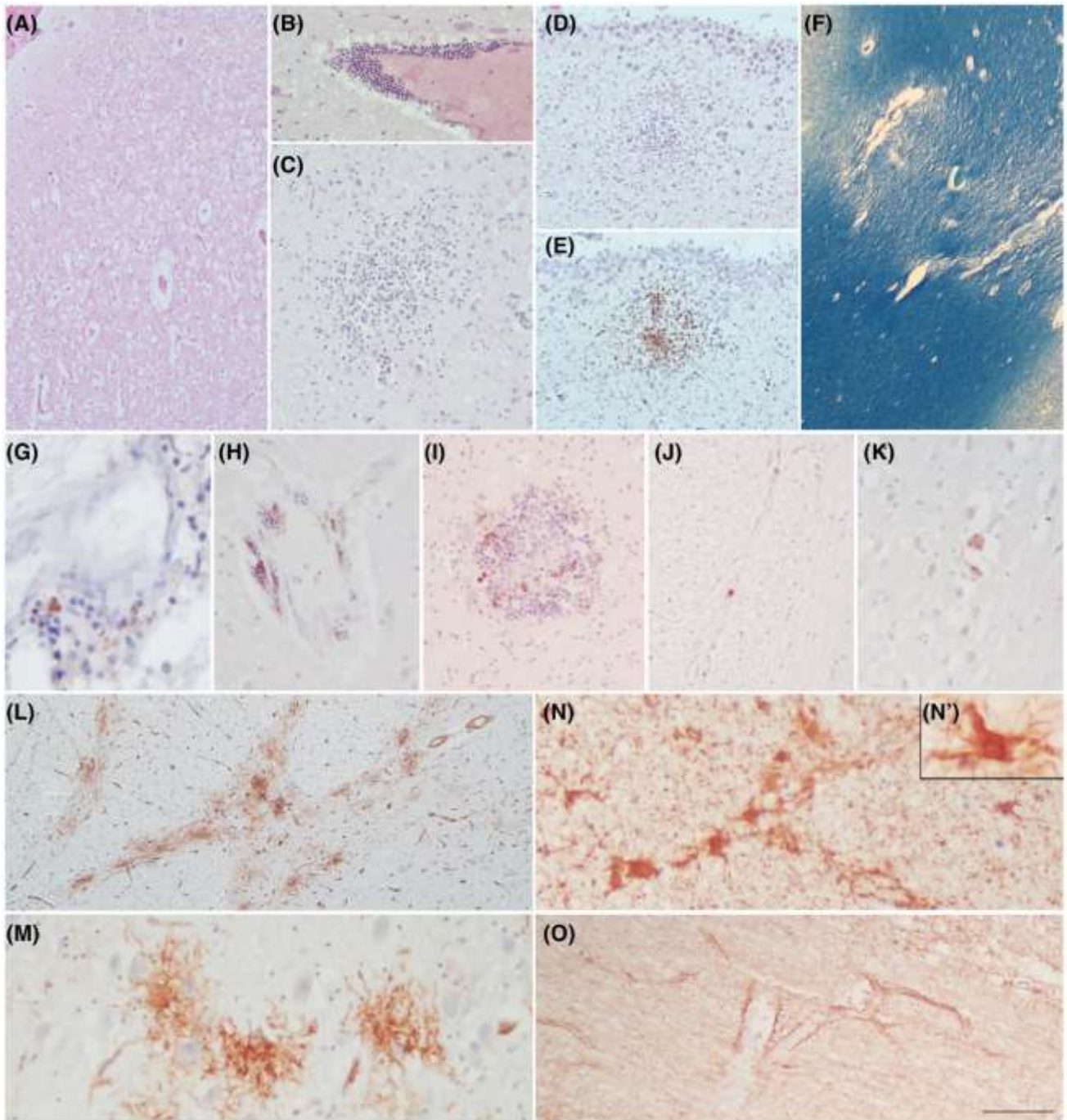


**Figure 6:** COVID-19 neuropathology. H&E reveals diffuse cortical oedema (A), inflammatory perivascular infiltrates (B), and micro nodules in the basal ganglia (C) and subependymal zone (D), which are also identified with CD68 marker (E). LFB shows myelin loss in the subcortical WM due to SVD (F). Rare foci of perivascular T-lymphocytes (G) and B-lymphocytes (H) are identified using anti-CD3 and anti-CD20 antibodies, respectively. B-lymphocytes are also observed within some inflammatory nodules (I). Rare SARS-Cov-2 positive cells are detected only in the lower brainstem of the one case (Cov3) (J, K). CD34 staining displays foci of abnormal tuft-like capillary features, particularly frequent in the pons (L, M). GFAP reveals mild to moderate gliosis with frequent reactive astrocytes (N, N'). GFAP enhancement in astrocytic end feet around blood vessels is a peculiar picture (O). Scale bars: 512  $\mu$ m (F); 288  $\mu$ m (A, L); 180  $\mu$ m (D, E); 106  $\mu$ m (B, J, O); 76  $\mu$ m (C, I); 47  $\mu$ m (H, K, M, N); 31  $\mu$ m (G); 17  $\mu$ m (N')

#### **4.4.1.2. Control non-COVID cases**

Non-COVID cases (n = 5) with dementia showed diffuse brain atrophy at gross examination. Moreover, two cases showed brain infarcts in the territories of the right middle cerebral artery and left posterior cerebral artery, respectively. Small vessel disease was present in 2 cases. Different degrees of AD pathology were noted in 4 cases, with a definite AD diagnosis in 3. Diffuse activation of microglia and microglial nodules were also observed in the non-COVID cases affected by AD; the distribution of parenchymal microglial nodules was similar to that of neuritic plaques. Rare perivascular T&B lymphocytes and sporadic parenchymal T lymphocytes were found. The 3 AD cases showed a higher number of lymphocytes. This phenomenon was not particularly prominent apart from one case, wherein a moderate presence of T lymphocytes was observed, especially in the hippocampus and mainly in perivascular zones. Normal vascular endothelium was identified using CD34 antibody. Although to a lesser extent in comparison with COVID-19 cases, tuft-like capillary structures were also present in the pons of non-COVID cases (rare to moderate tuft-like CD34 features). Widespread astrogliosis was seen in all 3 AD cases.

#### **4.4.1.3. Specific microglial features**

Pictures of microglial activation are presented in Figure 7. The first row demonstrates the patterns of cortical and hippocampal microglial activation in subjects with and without COVID-19, and with and without AD. Although a mild microglial reinforcement is detectable in AD cases who suffered from COVID-19, AD cases with and without COVID-19 are quite similar. In both, microglial nodules showed a topographical distribution comparable to that of amyloid and neuritic plaques (Figure 7A–C,E–G). Instead, the picture of non-AD/non-COVID cases is quite different with a normal microglial representation (Figure 7D,H). The second row displays the features of CD68-positive cells (activated amoeboid microglia) in COVID-19 cases, forming perivascular infiltrates and parenchymal inflammatory nodules. They were particularly

prominent in the olfactory bulbs, frontal cortex and hippocampus (Figure 7I–M), and even more prominent in the brainstem, where some macrophages engulfed neurons (neuronophagia) (Figure 7N–S).

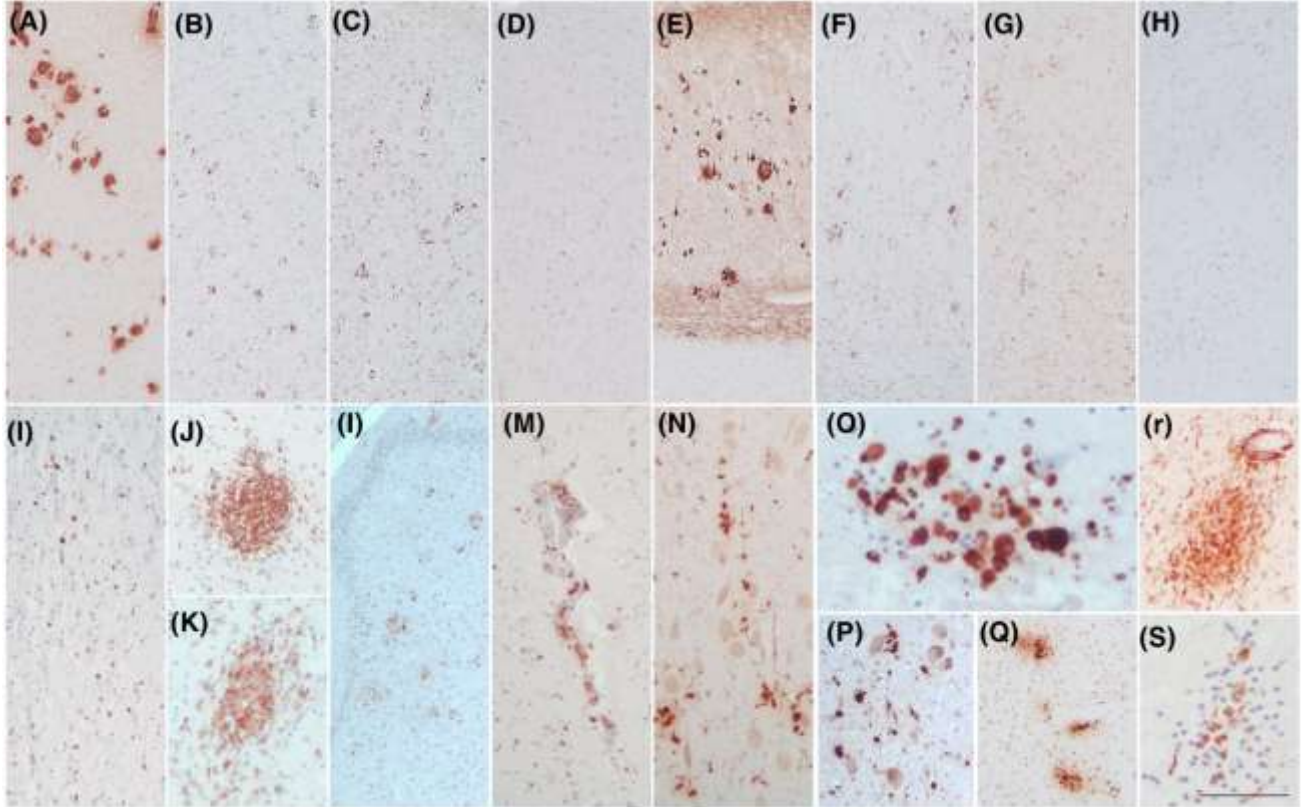


**Figure 7:** Microglial activation. The first row compares the neuropathological findings present in the frontal cortex (A–D) and the subiculum (E–H) of 2 AD cases (one AD/COVID-19 and one AD/non-COVID) and a non-AD/non-COVID case. The AD/COVID-19 case shows amyloid plaques (A, E), as well as moderate to severe microglial activation and nodules (CD68+) in a topographical distribution similar to that of the plaques (B, F). This microglial activation does not appear different from that seen in the AD/non-COVID case (C, G), while the same areas in the non-AD/non-COVID case are clearly diverse, with a normal microglial representation (D, H). The second row shows different pictures of activated microglia (CD68+) in COVID-19 cases, including amoeboid cells, perivascular infiltrates and nodules in the olfactory bulb (I), frontal cortex (J, K), hippocampus (L, M), midbrain (N: red nucleus; O: detail of a nodule with neuronophagia in the upper right sector), pons (P: locus coeruleus Q & R: raphe nuclei), and medulla oblongata (S: DMV area). Scale bars: 315  $\mu\text{m}$  (A–H, L); 137  $\mu\text{m}$  (I, M, N, P, Q); 60  $\mu\text{m}$  (J, K, R); 48  $\mu\text{m}$  (O, S)

#### 4.4.2. SEMI-QUANTITATIVE ANALYSIS OF MICROGLIAL ACTIVATION

An overview of CD68 semi-quantitative analysis revealed that, in COVID-19 cases, the microglial activation was particularly enhanced in the brainstem, mainly in the pons. The comparison between the whole brainstem (midbrain + pons + medulla) of all 9 COVID-19 and 5 non-COVID cases showed significantly greater microglial activation in COVID-19 cases (p

= 0.046). This did not happen at the level of the other hemispheric brain areas considered (frontal lobe and hippocampus) where the differences were modest and not significant (Table 10).

Considering the frontal cortex of the 9 COVID-19 cases, the presence of activated microglia was significantly greater in those with AD ( $n = 4$ ) compared to those without AD ( $n = 5$ ) ( $p = 0.018$ ). Likewise, considering the frontal cortex of the non-COVID cases, microglial scores were significantly higher in those with AD ( $n = 3$ ) than in those without AD ( $n = 2$ ) ( $p = 0.022$ ). Moreover, subjects belonging to the non-COVID/AD group ( $n = 3$ ) had a significantly higher microglial activation than those of the COVID-19/no or low AD group ( $n = 5$ ) ( $p = 0.028$ ). On the other hand, the comparison between the frontal cortical areas of AD cases with and without COVID-19 did not reveal any significant differences ( $p = 0.979$ ).

Comparing the 5 COVID-19 cases complicated by delirium (all of them had either mild- or major-NCD) and the 4 COVID-19 cases without delirium, a significantly stronger microglial activation was found in the hippocampus of cases with delirium ( $p = 0.048$ ). Interestingly, cases presenting with early delirium tended to exhibit more severe TAU pathology, but this trend did not reach statistical significance ( $p = 0.350$ ).

No significant differences in microglial activation were found between COVID-19 cases with and without sepsis.

Considering all cases, subjects with dementia showed significantly greater microglial activation in the cortex than subjects without dementia ( $p = 0.001$ ).



## 4.1. SARS-CoV 2 detection in frontal cortex

This part of the study was coordinated and mainly managed by S. Gagliardi and C. Cereda (Genomic and Post Genomic Unit, IRCCS Mondino Foundation, Pavia, Italy) and other colleagues.

The 9 COVID-19 cases were compared with frontal lobe samples from 8 non-COVID-19 cases provided by ABB.

RNA extracted from frontal cortex of both COVID-19 patients and controls have been analyzed for SARS-CoV-2 nucleocapsid gene 1 (nCoV\_N1) and human Ribonuclease P (hRP), as controls of RNA extraction. The analysis of viral RNA detection by qPCR was positive for viral RNA (nCoV\_N1) only in one patient while in all samples the expression of hRP gene was present, demonstrating that the RNA was correctly extracted. Moreover, the analysis was repeated by ddPCR, a more sensitive technique for RNA detection. The viral RNA was quantified in 8 (88%) samples of 9 examined patients.

### 4.1.1. *TRANSCRIPTOMIC RESULTS*

In COVID-19 patients, RNA-seq data reported 11 differentially expressed genes (DEGs), 10 were coding RNAs while 1 was a long non-coding RNAs (lncRNA). Concerning coding genes, 4 out of 10 have been found down-regulated while 6 out of 10 up-regulated.

The most deregulated genes are up-regulated mRNA coding for haemoglobin subunits (HBA, and HBB) and down-regulated genes associated to hypoxia and inflammation (SLC14A1, HIF3A and RGS5). This data also correlate with neuropathological findings that showed inflammatory infiltrates in COVID-19 patients' tissue.

Specific investigations (pathway analysis) have been performed to identify the most important pathways and molecular features associated to differentially expressed genes. The most relevant data showed that DEGs are associated to SARS coronavirus protease and Alpha

hemoglobin stabilizing protein (AHSP) pathway. Pathway analysis also underline the significant involvement of respiratory aspect in COVID-19 phenotype, with modifications in the response to oxidative stress, oxygen and gas transport and hydrogen peroxide catabolic and metabolic process. Moreover, also cellular detoxification and response to toxic substance pathways have been found involved. Analysis of molecular functions also confirmed the involvement of peroxide and antioxidant activity.

## 5. DISCUSSION

### 5.1. COVID-19 Pathology in the Lung, Kidney, Heart and Brain

Due to its intrinsic characteristics, SARS-CoV-2 infection is accompanied from the earliest stages by an extreme cytokine outpouring. This so-called “cytokine storm” is a form of severe inflammatory response syndrome due to a hyperactivation of the innate immune system with dysregulated and excessive production of pro-inflammatory cytokines, including IL-6, IL-1, IFN, and TNF-alpha. This type of reaction is specifically related to highly pathogenic beta-CoVs and is frequently observed among patients affected by severe COVID-19. Our results confirm that inflammatory and immune-mediated alterations augment the direct cytopathic damage induced by the virus, causing epithelial and endothelial damage, vascular leakage, and dampening of the T-cell response, accompanied by the over-activation of cells from the macrophage lineage. Hence, the severe form of COVID-19 is a multi-organ disease characterized by a combination of viral invasion, lympho-monocytic infiltration, and clotting alterations with mixed detrimental effects due to acute cytopathic injury, inflammation, microthrombosis, and chronic suffering leading to fibrosis. Further detrimental effects are induced by lung failure causing severe hypoxia in all tissues.

The main results to discuss are summarized in the following points:

- SARS-CoV-2 antigens: both pulmonary and renal tissues present capsid antigens, respectively, in the bronchial epithelia and alveolar pneumocytes, as well as in the tubular epithelial and capillary endothelial cells, but the organ with the heaviest burden of viral antigens is the lung, while their presence is negligible in the heart (rare endothelial cells of one case) and brain (rare pontine neurons of one case), with no evidence of active viral replication;

- inflammatory infiltrates: lymphocytic presence is most prominent in pulmonary and renal tissues, while the heart and brain display very scant lymphocytes with a clear predominance of the monocyte–macrophage–microglia compartment;
- comparison between COVID-19 and other types of pneumonia: T-lymphocytes were significantly more represented in the lungs infected by SARS-CoV-2;
- comparison between COVID-19 and control brains: in the frontal cortex of COVID-19 cases, there was a slight and non-significant microglial boosting that was probably related to pre-existing neurodegeneration (AD pathology), rather than to COVID-19, while microglial hyperactivation was significantly higher in the pons of COVID-19 cases, showing several microglial nodules that appeared to be specifically related to SARS-CoV-2 infection;
- microthrombosis: while it is a frequent finding across all organs, it appears to represent a specific COVID-19 feature only in the lungs.

### *5.1.1. SARS-CoV-2 ANTIGENS*

The parallel comparison between organs confirmed that each tissue interacted differently with SARS-CoV-2, showing interesting similarities and differences. As previously observed by us and other authors<sup>65,67,116</sup> SARS-CoV-2 replicates predominantly, and persists for longer periods, in the alveolar and bronchial epithelium (five cases), where it induces severe cytopathic effects (atypia and death of type-2 pneumocytes). These findings correlate with the abundance of ACE2, TMPRSS2 serine threonine transmembrane protease, and basigin (CD147), which are expressed not only in the alveolar epithelia, but also in the bronchial

epithelia. CD147 is now being recognized as a secondary docking site that may increase SARS-CoV-2 virulence and tropism for the upper airways compared with SARS-CoV<sup>117,118</sup>.

Similarly, but to a lesser degree, the kidneys showed occasional viral antigens inside the tubular epithelial and capillary endothelial cells. The presence of viral particles in the tubular epithelium has also been reported in other studies<sup>69,119</sup> and may contribute to renal damage. Acute tubular injury is, in fact, often observed in severe COVID-19, and the cause is likely multifactorial; it may result from hypoxia, vascular dysfunctions, severe inflammation, and cytokine release syndrome, along with renal viral tropism, and its consequent direct cytopathic effect on tubular epithelial cells<sup>120</sup>. In renal tissues, the co-expression of ACE2 receptors and TMPRSS2 protease has been reported<sup>121,22,123</sup>. This information, coupled with our results, suggests that some viral replication may also take place in the kidneys.

In the heart, SARS-CoV-2 positivity was found only in the endocardium and endothelium of a single case. Even though many have found the presence of ACE2 and TMPRSS2 to be consistent in the heart (especially in people with heart comorbidities), our results suggest that myocardial damage is not imputable to direct viral assault. The virus probably penetrates the heart, but the lack of cytopathic findings and the viral antigen negativity, observed by us as well as by others<sup>124</sup>, indicates that the virus does not replicate within the heart, despite the presence of ACE-2 receptors that are, however, mainly expressed by endothelial cells. Further studies are required to elucidate the biological reasons for the absence of active viral replication in the myocardium. It is possible that multiple alternative causes concur with the cardiac damage, among which, invariably, are generalized hypoxia, inflammatory damage, and microangiopathy<sup>62,125</sup>.

From a neuropathological standpoint, our data suggest that SARS-CoV-2 slightly penetrates the brain, but does not actively replicate within it. In the brain tissue, ACE2 and

TMPRSS2 are very scarcely present<sup>125,126</sup>. Indeed, our results demonstrate very limited traces of viral proteins in a cluster of neurons located in the pons of a single case. The antigen positivity likely results from virions or viral particles ascending from the respiratory and pharyngeal mucosa through the lower cranial nerves. This hypothesis is in line with the findings reported by Matschke et al.<sup>46</sup>, who identified SARS-CoV-2 in the lower cranial nerves. SARS-CoV-2 may also be present in the brain through the direct infection of endothelial cells that have a receptor structure favoring direct infection by the virus. Indeed, some authors have reported the sporadic presence of viral antigens within the brain endothelia<sup>44,54,127</sup> and the possible occurrence of endotheliitis<sup>52,53,128</sup>.

Our data suggest that SARS-CoV-2 causes an acute infection with progressive “cleaning” of the virus from the affected tissues. In particular, the virus was not detectable in four out of nine of the COVID-19 lungs, while a significant inflammatory infiltrate persisted in all cases. Along with other studies<sup>45,129</sup>, our data indicate that, similar to SARS-CoV and MERS-CoV, SARS-CoV-2 does not produce a persistent infection. Eventually, the virus is cleared from the tissues it infects; nonetheless, the consequences of the disease may last longer, resulting in persistent symptoms lasting weeks to months after the acute phase. Hence, an accurate analysis of the inflammatory phenomena that accompany SARS-CoV-2 infection is important.

### 5.1.2. INFLAMMATORY INFILTRATES

Examining the inflammatory infiltrates more closely, it is evident how the lymphocytic component is essentially more prominent in the lungs, less prevalent, but still relevant, in the kidneys, and negligible, if not absent, in the heart and brain. In particular, the sum of lymphocytes showed the highest scores in the pulmonary and renal tissues, where it tended to be superimposable. Although the lungs and kidneys seemed to behave similarly, the lungs

actively reacted to the massive viral invasion and replication, which was not so evident in the renal tissue. Indeed, T-lymphocytes were significantly more prominent inside the pulmonary infiltrates. This was probably a specific adaptive immune response against the intense viral replication, as demonstrated by the presence of the highest T-lymphocyte scores in association with the abiding positivity for SARS-CoV-2.

Contrarily, the heart and brain, which were less directly affected by the infection, displayed a scant lymphocytic presence, and the preponderance of macrophages and microglial cells, respectively, as a non-specific immune response (innate immunity) to antigenic perturbation and immune-complex formation. In the heart samples, we observed moderate macrophage infiltration in two cases. Such findings confirm the possibility of a macrophagic inflammatory response in the heart that has also been reported by others<sup>130</sup>. It is not yet clear whether this finding may represent a pathophysiological basis for the occasional reported cases of myocarditis and/or pericarditis in the literature<sup>131,132,133</sup>. Overall, pathological reports regarding the heart have yielded inconsistent results, and the mechanism of myocardial injury is probably multifactorial.

### *5.1.3. COMPARISON BETWEEN COVID-19 AND OTHER TYPES OF PNEUMONIA*

It is noteworthy that COVID-19 and non-COVID types of pneumonia share the same pathology with congestion, edema, DAD with septal lympho-monocytic infiltrates, and intra-alveolar exudate. A number of scientific articles have recently been published regarding the pulmonary features of COVID-19, describing several clinical, radiologic, and autopsy findings that closely resemble those seen in SARS and MERS cases, and also in other types of viral pneumonia, such as H1N1 flu cases<sup>68</sup>. These observations are consistent with ours; in particular, DAD emerges as a common key pathophysiological mechanism. Such findings suggest that the pathophysiology of alveolar damage in SARS-CoV-2 infection is the same as that of other known causes of acute respiratory distress syndrome (ARDS). Nonetheless, our results outline

the prominent T-lymphocyte response precisely in the site of the greatest viral replication. Indeed, even with a similar inflammatory infiltrate, a significantly greater presence of T lymphocytes was observed in COVID-19 lungs compared with the control ones. The relevant presence of T lymphocytes underlines the role of these cells in the specific response where viral replication is particularly active. We can assume that such a response may be common to other types of pneumonia with purely viral etiology.

#### *5.1.4. COMPARISON BETWEEN COVID-19 AND CONTROL BRAINS*

Brain pathology is characterized by the hyperactivation of microglia that exhibit amoeboid morphology and phagocytic properties, which have also been described by others<sup>50,53</sup>. In turn, microglial amoeboid cells tend to agglomerate into micronodules. When comparing the frontal lobe of people with COVID-19 with that of matched controls, we found similar features. It should be considered that they were almost always elderly people with cognitive problems affected by some degree of pre-existing vascular or degenerative pathologies that, per se, induced cortical hypoxia and inflammatory changes. Indeed, we have already reported that, in those cases with dementia, the distribution of the inflammatory nodules closely paralleled that of amyloid plaques, regardless of SARS-CoV-2 infection. Instead, regardless of the cognitive state, microglial hyperactivation was significantly more intense in the pontine structures of COVID-19 cases compared with controls. This phenomenon, also observed by others<sup>46,53</sup>, appears to be specific to the “COVID-19 encephalopathy” and may be activated by viral debris and isolated virions originating from the tracheobronchial and oropharyngeal mucosa through the lower cranial nerves<sup>46</sup>. Moreover, microglial activation in the brain is probably enhanced by infection-induced cytokine release and blood–brain barrier damage due to immune complex formation<sup>53</sup>. The topography of inflammatory lesions during SARS-CoV-2 infection represents the neuropathological basis of “COVID-19

encephalopathy”, which clinically presents as behavioral changes, lethargy, vegetative and autonomic dysfunctions, and absence of hypoxic drive<sup>43,53</sup>.

The overall impact triggered by hypoxia and inflammation may accelerate neurodegeneration, causing the so-called “brain fog” occurring after the acute phase of the disease. These phenomena may be enhanced in the elderly by the presence of a pre-existing degenerative burden, which causes microglial priming that, in turn, results in a more intense inflammatory response, favored by “immunological senescence” (lowered adaptive immunity with lower lymphocytic specific response) and “inflammaging” (age-related hyperactivation of innate immunity leading to an excessive non-specific inflammatory reaction)<sup>135,136,137</sup>. Where there was no active viral replication, a non-specific macrophage–microglial response predominated, which, in elderly subjects, can be favored by the neurodegenerative load, hence demonstrating the importance of a comparison that included patients with AD (the most common neurodegenerative disease).

Although several authors have proposed theories regarding a possible neurotropism of SARS-CoV-2 and its possible persistence in the CNS causing long-term consequences<sup>138,139</sup> in our cases, the brain showed scant lymphocytic infiltration and very limited traces of SARS-CoV-2 antigens with no associated evidence of viral replication and encephalitis. The pathological features we have shown are quite different from those of viral encephalitis caused by neurotropic viruses<sup>140</sup>, in which the presence of abundant viral antigens, abundant lymphocyte infiltrate, and direct cytopathic effects are observed, as well as that occurring in the lung. From these observations and literature analysis, it is inferred that SARS-CoV-2 is probably not a neurotropic virus and, importantly, there is no evidence proving its persistence within the brain after acute infection, at least in most cases.

#### 5.1.5. MICROTHROMBOSIS

Regarding the occurrence of thrombosis and microthrombosis, it should be considered that these phenomena, due to both clotting and endothelial alterations, are described in more than half of COVID-19, SARS, and MERS cases, while they are fairly less common in pneumonia caused by A/H1N1. Such findings suggest that thrombotic complications may be more specifically correlated with beta-CoVs than flu viruses<sup>68,141,142</sup>. In our study, we did not observe gross abnormalities, thrombosis of the large vessels, or infarcts; these phenomena have been reported by others<sup>143,144,145</sup> and are probably related to a protracted clinical course, which was not the case in our series. Nonetheless, we noted frequent microthrombosis in all organs. In particular, this phenomenon was significantly more prominent in COVID-19 lungs compared with control lungs affected by non-COVID pneumonia. This confirms that microthrombosis is an event specific to SARS-CoV-2 infection. The pathology of such a phenomenon may be explained by Virchow's triad: (1) the endothelial dysfunction and endothelial damage due to viral tropism and endotheliitis<sup>24</sup>; (2) the hypercoagulability state and increased blood viscosity due to the release of damage-associated molecular patterns (DAMPS) and to the higher load of cytokines, immunoglobulins, and immune complexes traveling within the blood<sup>146,147</sup>; and (3) the prolonged stasis that may result from immobilization during hospitalization. Microthrombosis in the lungs is an event specific to SARS-CoV-2 pneumonia and contributes to the clinical severity, lung failure, and mortality.

Our results confirm that thrombosis inside small pulmonary vessels is a COVID-specific phenomenon. The same cannot be stated for the small vessels of the brain, in which microthrombi are present both in cases and in controls, and are probably more related to prolonged agony, co-morbidities, and post-mortem phenomena, rather than to SARS-CoV-2 infection. Indeed, the only young case (COV2) with rapid death and no concomitant pathologies had little or no presence of microthrombi in all organs, suggesting a possible contribution of agony length, age, and co-morbidities to platelet aggregation inside small vessels.

## 5.2. COVID-19-related neuropathology and microglial activation

A further investigation was carried out of several part of brain samples. The main outcomes of this evaluation can be summarized in the following:

- All COVID-19 cases show remarkable non-SARS-CoV-2-specific changes including hypoxic-agonal alterations (without fresh infarcts), and a variable degree of neurodegeneration and/or pre-existent small vessels disease;
- The neuroinflammatory picture is dominated by the stimulated innate immune system (ameboid CD68 positive microglia), particularly prominent in the brainstem, while only scant lymphocytic presence and very few traces of SARS-CoV-2 have been detected;
- Microglial activation in the brainstem is significantly greater in COVID-19 cases than in non-COVID cases ( $p = 0.046$ ), and all COVID-19 cases without dementia show intense microglial activation particularly in the brainstem with a scarce cortical involvement;
- Microglial activation in the frontal cortex and hippocampus is associated with NCD due to AD pathology rather than COVID-19,
- In COVID-19 cases complicated by delirium (all with some degree of NCD), there is a significantly higher microglial activation in the hippocampus ( $p = 0.048$ ).

Fresh vascular lesions are described by other authors, mostly in patients with a history of atrial fibrillation, heart failure or mechanical ventilation<sup>46,52,148</sup>. In contrast, brain samples from our COVID-19 cases do not show acute vascular lesions, probably, due to their clinical characteristics. Indeed, they had no pre-existing severe heart disease, nor were they subjected to mechanical ventilation during their relatively short clinical course. This fact may suggest that

acute vascular changes are not directly associated with COVID-19 but mainly a consequence of heart complications, prolonged lung failure, and mechanical ventilation. In our series, as in Solomon's series<sup>48</sup>, diffuse brain congestion, cortical oedema, neuronal loss, and microvascular changes including microbleeds appear clearly attributable to non-specific hypoxic phenomena or to pre-existing SVD.

In all brain samples from our COVID-19 subjects, the monocyte-microglia component clearly prevails over the lymphocyte component and there is no evidence of the activation of specific lymphocyte clones within the CNS. This picture is quite different from that of autoimmune or viral encephalitis in which frequent viral inclusions are detectable in the brain tissue and/or many lymphocytes are present<sup>140,149</sup>. To compare lymphocytic pattern, we have searched for lymphocytes in the control non-COVID cases and found an overall low number of them. Nonetheless, the 3 non-COVID/AD cases present a slight increase in the number of T lymphocytes, a phenomenon that becomes particularly relevant in the BB138 case, which shows a moderate perivascular lymphocytic infiltrate in the hippocampus. These data are consistent with the findings of Zotova and Togo who reported a possible increase in T lymphocytes in AD, especially in the hippocampus<sup>150</sup>. In their COVID-19 series, Matschke et al. reported a variable presence of T lymphocytes (from absent to mild or moderate) predominantly in the perivascular brainstem zones. Overall, the authors detected T lymphocytes more frequently than us, but it should be considered that only 5 of the 43 cases reported by Matschke had NCD (less than 12% of cases)<sup>46</sup>, while our COVID-19 series includes mainly elderly with NCD. Our observation of a lower number of lymphocytes in AD patients with COVID-19 seems to confirm Rakic's work describing a diminution of T lymphocytes (brain immunosuppression) in cases suffering from both advanced AD and severe systemic infection. Furthermore, our COVID-19 cases had marked lymphopenia, which in turn may have contributed to the reduced number of lymphocytes we have observed in the brain. Zotova and

Togo did not find any correlation between the activation of innate immunity (microglia) and the presence of lymphocytes, and these two phenomena appear partially independent<sup>150,152</sup>. Precisely, COVID-19 might induce dissociation of innate (microglia) from adaptive (lymphocytes) immunity. Indeed, apart from single peculiar cases showing specific and severe para-infectious autoimmune pictures, such as haemorrhagic or disseminated encephalomyelitis<sup>148,153</sup> non-specific innate immunity activation (namely microglial activation) seems to be prevalent in the great majority of SARS-CoV-2-induced brain alterations<sup>50,51,53,154,155</sup>. This phenomenon may be particularly pronounced in elderly patients who tend to have a worse prognosis due to immunological senescence (reduced adaptive immunity with decreased specific immune responses) and “inflammaging” (excessive inflammatory activation in aging)<sup>135,136,137</sup>. At the same time, the elderly are prone to greater neurological injury, due to both cerebrovascular comorbidities and the presence of degenerative alterations recruiting inflammation and “priming” microglia. The role of inflammatory processes in the pathogenesis of dementias is well known. Specifically in AD, microglia and activated astrocytes are relevant for the disease pathogenesis and its histopathology<sup>156,157,158,159</sup>. Nonetheless, microglial cells are extremely dynamic and their topographical distribution and activation states are complex and dependent on multiple factors. This explains the different microglial patterns observed in different immunological situations. Frequently, an increase in microglial activity occurs concurrently with neurodegeneration, while in other situations a decrease is observed<sup>151,1527</sup>.

Where and how does SARS-CoV-2 affect inflammatory response in the brain of older people with and without AD? A first consideration is that COVID-19 induces significant microglial activation in the brainstem, regardless of cognitive status and age; in fact, it is also present in the Cov2 case (the only young subject in this series). Therefore, the microglial activation in brainstem seems to be a specific COVID-19 effect ( $p = 0.046$ ). The particular

intensity of microglial activation in such anatomical region is also confirmed by neuronophagia features, as observed by us and by other authors<sup>50,53</sup>. Our study combined with others authors' study describing an important involvement of the brainstem<sup>46,50,53,154</sup>, provide evidence that the trans-synaptic route through the cranial nerves may be the preferred point of entry of virions or viral antigens to the CNS. These viral particles then probably activate a response with a prevalent topographical distribution in this anatomic area. This interpretation is confirmed by the clear antigenic positivity for SARS-CoV-2 found by Matschke and colleagues in the lower cranial nerves. The clinical impact of these phenomena cannot be ascertained; however, it is possible that this inflammatory damage contributed to the lethargy, the neurovegetative alterations and the central component of respiratory failure manifested by some patients, as signs of brainstem dysfunction. On the other hand, the comparison between AD cases with and without COVID-19 demonstrates relevant cortical microglial activation and microglial nodules in AD, regardless of the SARS-CoV-2 infection. The occurrence of COVID-19 in AD cases appears to add only a slight boosting of the already present cortical microglial activation.

Nevertheless, microglial enhancement in the hippocampus appears to be clinically relevant in COVID-19 patients affected by NCD. Particularly, the hippocampi of cases Cov1,3,9 who all suffered from hyperactive delirium show higher inflammatory changes, and COVID-19 cases with delirium have a significantly higher microglial activation in the hippocampus than COVID-19 cases without delirium ( $p = 0.048$ ). Also, our data confirm and reinforce what was reported in a previous interesting study describing the inflammatory brain changes of 9 elderly patients who died in close temporal association with an episode of delirium, just like our COVID-19 cases. Probably for these reasons, COVID-19 patients with NCD are more prone to the "COVID-19 encephalopathic syndrome" with unfavourable clinical and prognostic consequences<sup>42,52,161</sup>. Through a tragic "natural experiment", SARS-CoV-2 is helping shed some light on the neuropathology underlying behavioural symptoms and delirium,

as signs of limbic system dysfunction, which seem to be related to both degenerative load and microglial boosting in the hippocampus.

Regarding the role of sepsis, in our COVID-19 cases there are no significant differences in microglial activation in relation to the absence or presence of severe bacterial superinfection. Nevertheless, it is interesting to note that our septic COVID-19 cases show a clear trend towards less microglial activation in the white matter. Although not statistically significant, again due to the low number of cases ( $p = 0.16$ ; Table 2), this trend is line with Rakic observation of microglial rarefaction in the white matter of advanced AD cases affected by severe bacterial infection<sup>151</sup>. Even if the neuropathology of “COVID-19 encephalopathic syndrome” resembles that of “septic encephalopathy”, which is also related to similar neurological manifestations including behavioural changes and delirium<sup>162,163</sup>, we observed some important qualitative differences between the neuropathology described in septic patients<sup>162</sup> and the one observed in our COVID-19 cases. Indeed, microglial activation in sepsis is much more disseminated and intense in the white matter with scant nodules. Instead, our cases showed several microglial nodules in the cortex and in the lower brainstem, and less in the white matter. It is intriguing to hypothesize that this topography may have a specific reason. It might be caused by the degenerative burden in the cortex and by the presence of viral antigens in the lower brainstem, where traces of viral immunoreactivity were found by us and others<sup>46,47</sup>. From this standpoint, we chose to include in the study a young SARS-CoV-2 positive individual, with no known symptoms, who died in a tragic fatality upon returning from work (Cov2 case). His neuropathology shows microglial activation with a peculiar topography (moderate in the frontal WM and severe in the lower brainstem). It is probable that, due to the absence of coexisting neurodegenerative lesions, neuroinflammation is not present in the brain cortex of this case, demonstrating that microglial reaction is case-specific and related to the personal clinical history.

As noted by Kantonen and other authors, the microvascular changes are caused by virus-triggered endotheliitis, hypoxia or pre-existing SVD<sup>51,52,53</sup>. We do not observe a clear picture of endotheliitis. However, a number of our COVID-19 cases (Cov1, 8, 9, 10) show perivascular gliosis with a very peculiar astrocytic endfeet enhancement, mainly at the capillary level, suggesting an inflammatory reinforcement of the blood-brain barrier. Moreover, in several of our cases (Cov1, 2, 5, 6, 9, 10 as well as BB118, 71, 137, 138, 210), we caught another peculiar feature of the capillary endothelium attributable to focal chaotic proliferation leading to the formation of ramified tuft-like structures. This alteration appears much more evident in the pons of COVID-19 cases but, to a lesser extent, it is also common in non-COVID cases. To the best of our knowledge, there are no similar descriptions for SARS-CoV-2 infection, mostly because CD34 staining for endothelium was not considered in previous studies. Instead, a very similar endothelial picture was observed in a case of encephalitis caused by the human BK polyomavirus<sup>164</sup>, occasionally in AD brains<sup>165</sup>, as observed by us, and in brain specimens from the temporal lobe of patients who previously underwent surgery for epilepsy. This CD34 picture has been described as “vascular buds” or “CD34-positive clusters”, and, currently, we report it as “CD34-tufts”. At the moment, the nature of these CD34-tufts is uncertain, but we can say they do not seem to possess any neoplastic proliferative characteristics nor are they associated with ischemic type lesions. In fact, examining the same sections with HE, no particular alteration of the tissue is noted. It is not clear whether CD34 tufts can be considered a form of endotheliitis, but their topographical association with activated microglia is evident. Therefore, CD34 tufts constitute a histological phenomenon associated with inflammation, and it is not surprising to find them abundantly in association with COVID-19, where they constitute a typical, although not specific, manifestation.

In line with the findings of other authors, our study confirms that the neuropathological alterations strictly attributable to the SARS-CoV-2 infection are overall modest, inflammatory

in nature and prevalent in the brainstem<sup>46,50,53,154</sup> where very rare viral inclusions were detected. Although traces of viral antigens and viral RNA (possibly blood-borne) have certainly been identified within the CNS by several authors<sup>46,48</sup> and also by us, such a few viral traces and scant lymphocytes argue against the presence of encephalitis and active viral replication within the CNS, and they do not suggest a neurotropism of SARS-CoV-2.

### **5.3. Presence of viral RNA in brain and Transcriptomic evaluations**

SARS-CoV-2 infection can cause severe pulmonary disease and complications with possible multi-organ consequences involving CNS<sup>167</sup>. The most frequent neurological manifestation of COVID-19 in patients with dementia is a non-specific encephalopathy with behavioural changes, such as psychomotor retardation and delirium, typical of several infective-inflammatory diseases<sup>43,112</sup>. These clinical manifestations may be due to non-specific pathological phenomena that can be attributed to inflammatory state, hypoxia, and sepsis, possibly superimposed on pre-existing neurodegenerative or vascular pathologies. At gross neuropathological examination, we could not find fresh macroscopic vascular lesions. All COVID-19 brains show congestion, oedema, and neuronal damage. These alterations are not SARS-CoV-2-specific but related to hypoxic-agonic and post-mortem phenomena. Also, other pathological findings such as AD pathology and SVD are clearly pre-existent conditions and cannot be considered virus-specific. On the other hand, we observed perivascular inflammatory infiltrates and nodules that are, probably, attributable to SARS-CoV-2. The inflammatory infiltrates consist essentially of cells of the innate immunity (monocyte-macrophage-microglia series) with very rare lymphocytes. Although the small number of cases does not allow us to draw firm conclusions, it is interesting to note that the inflammatory load appears greater in cases with dementia and with the greatest amount of viral RNA.

For a deeper understanding of the pathogenic processes induced by SARS-CoV-2 in the CNS, the neuropathological data should be supplemented with biochemical data. Therefore, detecting the presence of the virus in CNS, and the biochemical alterations induced by the virus, is crucial for the interpretation of the brain pathophysiology of COVID-19. Viral SARS-CoV-2 infection causes alterations in transcriptome of affected cells and tissues, as lung and peripheral blood mononuclear cells<sup>168,169,170</sup>. Starting from the evidence that transcriptomic

profile may be altered by SARS-CoV-2 infection and considering previous data<sup>44,171,172</sup> about a CNS involvement, a RNA-sequencing of frontal basal cortex was performed at Genomic and Post Genomic Unit, IRCCS Mondino Foundation to characterize the gene expression profile of COVID-19 patients.

First, we checked for the presence of viral RNA demonstrating that SARS-CoV-2 RNA was detectable by qRT-PCR only in one sample, while using a more sensitive method, ddPCR, it was appreciable in almost all COVID-19 samples (88%). Interestingly, literature reports that in COVID-19 brain tissue (not specifically in frontal cortex) viral RNA is detectable in few samples or fewer<sup>46,48,159</sup>. We showed that detection of virus in brain tissue was increasable to 90% through ddPCR<sup>174</sup>. Indeed, it should be considered that the time elapsed between the acute infection and the death is relevant for virus clearance and, probably, affects the presence of SARS-CoV-2 inside the brain. Thus, it is necessary to use an extremely sensitive method. In any case, the low amount of viral RNA detected does not allow to distinguish whether the virus is located in brain parenchyma or in brain blood vessels. However, these data, together with the absence of a specific neuropathological picture of encephalitis, testify to the absence of viral replicative activity within the brain.

About transcriptome profiling results, we found that 11 genes were differential expressed when frontal cortex of COVID-19 patients was compared to controls. These genes fall into categories including hypoxia, haemoglobin stabilizing protein, hydrogen peroxide processes, which all play important roles in SARS-CoV-2 infection<sup>175,176,177</sup>. Interesting, in our work three genes belongs to hypoxia-inducible factor (HIF) family genes have been found down-regulated. HIFs are transcription factors that respond to decrease in cellular environment oxygen or hypoxia<sup>178,179</sup>. Inhibition of specific HIFs has been found in SARS-CoV-2 infected cells<sup>180</sup> and it has been shown that inhibition of HIF-1 can promote replication of influenza A virus and severe inflammation mediated via promotion of autophagy<sup>181</sup>. Our data showed a

reduction of HIF suggesting a possible inhibition of defense capacity of macrophages in cases of infection. In fact, HIF pathway usually plays a protective role after injury and promotes cell recovery that in COVID-19 patients is not possible due to HIF down-regulation<sup>182</sup>. Previous work reported that the HIF response is variable depending upon the type of hypoxic stress<sup>183</sup>. Particularly, HIF was induced by chronic or intermittent hypoxia<sup>184</sup>. Our COVID-19 cases had a severe acute hypoxia due pulmonary failure, which was not corrected through mechanical ventilation. As highlighted by the neuropathological picture, this peculiar condition caused an extreme hypoxic suffering of the brain, which, probably, induced a down-regulation of the HIF response, thus creating a vicious circle that might be important in COVID-19 pathogenesis.

About up-regulated genes, the most relevant data concerned hemoglobin (HB) subunits increase. Hb up-regulation may be linked to downregulation of HIFs<sup>184</sup>. Moreover, Hb overexpression may be a protective system against oxidative stress. In fact, it has been demonstrated that Hb overexpression may be neuroprotective<sup>185</sup>.

About lncRNA CTB-36O1.7, an uncharacterized gene, it has been found associated to Multiple Sclerosis in brain. Although its role is still unknown, this finding may confirm a role of lncRNA CTB-36O1.7 in inflammation and in the regulation of microglia. The neuropathological picture observed in our COVID-19 cases is characterized by microglial activation, in the absence of clear signs of encephalitis due to viral replication. Thus, our data corroborates the involvement of lncRNA CTB-36O1.7 in the activation of microglia and innate immunity rather than in adaptive immunity linked to an active infection.

## 5.4. Limitations and strength of the study

This research work has some limitations:

- the low number of cases of mainly elderly people, who happen to constitute the most affected population, thus representing an interesting standpoint;
- this study essentially refers to patients of senile age, therefore, the generalizability of the results can only be referred to elderly subjects and should be interpreted with caution because of the small number of cases. The data would require confirmation from more extensive series
- the lack of RNA samples from all tissues apart from the frontal lobe, as most tissue samples from the autopsy were immediately formalin-fixed and paraffin-embedded for safety reasons, making subsequent RNA extraction very difficult in terms of quality and quantity;
- the predominance of superimposed bacterial infection in the control lungs, making them “not pure” controls for viral pneumonia; however, superimposed bacterial infection was also very frequent in SARS-CoV-2 pneumonia.
- PMI varies greatly among controls and COVID-19 subjects. The control ABB cases differ from the COVID-19 cases for the post mortem-time which was much shorter (from 2 to 16 h). The PMD was necessarily different because the ABB protocol implies an autopsy performed no later than 30 h after death. Instead, the COVID-19 autopsies followed the course of the forensic roles. Anyway, there was no evident impact on immunohistochemical reactions used for this study.

The strength of this research is the focus on histological differences between organs and tissues of clinically well-documented COVID-19 cases, along with the comparison with

lungs and brains from non-COVID matched controls to estimate the specific role of SARS-CoV-2 in determining the pathological changes. Furthermore, we developed a method for histological assessment that considered large areas of tissue to select the most affected zones of an individual organ, which were used for scoring. This approach was proven effective in characterizing and comparing the inflammatory infiltrates.

## 6. CONCLUSIONS

We can conclude that:

- Hypoxia, a well-known condition associated to COVID-19 infection, is a multi-organ feature (lung, kidney, and hearth) that marks even the CNS, and specifically brain cortex. Our data showed an important deregulation of hypoxia inducing factor system that inhibits defense system from infection.
- Viral RNA is present at very low amount in frontal cortex tissues. As a matter of fact, COVID-19 detection is variable; therefore a sensitive method is required to reveal the viral RNA. The quantity of viral RNA is minimal, thus, it is likely that SARS-CoV-2 does not actively infect and replicate in the brain.
- COVID-19 patients with NCD and delirium are characterized by microglial boosting in the hippocampus – microglial activation associated with TAU-pathology.
- viral replication appears to be active and have a direct pathogenetic role in the lungs and, to a lesser degree, in the kidneys;
- the type of infiltrate depends on the relationship that the virus establishes with the tissue; in particular, the more active viral replication is, the more T-lymphocytes are present, while a macrophage–microglial response predominates where there is no evidence of active viral replication;
- the most specific COVID-19 pathological features consist of an abundance of T-lymphocytes and microthrombosis at the pulmonary level, and relevant microglial hyperactivation in the brainstem.

A careful examination of the pathological pictures present in the various tissues is the basis for understanding acute and long-term symptoms. Overall, our findings suggest that tissue

damage in the lungs and kidneys may be caused by a direct viral cytopathic effect along with inflammation-mediated mechanisms. On the other hand, the heart and brain may be damaged mainly by an abnormal and persistent inflammation. The presence of sequelae across all organs appears to be the result of a combination of the aforementioned factors. It is probable that a complete recovery from COVID-19 requires the termination of both viral infection and the associated inflammation, which can take many months. The biologically detrimental effects of SARS-CoV-2 infection and related inflammatory changes are at least partially reversible. A deeper understanding of these phenomena is important to improve the management of COVID-19 patients, also after the acute phase.

The analysis carried out presents considerable points of interest for the interpretation of the interactions between neurodegenerative diseases, systemic inflammation and behavioral disorders, even beyond the SARS-CoV-2 infection. A better understanding of the pathogenesis of behavioral alterations in neuro-cognitive disorders may have practical repercussions on therapeutic approaches for delirium. If delirium occurs in a context of systemic inflammation with microglial activation, it could greatly benefit from drugs capable of inhibiting microglia, such as simple corticosteroids. In this perspective, COVID-19 can represent a useful “natural experiment” of severe systemic inflammation, from which much can be learned.

A handwritten signature in black ink, reading "Matteo Moretti". The signature is written in a cursive, slightly slanted style. The first name "Matteo" is written with a large, sweeping initial 'M', and the last name "Moretti" follows with a similar style.

## 7. REFERENCES

1. Lu R, Zhao X, Li J, Niu P, Yang B, Wu H, Wang W, Song H, Huang B, Zhu N, Bi Y, Ma X, Zhan F, Wang L, Hu T, Zhou H, Hu Z, Zhou W, Zhao L, Chen J, Meng Y, Wang J, Lin Y, Yuan J, Xie Z, Ma J, Liu WJ, Wang D, Xu W, Holmes EC, Gao GF, Wu G, Chen W, Shi W, Tan W. Genomic characterisation and epidemiology of 2019 novel coronavirus: implications for virus origins and receptor binding. *Lancet*. 2020 Feb 22;395(10224):565-574. doi: 10.1016/S0140-6736(20)30251-8. Epub 2020 Jan 30. PMID: 32007145; PMCID: PMC7159086.
2. WHO website [https://www.who.int/emergencies/diseases/novel-coronavirus-2019?gclid=EAIaIQobChMI98fR-4qO6glVsbTtCh1hVwulEAAYASAAEgJE7fD\\_BwE](https://www.who.int/emergencies/diseases/novel-coronavirus-2019?gclid=EAIaIQobChMI98fR-4qO6glVsbTtCh1hVwulEAAYASAAEgJE7fD_BwE)
3. Wuhan City Health Committee (WCHC). Wuhan Municipal Health and Health Commission's briefing on the current pneumonia epidemic situation in our city 2019. updated 31 December 2019-14 January 2020. <http://wjw.wuhan.gov.cn/front/web/showDetail/2019123108989>
4. Tan WJ, Zhao X, et al. A novel coronavirus genome identified in a cluster of pneumonia cases - Wuhan, China 2019-2020. *China CDC Weekly* 2020;2:61-2.
5. Lvov DK, Alkhovskiy SV, Kolobukhina LV, Burtseva EI. [Etiology of epidemic outbreaks COVID-19 on Wuhan, Hubei province, Chinese People Republic associated with 2019-nCoV (Nidovirales, Coronaviridae, Coronavirinae, Betacoronavirus, Subgenus Sarbecovirus): lessons of SARS-CoV outbreak.]. *Vopr Virusol*. 2020;65(1):6-15. Russian. doi: 10.36233/0507-4088-2020-65-1-6-15. PMID: 32496715
6. Guo YR, Cao QD, Hong ZS, Tan YY, Chen SD, Jin HJ, Tan KS, Wang DY, Yan Y. The origin, transmission and clinical therapies on coronavirus disease 2019 (COVID-19) outbreak - an update on the status. *Mil Med Res*. 2020 Mar 13;7(1):11. doi: 10.1186/s40779-020-00240-0. PMID: 32169119; PMCID: PMC7068984.
7. Zhu, Z.; Lian, X.; Su, X.; Wu, W.; Marraro, G.A.; Zeng, Y. From SARS and MERS to COVID-19: A brief summary and comparison of severe acute respiratory infections caused by three highly pathogenic human coronaviruses. *Respir. Res*. 2020, 21, 224.
8. Worobey M, Levy JI, Malpica Serrano L, Crits-Christoph A, Pekar JE, Goldstein SA, Rasmussen AL, Kraemer MUG, Newman C, Koopmans MPG, Suchard MA, Wertheim JO, Lemey P, Robertson DL, Garry RF, Holmes EC, Rambaut A, Andersen KG. The Huanan Seafood Wholesale Market in Wuhan was the early epicenter of the COVID-19 pandemic. *Science*. 2022 Aug 26;377(6609):951-959. doi: 10.1126/science.abp8715. Epub 2022 Jul 26. PMID: 35881010; PMCID: PMC9348750.
9. J. Pekar, M. Worobey, N. Moshiri, K. Scheffler, J. O. Wertheim, Timing the SARS-CoV-2 index case in Hubei province. *Science* 372, 412–417 (2021).
10. Yadav R, Chaudhary JK, Jain N, Chaudhary PK, Khanra S, Dhamija P, et al. Role of structural and non-structural proteins and therapeutic targets of SARS-CoV-2 for COVID-19. *Cells*. (2021) 10:821. doi: 10.3390/cells10040821
11. Wang H, Li X, Li T, Zhang S, Wang L, Wu X, Liu J. The genetic sequence, origin, and diagnosis of SARS-CoV-2. *Eur J Clin Microbiol Infect Dis*. 2020 Sep;39(9):1629-1635. doi: 10.1007/s10096-020-03899-4. Epub 2020 Apr 24. PMID: 32333222; PMCID: PMC7180649.
12. Pavan M, Bassani D, Sturlese M, Moro S. From the Wuhan-Hu-1 strain to the XD and XE variants: is targeting the SARS-CoV-2 spike protein still a pharmaceutically relevant option against COVID-19? *J Enzyme Inhib Med Chem*. 2022 Dec;37(1):1704-1714. doi: 10.1080/14756366.2022.2081847. PMID: 35695095; PMCID: PMC9196651.
13. F. Hikmet, L. Méar, M. Uhlén, C. Lindskog The protein expression profile of ACE2 in human tissues  
BioRxiv, 2020 (2020) 2003.2031.016048
14. F. Qi, S. Qian, S. Zhang, Z. Zhang Single cell RNA sequencing of 13 human tissues identify cell types and receptors of human coronaviruses *Biochem. Biophys. Res. Commun.*, 526 (2020), pp. 135-140
15. Y. Zhao, Z. Zhao, Y. Wang, Y. Zhou, Y. Ma, W. Zuo Single-cell RNA expression profiling of ACE2, the receptor of SARS-CoV-2 *BioRxiv*, 2020 (2020) 2001.2026.919985

16. Kirtipal N, Kumar S, Dubey SK, Dwivedi VD, Gireesh Babu K, Malý P, Bharadwaj S. Understanding on the possible routes for SARS CoV-2 invasion via ACE2 in the host linked with multiple organs damage. *Infect Genet Evol.* 2022 Apr;99:105254. doi: 10.1016/j.meegid.2022.105254. Epub 2022 Feb 23. PMID: 35217145; PMCID: PMC8863418.
17. Jain U. Effect of COVID-19 on the Organs. *Cureus.* 2020 Aug 3;12(8):e9540. doi: 10.7759/cureus.9540. PMID: 32905500; PMCID: PMC7470660.
18. Wei, J., Alfajaro, M. M., DeWeirdt, P. C., Hanna, R. E., Lu-Culligan, W. J., Cai, W. L., et al. (2021). Genome-wide CRISPR Screens Reveal Host Factors Critical for SARS-CoV-2 Infection. *Cell* 184, 76–91.e13. doi:10.1016/j.cell.2020.10.028
19. Valero N, Larreal Y, Mosqueray J, Rincón E. Síndrome respiratorio agudo severo (SRAS). Lecciones y retos [Severe acute respiratory syndrome (SARS). Lesson and challenges]. *Invest Clin.* 2005 Mar;46(1):75-95. Spanish. PMID: 15782539.
20. Hwang SM, Na BJ, Jung Y, Lim HS, Seo JE, Park SA, Cho YS, Song EH, Seo JY, Kim SR, Lee GY, Kim SJ, Park YS, Seo H. Clinical and Laboratory Findings of Middle East Respiratory Syndrome Coronavirus Infection. *Jpn J Infect Dis.* 2019 May 23;72(3):160-167. doi: 10.7883/yoken.JJID.2018.187. Epub 2018 Dec 25. PMID: 30584196.
21. Hernandez Acosta RA, Esquer Garrigos Z, Marcelin JR, Vijayvargiya P. COVID-19 Pathogenesis and Clinical Manifestations. *Infect Dis Clin North Am.* 2022 Jun;36(2):231-249. doi: 10.1016/j.idc.2022.01.003. Epub 2022 Feb 1. PMID: 35636898; PMCID: PMC8806149.
22. Deshmukh, V.; Motwani, R.; Kumar, A.; Kumari, C.; Raza, K. Histopathological observations in COVID-19: A systematic review. *J. Clin. Pathol.* 2021, 74, 76–83.
23. Caramaschi, S.; Kapp, M.E.; Miller, S.E.; Eisenberg, R.; Johnson, J.; Epperly, G.; Maiorana, A.; Silvestri, G.; Giannico, G.A. Histopathological findings and clinicopathologic correlation in COVID-19: A systematic review. *Mod. Pathol.* 2021, 34, 1614–1633.
24. Wong, D.W.L.; Klinkhammer, B.M.; Djurdjaj, S.; Villwock, S.; Timm, M.C.; Buhl, E.M.; Wucherpfennig, S.; Cacchi, C.; Braunschweig, T.; Knüchel-Clarke, R.; et al. Multisystemic cellular tropism of SARS-CoV-2 in autopsies of COVID-19 patients. *Cells* 2021, 10, 1900.
25. Menter, T.; Haslbauer, J.D.; Nienhold, R.; Savic, S.; Hopfer, H.; Deigendesch, N.; Frank, S.; Turek, D.; Willi, N.; Pargger, H.; et al. Postmortem examination of COVID-19 patients reveals diffuse alveolar damage with severe capillary congestion and variegated findings in lungs and other organs suggesting vascular dysfunction. *Histopathology* 2020, 77, 198–209.
26. Wang M, Zhang N. Focus on the 2019 novel coronavirus (SARS-CoV-2). *Future Microbiol.* 2020 Jul;15:905-918. doi: 10.2217/fmb-2020-0063. Epub 2020 Jun 11. Erratum in: *Future Microbiol.* 2021 Mar;16:370. PMID: 32524843; PMCID: PMC729195.
27. Vakili K, Fathi M, Pezeshgi A, Mohamadkhani A, Hajiesmaeili M, Rezaei-Tavirani M, Sayehmiri F. Critical complications of COVID-19: A descriptive meta-analysis study. *Rev Cardiovasc Med.* 2020 Sep 30;21(3):433-442. doi: 10.31083/j.rcm.2020.03.129. PMID: 33070547.
28. Matsunaga N, Hayakawa K, Asai Y, et al. Clinical characteristics of the first three waves of hospitalised patients with COVID-19 in Japan prior to the widespread use of vaccination: a nationwide observational study. *Lancet Reg Health West Pac.* 2022 Mar 16;22:100421. doi: 10.1016/j.lanwpc.2022.100421. PMID: 35300186; PMCID: PMC8923875.
29. Hariyanto TI, Putri C, Arisa J, Situmeang RFV, Kurniawan A. Dementia and outcomes from coronavirus disease 2019 (COVID-19) pneumonia: a systematic review and meta-analysis. *Arch Gerontol Geriatr.* 2021;93:104299.
30. Wei Y, Wei L, Liu Y, Huang L, Shen S, Zhang R, Chen J, Zhao Y, Shen H, Chen F. Comprehensive estimation for the length and dispersion of COVID-19 incubation period: a systematic review and meta-analysis. *Infection.* 2022 Aug;50(4):803-813. doi: 10.1007/s15010-021-01682-x. Epub 2021 Aug 18. PMID: 34409563; PMCID: PMC8372687.
31. Zayet S, Kadiane-Oussou NJ, Lepiller Q, Zahra H, Royer PY, Toko L, Gendrin V, Klopfenstein T. Clinical features of COVID-19 and influenza: a comparative study on Nord Franche-Comte cluster. *Microbes Infect.* 2020 Oct;22(9):481-488. doi: 10.1016/j.micinf.2020.05.016. Epub 2020 Jun 16. PMID: 32561409; PMCID: PMC7297177.
32. Shang W, Kang L, Cao G, Wang Y, Gao P, Liu J, Liu M. Percentage of Asymptomatic Infections among SARS-CoV-2 Omicron Variant-Positive Individuals: A Systematic Review

- and Meta-Analysis. *Vaccines* (Basel). 2022 Jun 30;10(7):1049. doi: 10.3390/vaccines10071049. PMID: 35891214; PMCID: PMC9321237.
33. Bao C, Liu X, Zhang H, Li Y, Liu J. Coronavirus Disease 2019 (COVID-19) CT Findings: A Systematic Review and Meta-analysis. *J Am Coll Radiol*. 2020 Jun;17(6):701-709. doi: 10.1016/j.jacr.2020.03.006. Epub 2020 Mar 25. PMID: 32283052; PMCID: PMC7151282.
  34. Toori KU, Qureshi MA, Chaudhry A. Lymphopenia: A useful predictor of COVID-19 disease severity and mortality. *Pak J Med Sci*. 2021 Nov-Dec;37(7):1984-1988. doi: 10.12669/pjms.37.7.4085. PMID: 34912430; PMCID: PMC8613069.
  35. Rodriguez L, Pekkarinen PT, Lakshmikanth T, et al P. Systems-Level Immunomonitoring from Acute to Recovery Phase of Severe COVID-19. *Cell Rep Med*. 2020 Aug 25;1(5):100078. doi: 10.1016/j.xcrm.2020.100078. Epub 2020 Aug 5. PMID: 32838342; PMCID: PMC7405891.
  36. Priyadarshni S, Westra J, Kuo YF, Baillargeon JG, Khalife W, Raji M. COVID-19 Infection and Incidence of Myocarditis: A Multi-Site Population-Based Propensity Score-Matched Analysis. *Cureus*. 2022 Feb 3;14(2):e21879. doi: 10.7759/cureus.21879. PMID: 35265414; PMCID: PMC8898072.
  37. Rathore SS, Rojas GA, Sondhi M, Pothuru S, Pydi R, Kancharla N, Singh R, Ahmed NK, Shah J, Tousif S, Baloch UT, Wen Q. Myocarditis associated with Covid-19 disease: A systematic review of published case reports and case series. *Int J Clin Pract*. 2021 Nov;75(11):e14470. doi: 10.1111/ijcp.14470. Epub 2021 Jul 7. PMID: 34235815.
  38. Mao L, Jin H, Wang M, Hu Y, Chen S, He Q, et al. Neurologic manifestations of hospitalized patients with coronavirus disease 2019 in Wuhan, China. *JAMA Neurol*. 2020;77:683–90.
  39. Zubair AS, McAlpine LS, Gardin T, Farhadian S, Kuruvilla DE, Spudich S. Neuropathogenesis and neurologic manifestations of the coronaviruses in the age of coronavirus disease 2019: a review. *JAMA Neurol*. 2020;77:1018–27.
  40. Dantzer R. Cytokine-induced sickness behaviour: a neuroimmune response to activation of innate immunity. *Eur J Pharmacol*. 2004;500:399–411.
  41. Holmes C, Cunningham C, Zotova E, Culliford D, Perry VH. Proinflammatory cytokines, sickness behavior, and Alzheimer disease. *Neurology*. 2011;77:212–8.
  42. Kennedy M, Helfand BKI, Gou RY, Gartaganis SL, Webb M, Moccia JM, et al. Delirium in older patients with COVID-19 presenting to the emergency department. *JAMA Netw Open*. 2020;3:e2029540.
  43. Poloni TE, Carlos AF, Cairati M, Cutaia C, Medici V, Marelli E, et al. Prevalence and prognostic value of Delirium as the initial presentation of COVID-19 in the elderly with dementia: an Italian retrospective study. *EClinicalMedicine*. 2020;26:100490.
  44. Baig AM, Sanders EC. Potential neuroinvasive pathways of SARS-CoV-2: deciphering the spectrum of neurological deficit seen in coronavirus disease-2019 (COVID-19). *J Med Virol*. 2020;92:1845–57.
  45. Iadecola C, Anrather J, Kamel H. Effects of COVID-19 on the nervous system. *Cell*. 2020;183:16–27.
  46. Matschke J, Lütgehetmann M, Hagel C, Sperhake JP, Schröder AS, Edler C, et al. Neuropathology of patients with COVID-19 in Germany: a post-mortem case series. *Lancet Neurol*. 2020;19:919–29.
  47. Meinhardt J, Radke J, Dittmayer C, Franz J, Thomas C, Mothes R, et al. Olfactory transmucosal SARS-CoV-2 invasion as a port of central nervous system entry in individuals with COVID-19. *Nat Neurosci*. 2021;24:168–75.
  48. Solomon I.H., Normandin E., Bhattacharyya S., Mukerji S.S., Keller K., Ali A.S. Neuropathological Features of Covid-19. *N Engl J Med*. 2020
  49. von Weyhern C.H., Kaufmann I., Neff F., Kremer M. Early evidence of pronounced brain involvement in fatal COVID-19 outcomes. *Lancet*. 2020;395(10241) doi: 10.1016/S0140-6736(20)31282-4.
  50. Al-Dalahmah O., Thakur K.T., Nordvig A.S., Prust M.L., Roth W., Lignelli A., Uhlemann A.-C., Miller E.H., Kunnath-Velayudhan S., del Portillo A., et al. Neuronophagia and microglial nodules in a SARS-CoV-2 patient with cerebellar hemorrhage. *Acta Neuropathol. Commun*. 2020;8:147. doi: 10.1186/s40478-020-01024-2.

51. Jaunmuktane Z., Mahadeva U., Green A., Sekhawat V., Barrett N.A., Childs L., Shankar-Hari M., Thom M., Jäger H.R., Brandner S. Microvascular injury and hypoxic damage: Emerging neuropathological signatures in COVID-19. *Acta Neuropathol.* 2020;140:397–400. doi: 10.1007/s00401-020-02190-2.
52. Kirschenbaum D., Imbach L.L., Rushing E.J., Frauenknecht K.B.M., Gascho D., Ineichen B.V., Keller E., Kohler S., Lichtblau M., Reimann R.R., et al. Intracerebral endotheliitis and microbleeds are neuropathological features of COVID-19. *Neuropathol. Appl. Neurobiol.* 2021;47:454–459. doi: 10.1111/nan.12677.
53. Lee M.-H., Perl D.P., Nair G., Li W., Maric D., Murray H., Dodd S.J., Koretsky A.P., Watts J.A., Cheung V., et al. Microvascular Injury in the Brains of Patients with COVID-19. *N. Engl. J. Med.* 2021;384:481–483. doi: 10.1056/NEJMc2033369.
54. Bryce C., Grimes Z., Pujadas E., Ahuja S., Beth Beasley M., Albrecht R., Hernandez T., Stock A., Zhao Z., Al Rasheed M., et al. Pathophysiology of SARS-CoV-2: Targeting of endothelial cells renders a complex disease with thrombotic microangiopathy and aberrant immune response. *The Mount Sinai COVID-19 autopsy experience. Mod. Pathol.* 2021;34:1456–1467. doi: 10.1038/s41379-021-00793-y.
55. Kantonen J., Mahzabin S., Mäyränpää M.I., Tynnenen O., Paetau A., Andersson N., Sajantila A., Vapalahti O., Carpén O., Kekäläinen E., et al. Neuropathologic features of four autopsied COVID-19 patients. *Brain Pathol.* 2020;30:1012–1016. doi: 10.1111/bpa.12889
56. Crunfli F, Carregari VC, Veras FP, et al Morphological, cellular, and molecular basis of brain infection in COVID-19 patients. *Proc Natl Acad Sci U S A.* 2022 Aug 30;119(35):e2200960119. doi: 10.1073/pnas.2200960119. Epub 2022 Aug 11. PMID: 35951647; PMCID: PMC9436354.
57. Vasquez-Bonilla, W.O.; Orozco, R.; Argueta, V.; Sierra, M.; Zambrano, L.I.; Muñoz-Lara, F.; López-Molina, D.S.; Arteaga-Livias, K.; Grimes, Z.; Bryce, C.; et al. A review of the main histopathological findings in coronavirus disease 2019. *Hum. Pathol.* 2020, 105, 74–83.
58. Falasca, L.; Nardacci, R.; Colombo, D.; Lalle, E.; Di Caro, A.; Nicastri, E.; Antinori, A.; Petrosillo, N.; Marchioni, L.; Biava, G.; et al. Postmortem Findings in Italian Patients with COVID-19: A Descriptive Full Autopsy Study of Cases with and without Comorbidities. *J. Infect. Dis.* 2020, 222, 1807–1815.
59. Fox, S.E.; Akmatbekov, A.; Harbert, J.L.; Li, G.; Quincy Brown, J.; Vander Heide, R.S. Pulmonary and cardiac pathology in African American patients with COVID-19: An autopsy series from New Orleans. *Lancet Respir. Med.* 2020, 681–686.
60. Grosse, C.; Grosse, A.; Salzer, H.J.F.; Dünser, M.W.; Motz, R.; Langer, R. Analysis of cardiopulmonary findings in COVID-19 fatalities: High incidence of pulmonary artery thrombi and acute suppurative bronchopneumonia. *Cardiovasc. Pathol.* 2020, 49, 107263.
61. Edler, C.; Schröder, A.S.; Aepfelbacher, M.; Fitzek, A.; Heinemann, A.; Heinrich, F.; Klein, A.; Langenwalder, F.; Lütgehetmann, M.; Meißner, K.; et al. Dying with SARS-CoV-2 infection—An autopsy study of the first consecutive 80 cases in Hamburg, Germany. *Int. J. Leg. Med.* 2020, 134, 1275–1284.
62. Romanova, E.S.; Vasilyev, V.V.; Startseva, G.; Karev, V.; Rybakova, M.G.; Platonov, P.G. Cause of death based on systematic post-mortem studies in patients with positive SARS-CoV-2 tissue PCR during the COVID-19 pandemic. *J. Intern. Med.* 2021, 290, 655–665.
63. Borczuk, A.C.; Salvatore, S.P.; Seshan, S.V.; Patel, S.S.; Bussel, J.B.; Mostyka, M.; Elsoukary, S.; He, B.; DEL Vecchio, C.; Fortarezza, F.; et al. COVID-19 pulmonary pathology: A multi-institutional autopsy cohort from Italy and New York City. *Mod. Pathol.* 2020, 33, 2156–2168.
64. Schaller, T.; Hirschbühl, K.; Burkhardt, K.; Braun, G.; Trepel, M.; Märkl, B.; Claus, R. Postmortem Examination of Patients with COVID-19. *JAMA* 2020, 323, 2518–2520.
65. Bradley, B.T.; Maioli, H.; Johnston, R.; Chaudhry, I.; Fink, S.L.; Xu, H.; Najafian, B.; Deutsch, G.; Lacy, J.M.; Williams, T.; et al. Histopathology and ultrastructural findings of fatal COVID-19 infections in Washington State: A case series. *Lancet* 2020, 396, 320–332.
66. Duarte-Neto, A.N.; Monteiro, R.; Da Silva, L.F.F.; Malheiros, D.M.A.C.; De Oliveira, E.P.; Theodoro-Filho, J.; Pinho, J.R.R.; Gomes-Gouvêa, M.S.; Salles, A.P.M.; De Oliveira, I.R.S.; et

- al. Pulmonary and systemic involvement in COVID-19 patients assessed with ultrasound-guided minimally invasive autopsy. *Histopathology* 2020, 77, 186–197.
67. Elsoukkary, S.S.; Mostyka, M.; Dillard, A.; Berman, D.R.; Ma, L.X.; Chadburn, A.; Yantiss, R.K.; Jessurun, J.; Seshan, S.V.; Borczuk, A.C.; et al. Autopsy Findings in 32 Patients with COVID-19: A Single-Institution Experience. *Pathobiology* 2021, 88, 56–68.
  68. Hariri, L.P.; North, C.M.; Shih, A.R.; Israel, R.A.; Maley, J.H.; Villalba, J.A.; Vinarsky, V.; Rubin, J.; Okin, D.A.; Sclafani, A.; et al. Lung Histopathology in Coronavirus Disease 2019 as Compared With Severe Acute Respiratory Syndrome and H1N1 Influenza: A Systematic Review. *Chest* 2021, 159, 73–84.
  69. Su H, Yang M, Wan C, et al. Renal histo-pathological analysis of 26 postmortem findings of patients with COVID-19 in China. *Kidney Int* 2020;98:219-27
  70. Sánchez Tinajero Á, González Cueto E, Martínez Orozco JA, Becerril Vargas E, Ruiz Santillán DP, Reséndiz Escobar H. A 65-year-old woman with a history of type 2 diabetes mellitus and hypertension and a 15-day history of dry cough and fever who presented with acute renal failure due to infection with SARS-Cov-2. *Am J Case Rep* 2020;21:e926737
  71. Vishwajeet V, Krishna H, Ghatak S, Elhence PA, Ambwani S, Varthya SB. Renal Histopathological Changes in Coronavirus Disease 2019 Patients: A Systematic Review and Meta-analysis of Individual Patient Data. *Saudi J Kidney Dis Transpl.* 2021 Nov-Dec;32(6):1523-1544. doi: 10.4103/1319-2442.352410. PMID: 35946265.
  72. Roufousse C, Curtis E, Moran L, et al. Electron microscopic investigations in COVID-19: Not all crowns are coronas. *Kidney Int* 2020;98: 505-6.
  73. Santoriello, D.; Khairallah, P.; Bomback, A.S.; Xu, K.; Kudose, S.; Batal, I.; Barasch, J.; Radhakrishnan, J.; D’Agati, V.; Markowitz, G. Postmortem Kidney Pathology Findings in Patients with COVID-19. *J. Am. Soc. Nephrol.* 2020, 31, 2158–2167.
  74. Ahmed J, Rizwan T, Malik F, Akhter R, Malik M, Ahmad J, Khan AW, Chaudhary MA, Usman MS. COVID-19 and liver injury: a systematic review and meta-analysis. *Cureus.* 2020;12(7):e9424
  75. Phipps MM, Barraza LH, LaSota ED, Sobieszczyk ME, Pereira MR, Zheng EX, Fox AN, Zucker J, Verna EC. Acute liver injury in COVID-19: prevalence and association with clinical outcomes in a large US cohort. *Hepatology.* 2020;72(3):807–817. doi: 10.1002/hep.31404
  76. Lagana SM, Kudose S, Iuga AC, Lee MJ, Fazlollahi L, Remotti HE, Del Portillo A, De Michele S, de Gonzalez AK, Saqi A, Khairallah P, Chong AM, Park H, Uhlemann A-C, Lefkowitz JH, Verna EC. Hepatic pathology in patients dying of COVID-19: a series of 40 cases including clinical, histologic, and virologic data. *Mod Pathol.* 2020;33(11):2147–2155. doi: 10.1038/s41379-020-00649-x
  77. Bangash MN, Patel J, Parekh D. COVID-19 and the liver: little cause for concern. *Lancet Gastroenterol Hepatol.* 2020;5(6):529. doi: 10.1016/S2468-1253(20)30084-4.
  78. Mohammed SA, Eid KM, Anyiam FE, Wadaaallah H, Muhamed MAM, Morsi MH, Dahman NBH. Liver injury with COVID-19: laboratory and histopathological outcome-systematic review and meta-analysis. *Egypt Liver J.* 2022;12(1):9. doi: 10.1186/s43066-022-00171-6. Epub 2022 Jan 21. PMID: 35096428; PMCID: PMC8781706.
  79. Zhang Y., Zheng L., Liu L., Zhao M., Xiao J., Zhao Q. Liver impairment in COVID-19 patients: A retrospective analysis of 115 cases from a single centre in Wuhan city, China. *Liver Int.* 2020;40:2095–2103. doi: 10.1111/liv.14455.
  80. Başkiran A., Akbulut S., Şahin T.T., Tunçer A., Kaplan K., Bayındır Y., Yılmaz S. Coronavirus Precautions: Experience of High Volume Liver Transplant Institute. *Turk. J. Gastroenterol.* 2022;33:145–152. doi: 10.5152/tjg.2022.21748.
  81. Sahin T.T., Akbulut S., Yılmaz S. COVID-19 pandemic: Its impact on liver disease and liver transplantation. *World J. Gastroenterol.* 2020;26:2987–2999. doi: 10.3748/wjg.v26.i22.2987.
  82. Nalbandian, A.; Sehgal, K.; Gupta, A.; Madhavan, M.V.; McGroder, C.; Stevens, J.S.; Cook, J.R.; Nordvig, A.S.; Shalev, D.; Sehrawat, T.S.; et al. Post-acute COVID-19 syndrome. *Nat. Med.* 2021, 27, 601–615.
  83. Yende, S.; Parikh, C.R. Long COVID and kidney disease. *Nat. Rev. Nephrol.* 2021, 17, 792–793.

84. Raveendran, A.V.; Jayadevan, R.; Sashidharan, S. Long COVID: An overview. *Diabetes Metab. Syndr. Clin. Res. Rev.* 2021, 15, 869–875.
85. Hampshire, A.; Trender, W.; Chamberlain, S.R.; Jolly, A.E.; Grant, J.E.; Patrick, F.; Mazibuko, N.; Williams, S.C.R.; Barnby, J.M.; Hellyer, P.; et al. Cognitive deficits in people who have recovered from COVID-19. *eClinicalMedicine* 2021, 39, 101044.
86. College of American Pathologists. COVID-19 Autopsy Guideline Statement from the CAP Autopsy Committee. <https://documents.cap.org/documents/COVID-Autopsy-Statement-05may2020.pdf>. Accessed 15 May 2022.
87. Carsana L, Sonzogni A, Nasr A, Rossi R, Pellegrinelli A, Zerbi P, et al. Pulmonary post-mortem findings in a large series of COVID-19 cases from Northern Italy. *medRxiv* (preprint). 2020. 10.1101/2020.04.19.20054262
88. Wichmann D, Sperhake JP, Lütgehetmann M, Steurer S, Edler C, Heinemann A, et al. Autopsy findings and venous thromboembolism in patients with COVID-19: a prospective cohort study. *Ann Intern Med.* 2020 doi: 10.7326/M20-2003
89. Chong PY, Chui P, Ling AE, et al. Analysis of deaths during the severe acute respiratory syndrome (SARS) epidemic in Singapore: challenges in determining a SARS diagnosis. *Arch Pathol Lab Med.* 2004;128:195–204. doi: 10.5858/2004-128-195-AODDTS.
90. Liu Y., Li T., Deng Y., Liu S., Zhang D., Li H., Wang X., Jia L., Han J., Bei Z., Li L., Li J. Stability of SARS-CoV-2 on environmental surfaces and in human excreta. *J Hosp Infect.* 2021;107:105–107
91. Chin A.W.H., Chu J.T.S., Perera M.R.A., Hui K.P.Y., Yen H.-L., Chan M.C.W., Peiris M., Poon L.L.M. Stability of SARS-CoV-2 in different environmental conditions. *Lancet Microbe.* 2020;1:e10. doi: 10.1016/S2666-5247(20)30003-3
92. Baker CA, Gibson KE. Persistence of SARS-CoV-2 on surfaces and relevance to the food industry. *Curr Opin Food Sci.* 2022 Oct;47:100875. doi: 10.1016/j.cofs.2022.100875. Epub 2022 Jun 3. PMID: 35784376; PMCID: PMC9238272.
93. Circolare Fani. Italian Ministerial Circular n. 1665 of 30/6/1910 and Ministerial Circular n. 1667 of 24/7/1910. <https://www.funerali.org/wp-content/uploads/File/Circolari/cg91006300.htm>. Accessed 15 May 2022
94. Italian Regulation on the Mortuary Police. Art. 5 (D.P.R. 285/1990). [http://presidenza.governo.it/USRI/ufficio\\_studi/normativa/D.P.R.%2010%20settembre%201990,%20n.%20285.pdf](http://presidenza.governo.it/USRI/ufficio_studi/normativa/D.P.R.%2010%20settembre%201990,%20n.%20285.pdf). Accessed 15 May 2022.
95. di Vella G, Campobasso CP. Death investigation and certification in Italy. *Acad Forensic Pathol.* 2015;5:454–61. doi: 10.23907/2015.050
96. Turnbull A, Osborn M, Nicholas N. Hospital autopsy: Endangered or extinct? *J Clin Pathol.* 2015;68:601–4. doi: 10.1136/jclinpath-2014-202700.
97. Moretti M, Malhotra A, Visonà SD, Finley SJ, Osculati AMM, Javan GT. The roles of medical examiners in the COVID-19 era: a comparison between the United States and Italy. *Forensic Sci Med Pathol.* 2021 Jun;17(2):262-270. doi: 10.1007/s12024-021-00358-0. Epub 2021 Feb 13. PMID: 33582936; PMCID: PMC7882048.
98. Boseley S. WHO declares coronavirus a global health emergency. *The Guardian.* 2020. <https://www.theguardian.com/world/2020/jan/30/who-declares-coronavirus-a-global-health-emergency>. Accessed 30 March 2022.
99. Hanley B, Lucas SB, Youd E, et al. Autopsy in suspected COVID-19 cases. *J Clin Pathol.* 2020;73:239–42. doi: 10.1136/jclinpath-2020-206522
100. Sriwijitalai W, Wiwanitkit V. COVID-19 in forensic medicine unit personnel: Observation from Thailand. *J Forensic Leg Med.* 2020;72:101964. doi: 10.1016/j.jflm.2020.101964.
101. Sriwijitalai W, Wiwanitkit V. Corrigendum to "COVID-19 in forensic medicine unit personnel: Observation from Thailand" [J Forensic Legal Med 72 May 2020, 101964] *J Forensic Leg Med.* 2020;72:101967. doi: 10.1016/j.jflm.2020.101967
102. Taylor M. COVID-19 was not spread to medical examiner from body. *Forensic: on the scene and in the lab.* 24 April 2020. <https://www.forensicmag.com/563597-Authors-Journal-Issue-Correction-COVID-19-Was-Not-Spread-to-Medical-Examiner-from-Body/>. Accessed 10 May 2020

103. Centers for Disease Control and Prevention (CDC). Collection and submission of postmortem specimens from deceased persons with known or suspected COVID-19, March 2020 (Interim Guidance). 2020. <https://www.cdc.gov/coronavirus/2019-ncov/hcp/guidance-postmortem-specimens.html>. Accessed 10 June 2020
104. European Centre for Disease Prevention and Control. - Italian National Institute of Health - ISS. <https://www.ecdc.europa.eu/en/instituto-superiore-di-sanita-epiet>. Accessed 20 May 2021.
105. Italian National Institute of Statistics. COVID-19: instructions for completing the death certificate. 2020. [https://www.istat.it/it/files//2020/03/Covid\\_Indicazioni\\_scheda\\_morte.pdf](https://www.istat.it/it/files//2020/03/Covid_Indicazioni_scheda_morte.pdf). Accessed 11 May 2022.
106. Circular published by the Ministry of Health on 25 February 2020. <http://www.trovanorme.salute.gov.it/norme/renderNormsanPdf?anno=2020&codLeg=73368&parte=1%20&serie=null>. Accessed 15 May 2020.
107. Istituto Superiore di Sanità. National surveillance (epidemiological and virological) of COVID-19 cases in Italy - Epidemiology for public health. <https://www.epicentro.iss.it/en/coronavirus/sars-cov-2-analysis-of-deaths>. Accessed 12 May 2020.
108. Ministry of Health. Ministerial circular n. 1997 of 22 January 2020. [https://www.lavoripubblici.it/documenti2020/lvpb1/Circolare\\_Min\\_Salute\\_22\\_01\\_2020\\_1997.pdf](https://www.lavoripubblici.it/documenti2020/lvpb1/Circolare_Min_Salute_22_01_2020_1997.pdf). Accessed 12 May 2020.
109. Indicazioni emergenziali connesse ad epidemia COVID-19 riguardanti il settore funebre, cimiteriale e di cremazione. Ministero della Salute-Direzione Generale Della Prevenzione Sanitaria. Ufficio 4 - 0011285-01/04/2020-DGPRES-DGPRES-P. <http://www.trovanorme.salute.gov.it/norme/renderNormsanPdf?anno=2020&codLeg=73789&parte=1%20&serie=null> Accessed 7 May 2020.
110. P. Fais, S. Gavelli, G. Bolino, C. P. Campobasso, G. Cecchetto, R. Cecchi, R. Demontis, C. D'Ovidio, M. Moretti, M. Neri, A. Oliva, G. Pierucci, E. Ventura Spagnolo Elvira, F. Ventura, G. Di Vella. "Focus on COVID-19 buone pratiche per l'autopsia medico-legale nei cadaveri con sospetta infezione da SARS-CoV-2. Un aggiornamento dalla task force del gruppo italiano di patologia forense. *Rivista Italiana di Medicina Legale e del Diritto In Campo Sanitario*, ISSN: 2499-2852
111. Cattaneo C. Forensic medicine in the time of COVID 19: An editorial from Milano. Italy. *Forensic Sci Int.* 2020;312:110308. doi: 10.1016/j.forsciint.2020.110308.
112. Poloni T.E., Medici V., Carlos A.F., Davin A., Ceretti A., Mangieri M., Cassini P., Vaccaro R., Zaccaria D., Abbondanza S., et al., Bordoni M, Fantini V, Fogato E, Cereda C, Ceroni M, Guaita A. Abbiategrosso Brain Bank Protocol for Collecting, Processing and Characterizing Aging Brains. *J. Vis. Exp.* 2020;2020:e60296. Jun 3;(160). doi: 10.3791/60296.
113. Poloni TE, Medici V, Moretti M, Visonà SD, Cirrincione A, Carlos AF, Davin A, Gagliardi S, Pansarasa O, Cereda C, Tronconi L, Guaita A, Ceroni M. COVID-19-related neuropathology and microglial activation in elderly with and without dementia. *Brain Pathol.* 2021 Sep;31(5):e12997. doi: 10.1111/bpa.12997. Epub 2021 Jun 18. PMID: 34145669; PMCID: PMC8412067.
114. Moretti M., Belli G., Morini L., Monti M.C., Osculati A.M.M., Visonà S.D. Drug abuse-related neuroinflammation in human postmortem brains: An immunohistochemical approach. *J. Neuropathol. Exp. Neurol.* 2019;78:1059–1065. doi: 10.1093/jnen/nlz084
115. Gagliardi S, Poloni ET, Pandini C, Garofalo M, Dragoni F, Medici V, Davin A, Visonà SD, Moretti M, Sproviero D, Pansarasa O, Guaita A, Ceroni M, Tronconi L, Cereda C. Detection of SARS-CoV-2 genome and whole transcriptome sequencing in frontal cortex of COVID-19 patients. *Brain Behav Immun.* 2021 Oct;97:13-21. doi: 10.1016/j.bbi.2021.05.012. Epub 2021 May 19. PMID: 34022369; PMCID: PMC8132498.
116. Hanley B., Naresh K.N., Roufousse C., Nicholson A.G., Weir J., Cooke G.S., Thursz M., Manousou P., Corbett R., Goldin R., et al. Articles Histopathological findings and viral tropism in UK patients with severe fatal COVID-19: A post-mortem study. *Lancet Microbe.* 2020;1:e245–e253. doi: 10.1016/S2666-5247(20)30115-4
117. Zhang Y., Tang L.V. Overview of Targets and Potential Drugs of SARS-CoV-2 According to the Viral Replication. *J. Proteome Res.* 2021;20:49–59. doi: 10.1021/acs.jproteome.0c00526.

118. Wang K., Chen W., Zhang Z., Deng Y., Lian J.-Q., Du P., Wei D., Zhang Y., Sun X.-X., Gong L., et al. CD147-spike protein is a novel route for SARS-CoV-2 infection to host cells. *Signal Transduct. Target. Ther.* 2020;5:283. doi: 10.1038/s41392-020-00426-x.
119. Farkash E.A., Wilson A.M., Jentzen J.M. Ultrastructural Evidence for Direct Renal Infection with SARS-CoV-2. *JASN.* 2020;31:1683–1687. doi: 10.1681/ASN.2020040432
120. Lynch M.R., Tang J. COVID-19 and Kidney Injury. *Rhode Isl. Med. J.* 2020;103:24–28
121. Pan X.W., Xu D., Zhang H., Zhou W., Wang L.H., Cui X.G. Identification of a potential mechanism of acute kidney injury during the COVID-19 outbreak: A study based on single-cell transcriptome analysis. *Intensive Care Med.* 2020;46:1114–1116. doi: 10.1007/s00134-020-06026-1
122. Hassanein M., Radhakrishnan Y., Sedor J., Vachharajani T., Vachharajani V.T., Augustine J., Demirjian S., Thomas G. COVID-19 and the kidney. *Clevel. Clin. J. Med.* 2020;87:619–631. doi: 10.3949/ccjm.87a.20072
123. Mizuri S. ACE and ACE2 in kidney disease. *World J. Nephrol.* 2015;4:74–82. doi: 10.5527/wjn.v4.i1.74
124. Dal Ferro M., Bussani R., Paldino A., Nuzzi V., Collesi C., Zentilin L., Schneider E., Correa R., Silvestri F., Zacchigna S., et al. SARS-CoV-2, myocardial injury and inflammation: Insights from a large clinical and autopsy study. *Clin. Res. Cardiol.* 2021;110:1822–1831. doi: 10.1007/s00392-021-01910-2.
125. Sang C.J., Burkett A., Heindl B., Litovsky S.H., Prabhu S.D., Benson P.V., Rajapreyar I. Cardiac pathology in COVID-19: A single center autopsy experience. *Cardiovasc. Pathol.* 2021;54:107370. doi: 10.1016/j.carpath.2021.107370.
126. Liu J., Li Y., Liu Q., Yao Q., Wang X., Zhang H., Chen R., Ren L., Min J., Deng F., et al. SARS-CoV-2 cell tropism and multiorgan infection. *Cell Discov.* 2021;7:17. doi: 10.1038/s41421-021-00249-2.
127. Beyerstedt S., Barbosa Casaro E., Bevilacqua Rangel É. COVID-19: Angiotensin-converting enzyme 2 (ACE2) expression and tissue susceptibility to SARS-CoV-2 infection. *Eur. J. Clin. Microbiol. Infect. Dis.* 2021;40:905–919. doi: 10.1007/s10096-020-04138-6
128. Varga Z., Flammer A.J., Steiger P., Haberecker M., Andermatt R., Zinkernagel A.S., Mehra M.R., Schuepbach R.A., Ruschitzka F., Moch H. Endothelial cell infection and endotheliitis in COVID-19. *Lancet.* 2020;395:1417–1418. doi: 10.1016/S0140-6736(20)30937-5
129. Boldrini M., Canoll P.D., Klein R.S. How COVID-19 Affects the Brain. *JAMA Psychiatry.* 2021;78:682–683. doi: 10.1001/jamapsychiatry.2021.0500.
130. Basso C., Leone O., Rizzo S., De Gaspari M., Van Der Wal A.C., Aubry M.-C., Bois M.C., Lin P.T., Maleszewski J.J., Stone J.R. Pathological features of COVID-19-associated myocardial injury: A multicentre cardiovascular pathology study. *Eur. Heart J.* 2020;41:3827–3835. doi: 10.1093/eurheartj/ehaa664.
131. Paul J.F., Charles P., Richaud C., Caussin C., Diakov C. Myocarditis revealing COVID-19 infection in a young patient. *Eur. Heart J. Cardiovasc. Imaging.* 2020;21:776. doi: 10.1093/ehjci/jeaa107
132. Mele D., Flamigni F., Rapezzi C., Ferrari R. Myocarditis in COVID-19 patients: Current problems. *Intern. Emerg. Med.* 2021;16:1123–1129. doi: 10.1007/s11739-021-02635-w.
133. Kumar R., Kumar J., Daly C., Edroos S.A. Acute pericarditis as a primary presentation of COVID-19. *BMJ Case Rep.* 2020;13:e237617. doi: 10.1136/bcr-2020-237617
134. Lee M.H., Perl D.P., Steiner J., Pasternack N., Li W., Maric D., Safavi F., Horkayne-Szakaly I., Jones R., Stram M.N., et al. Neurovascular injury with complement activation and inflammation in COVID-19. *Brain.* 2022;145:2555–2568. doi: 10.1093/brain/awac151
135. Akbar A.N., Gilroy D.W. Aging immunity may exacerbate COVID-19. *Science. Am. Assoc. Adv. Sci.* 2020;369:256–257
136. Mueller A.L., Mcnamara M.S., Sinclair D.A. Why does COVID-19 disproportionately affect older people? *Aging.* 2020;12:9959–9981. doi: 10.18632/aging.103344
137. Salimi S., Hamlyn J.M., Le Couteur D. COVID-19 and Crosstalk with the Hallmarks of Aging. *J. Gerontol. Ser. A Biol. Sci. Med. Sci.* 2020;75:e34–e41. doi: 10.1093/gerona/glaa149

138. Yachou Y., El Idrissi A., Belapasov V., Ait Benali S. Neuroinvasion, neurotropic, and neuroinflammatory events of SARS-CoV-2: Understanding the neurological manifestations in COVID-19 patients. *Neurol. Sci.* 2020;41:2657–2669. doi: 10.1007/s10072-020-04575-3
139. Dong M., Zhang J., Ma X., Tan J., Chen L., Liu S., Xin Y., Zhuang L. ACE2, TMPRSS2 distribution and extrapulmonary organ injury in patients with COVID-19. *Biomed. Pharmacother.* 2020;131:110678. doi: 10.1016/j.biopha.2020.110678
140. Ludlow M., Kortekaas J., Herden C., Hoffmann B., Tappe D., Trebst C., Griffin D.E., Brindle H., Solomon T., Brown A.S., et al. Neurotropic virus infections as the cause of immediate and delayed neuropathology. *Acta Neuropathol.* 2016;131:159–184. doi: 10.1007/s00401-015-1511-3
141. Ackermann M., Verleden S.E., Kuehnel M., Haverich A., Welte T., Laenger F., Vanstapel A., Werlein C., Stark H., Tzankov A., et al. Pulmonary Vascular Endothelialitis, Thrombosis, and Angiogenesis in COVID-19. *N. Engl. J. Med.* 2020;383:120–128. doi: 10.1056/NEJMoa2015432
142. McFadyen J.D., Stevens H., Peter K. The Emerging Threat of (Micro)Thrombosis in COVID-19 and Its Therapeutic Implications. *Circ. Res.* 2020;127:571–587. doi: 10.1161/CIRCRESAHA.120.317447
143. Pisano T.J., Hakkinen I., Rybinnik I. Large Vessel Occlusion Secondary to COVID-19 Hypercoagulability in a Young Patient: A Case Report and Literature Review. *J. Stroke Cerebrovasc. Dis.* 2020;29:105307. doi: 10.1016/j.jstrokecerebrovasdis.2020.105307.
144. Baram A., Kakamad F.H., Abdullah H.M., Mohammed-Saeed D.H., Hussein D.A., Mohammed S.H., Abdulrahman B.B., Mirza A.J., Abdulla B.A., Rahim H.M., et al. Large vessel thrombosis in patient with COVID-19, a case series. *Ann. Med. Surg.* 2020;60:526–530. doi:10.1016/j.amsu.2020.11.030.
145. Avila J., Long B., Holladay D., Gottlieb M. Thrombotic complications of COVID-19. *Am. J. Emerg. Med.* 2021;39:213–218. doi: 10.1016/j.ajem.2020.09.065.
146. Iba T., Levy J.H., Levi M., Thachil J. Coagulopathy in COVID-19. *J. Thromb. Haemost.* 2020;18:2103–2109. doi: 10.1111/jth.14975.
147. Soy M., Keser G., Atagündüz P., Tabak F., Atagündüz I., Kayhan S. Cytokine storm in COVID-19: Pathogenesis and overview of anti-inflammatory agents used in treatment. *Clin. Rheumatol.* 2020;39:2085–2094. doi: 10.1007/s10067-020-05190-5
148. Reichard RR, Kashani KB, Boire NA, Constantopoulos E, Guo Y, Lucchinetti CF. Neuropathology of COVID-19: a spectrum of vascular and acute disseminated encephalomyelitis (ADEM)-like pathology. *Acta Neuropathol.* 2020;140:1–6.
149. Tröschler AR, Wimmer I, Quemada-Garrido L, Köck U, Gessler D, Verberk SGS, et al. Microglial nodules provide the environment for pathogenic T cells in human encephalitis. *Acta Neuropathol.* 2019;137:619–35.
150. Togo T, Akiyama H, Iseki E, Kondo H, Ikeda K, Kato M, et al. Occurrence of T cells in the brain of Alzheimer's disease and other neurological diseases. *J Neuroimmunol.* 2002;124:83–92
151. Rakic S, Hung YMA, Smith M, So D, Tayler HM, Varney W, et al. Systemic infection modifies the neuroinflammatory response in late stage Alzheimer's disease. *Acta Neuropathol Commun.* 2018;6:88.
152. Zotova E, Bharambe V, Cheaveau M, Morgan W, Holmes C, Harris S, et al. Inflammatory components in human Alzheimer's disease and after active amyloid- $\beta$ 42 immunization. *Brain.* 2013;136:2677–96.
153. Poyiadji N, Shahin G, Noujaim D, Stone M, Patel S, Griffith B. COVID-19-associated acute hemorrhagic necrotizing encephalopathy: imaging features. *Radiology.* 2020;296:E119–20.
154. Al-Sarraj S, Troakes C, Hanley B, Osborn M, Richardson MP, Hotopf M, et al. Invited Review: the spectrum of neuropathology in COVID-19. *Neuropathol Appl Neurobiol.* 2021;47:3–16
155. Deigendesch N, Sironi L, Kutza M, Wischniewski S, Fuchs V, Hench J, et al. Correlates of critical illness-related encephalopathy predominate postmortem COVID-19 neuropathology. *Acta Neuropathol.* 2020;140:583–6

156. Felsky D, Roostaei T, Nho K, Risacher SL, Bradshaw EM, Petyuk V, et al. Neuropathological correlates and genetic architecture of microglial activation in elderly human brain. *Nat Commun.* 2019;10:409. 10.1038/s41467-018-08279-3.
157. Hansen DV, Hanson JE, Sheng M. Microglia in Alzheimer's disease. *J Cell Biol.* 2018;217:459–72.
158. Santos LE, Beckman D, Ferreira ST. Microglial dysfunction connects depression and Alzheimer's disease. *Brain Behav Immun.* 2016;55:151–65.
159. Serrano-Pozo A, Muzikansky A, Gómez-Isla T, Growdon JH, Betensky RA, Frosch MP, et al. Differential relationships of reactive astrocytes and microglia to fibrillar amyloid deposits in alzheimer disease. *J Neuropathol Exp Neurol.* 2013;72:462–71.
160. Van Munster BC, Aronica E, Zwinderman AH, Eikelenboom P, Cunningham C, De Rooij SEJA. Neuroinflammation in delirium: a postmortem case-control study. *Rejuvenation Res.* 2011;14:615–22
161. Davis DHJ, Muniz Terrera G, Keage H, Rahkonen T, Oinas M, Matthews FE, et al. Delirium is a strong risk factor for dementia in the oldest-old: a population-based cohort study. *Brain.* 2012;135:2809–16
162. Lemstra AW, Groen in't Woud JCM, Hoozemans JJM, van Haastert ES, Rozemuller AJM, Eikelenboom P, van Gool WA Microglia activation in sepsis: a case-control study. *J Neuroinflammation.* 2007;4:4.
163. Michels M, Danielski L, Dal-Pizzol F, Petronilho F. Neuroinflammation: microglial activation during sepsis. *Curr Neurovasc Res.* 2014;11:262–70
164. Darbinyan A, Major EO, Morgello S, Holland S, Ryschkewitsch C, Monaco MC, et al. BK virus encephalopathy and sclerosing vasculopathy in a patient with hypohidrotic ectodermal dysplasia and immunodeficiency. *Acta Neuropathol Commun.* 2016;4:73
165. Kalaria RN, Kroon SN. Expression of leukocyte antigen CD34 by brain capillaries in Alzheimer's disease and neurologically normal subjects. *Acta Neuropathol.* 1992;84:606–12
166. Blümcke I, Giencke K, Wardelmann E, Beyenburg S, Kral T, Sarioglu N, et al. The CD34 epitope is expressed in neoplastic and malformative lesions associated with chronic, focal epilepsies. *Acta Neuropathol.* 1999;97:481–90.
167. Renu K, Prasanna PL, Valsala Gopalakrishnan A. Coronaviruses pathogenesis, comorbidities and multi-organ damage - A review. *Life Sci.* 2020 Aug 15;255:117839. doi: 10.1016/j.lfs.2020.117839. Epub 2020 May 22. PMID: 32450165; PMCID: PMC7243768.
168. Islam ABMMK, Khan MA. Lung transcriptome of a COVID-19 patient and systems biology predictions suggest impaired surfactant production which may be druggable by surfactant therapy. *Sci Rep.* 2020 Nov 10;10(1):19395. doi: 10.1038/s41598-020-76404-8
169. Yang S., Wu S., Yu Z., Huang J., Zhong X., Liu X., Zhu H., Xiao L., Deng Q., Sun W. Transcriptomic analysis reveals novel mechanisms of SARS-CoV-2 infection in human lung cells. *Immun Inflamm Dis.* 2020;8(4):753–762. doi: 10.1002/iid3.366.
170. Xiong Y., Liu Y., Cao L., Wang D., Guo M., Jiang A., Guo D., Hu W., Yang J., Tang Z., Wu H., Lin Y., Zhang M., Zhang Q., Shi M., Liu Y., Zhou Y., Lan K., Chen Y. Transcriptomic characteristics of bronchoalveolar lavage fluid and peripheral blood mononuclear cells in COVID-19 patients. *Emerg Microbes Infect.* 2020;9(1):761–770. doi: 10.1080/22221751.2020.1747363.
171. Asadi-Pooya A.A., Simani L. Central nervous system manifestations of COVID-19: A systematic review. *J Neurol Sci.* 2020;15(413) doi: 10.1016/j.jns.2020.116832. PMID: 32299017; PMCID: PMC7151535.
172. Koralnik I.J., Tyler K.L. COVID-19: A Global Threat to the Nervous System. *Ann Neurol.* 2020;88(1):1–11. doi: 10.1002/ana.25807. PMID: 32506549; PMCID: PMC7300753.
173. Serrano GE, Walker JE, Tremblay C, et al. SARS-CoV-2 Brain Regional Detection, Histopathology, Gene Expression, and Immunomodulatory Changes in Decedents with COVID-19. *J Neuropathol Exp Neurol.* 2022 Aug 16;81(9):666-695. doi: 10.1093/jnen/nlac056. PMID: 35818336; PMCID: PMC9278252.
174. T. Suo, X. Liu, J. Feng, M. Guo, W. Hu, D. Guo, H. Ullah, Y. Yang, Q. Zhang, X. Wang, M. Sajid, Z. Huang, L. Deng, T. Chen, F. Liu, K. Xu, Y. Liu, Q. Zhang, Y. Liu, Y. Xiong, Y. Chen

- ddPCR: a more accurate tool for SARS-CoV-2 detection in low viral load specimens *Emerging microbes & infections*, 9 (1) (2020), pp. 1259-1268,
175. Cavezzi, E. Troiani, S. Corrao COVID-19: hemoglobin, iron, and hypoxia beyond inflammation. A narrative review *Clin Pract.*, 10 (2) (2020), p. 1271, 10.4081/cp.2020.1271
  176. M. Jahani, S. Dokaneheifard, K. Mansouri Hypoxia: A key feature of COVID-19 launching activation of HIF-1 and cytokine storm *J Inflamm*, 17 (2020), p. 33, 10.1186/s12950-020-00263-3
  177. Thomas T, Stefanoni D, Dzieciatkowska M, Issaian A, Nemkov T, Hill RC, Francis RO, Hudson KE, Buehler PW, Zimring JC, Hod EA, Hansen KC, Spitalnik SL, D'Alessandro A. Evidence of Structural Protein Damage and Membrane Lipid Remodeling in Red Blood Cells from COVID-19 Patients. *J Proteome Res.* 2020 Nov 6;19(11):4455-4469. doi: 10.1021/acs.jproteome.0c00606. Epub 2020 Oct 26. PMID: 33103907; PMCID: PMC7640979.
  178. T.G. Smith, P.A. Robbins, P.J. Ratcliffe The human side of hypoxia-inducible factor *Br J Haematol.*, 141 (3) (2008), pp. 325-334, 10.1111/j.1365-2141.2008.07029.x
  179. S.E. Wilkins, M.I. Abboud, R.L. Hancock, C.J. Schofield Targeting Protein-Protein Interactions in the HIF System *ChemMedChem*, 11 (2016), p. 773
  180. K.S. Appelberg S. Gupta svensson akujsÅrvi, Sara & Ambikan, Anoop & Mikaeloff, Flora & Saccon, , Akos & Benfeitas, Rui & Sperk, Maïke & StÅ¥hlberg, Marie & Krishnan, Shuba & Singh, Kamal & Penninger, Josef & Mirazimi, Ali & Neogi, Ujjwal. Dysregulation in Akt/mTOR/HIF-1 signaling identified by proteo-transcriptomics of SARS-CoV-2 infected cells. *Emerging Microbes & Infections.* 9 2020 1 36 10.1080/22221751.2020.1799723.
  181. H. Zhao, D. Shen, H. Zhou, J. Liu, S. Chen Guillain-Barré syndrome associated with SARS-CoV-2 infection: causality or coincidence? *Lancet Neurol [Internet].*, 19 (5) (2020), pp. 383-384, 10.1016/S1474-4422(20)30109-5
  182. C. Corrado, S. Fontana Hypoxia and HIF Signaling: One Axis with Divergent Effects *Int. J. Mol. Sci.*, 21 (2020), p. 5611, 10.3390/ijms21165611
  183. Mandic M., Tzaneva V., Careau V., Perry, S.F. Hif-1 $\alpha$  paralogs play a role in the hypoxic ventilatory response of larval and adult zebrafish (*Danio rerio*) *J Exp Biol.* 222 2018 jeb.195198 10.1242/jeb.195198.
  184. F.L. Powell, Z. Fu HIF-1 and ventilatory acclimatization to chronic hypoxia *Respir Physiol Neurobiol.*, 164 (1–2) (2008), pp. 282-287, 10.1016/j.resp.2008.07.017 PMID: 18708172; PMCID: PMC2700119
  185. M. Codrich, M. Bertuzzi, R. Russo, M. Francescato, S. Espinoza, L. Zentilin, M. Giacca, D. Cesselli, A.P. Beltrami, P. Ascenzi, S. Zucchelli, F. Persichetti, G. Leanza, S. Gustincich Neuronal hemoglobin affects dopaminergic cells' response to stress *Cell Death Dis.*, 8 (1) (2017), Article e2538, 10.1038/cddis.2016.458 PMID: 28055011; PMCID: PMC5386368

## **8. Acknowledgements**

I want to deeply thank Emanuele Poloni and Valentina Medici for the hard work done during these difficult three years. The pandemic and sudden deaths have turned our lives upside down, but it has been a real pleasure to meet them and to work with these two special persons. This research work was only possible thanks to their efforts.

Thanks to all the staff of the Golgi-Cenci Foundation, Unit of Legal Medicine of Pavia, Genomic and IRCCS Mondino Foundation, and in particular to Silvia Visonà, Stella Gagliardi, Antonio Guaita, Mauro Ceroni, Cristina Cereda for their experience and expertise.

Thanks to Professor Politi for his patience and for treating me like a colleague.

Thanks to Giulia Rosi, Anna Milione, Giacomo Belli, Elena Cavriani and Marco Garatti for technical and scientific support.

Thanks and greetings to my mentor Prof. Antonio Osculati, who passed away suddenly. His teachings are a fundamental part of my present and my future. I hope you can always be proud of me.

As always, thanks to Professor Luca Morini, friend and guide, for everything he has done for me.